SAND2007-0552C

How did X-ray Sources Perform on Z?

M. E. Cuneo, D. B. Sinars,
W. A. Stygar, E. M. Waisman,
R. A. Aragon, B. M. Jones

J. H. Hammer, O. A. Hurricane,
S. MacLaren, B. Blue

LLNL-Sandia Workshop

January 23-25, 2007

Lawrence Livermore National Laboratory

Sandia is a multiprogram laboratory operated by Sandia Corporation, a Lockheed Martin Company, for the United States Department of Energy's National Nuclear Security Administration under contract DE-AC04-94AL85000.

Shots 1641, 1642, 1643 and 1695 were in this feed geometry

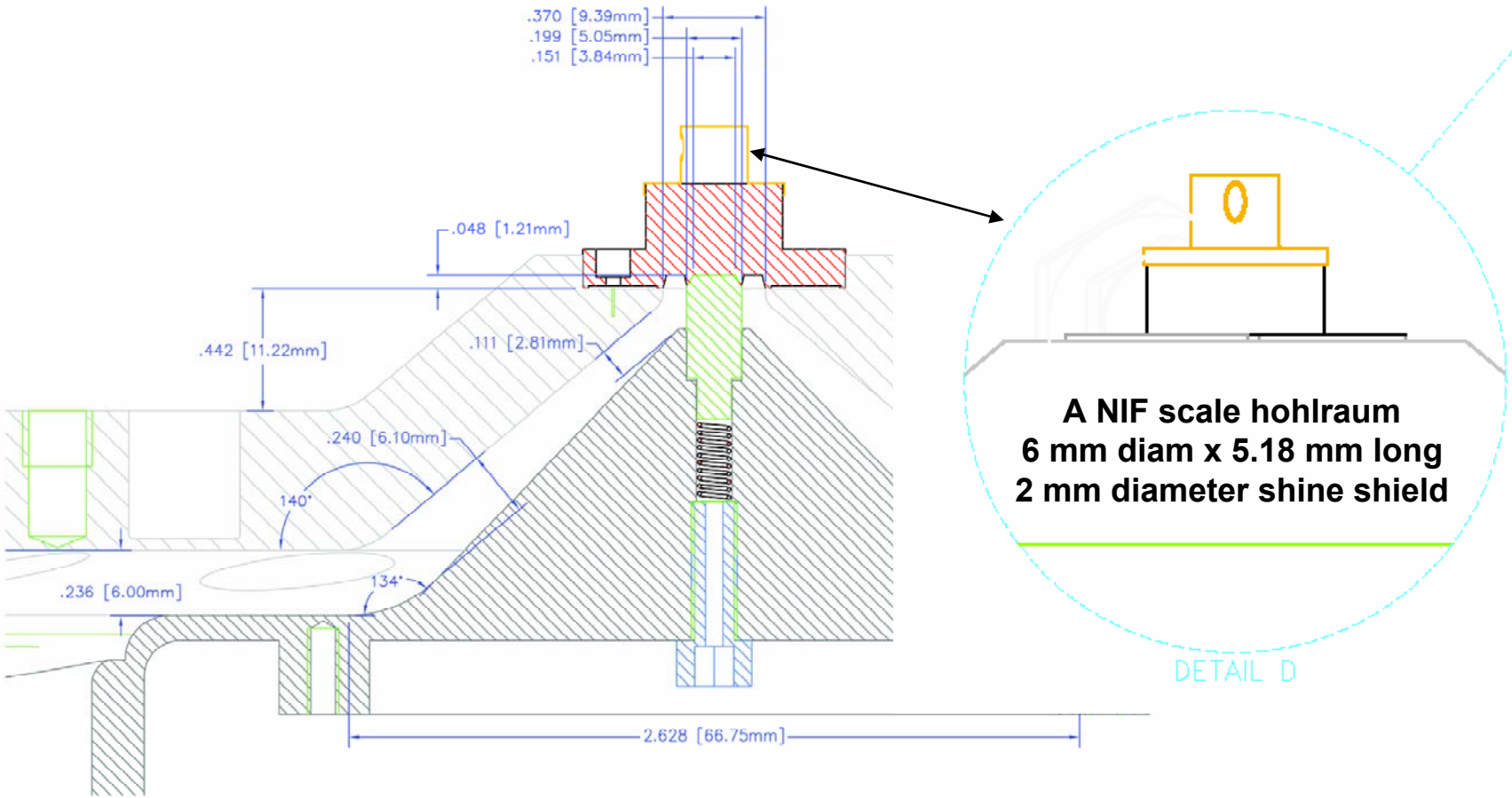

- L_{feed} = 4.0 ± 0.40 nH. Raised to allow backlighter line of sight on Z (which was not necessary for this experiment).
- Optimization for ZR might reduce this by 1 to 2 nH.

Shot 1736 was in this feed geometry compatible with two sided drive (MacLaren)

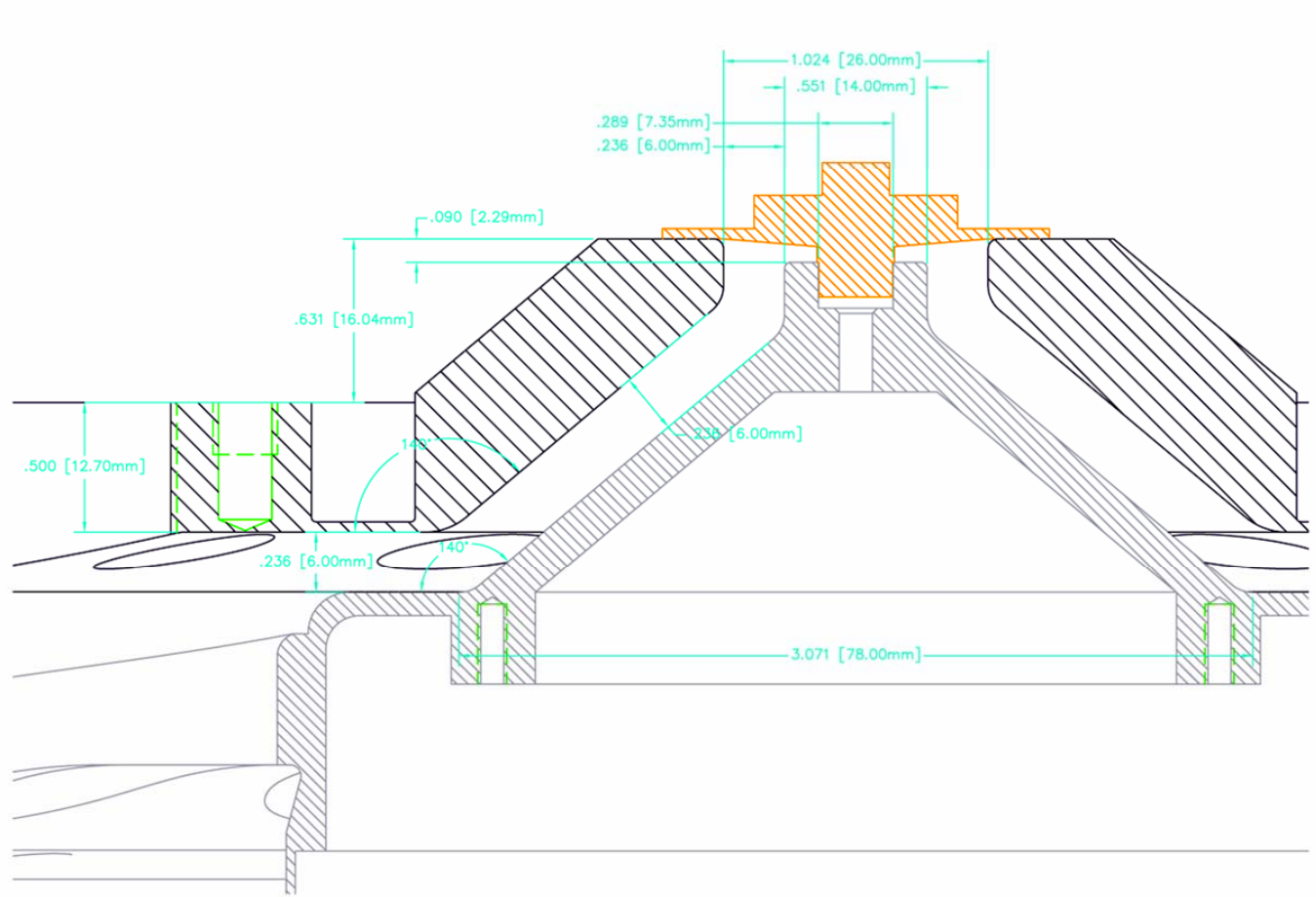

- Lfeed = 3.94 ± 0.39 nH. Again raised for backlighter line of sight.
- Again, should try to trim 1 to 2 nH from this.

Five experiments were performed in these experimental configurations before Z shut down

Shot	Liner Style	Shine Shield Thick. (μm)	Shine Shield Diam. (mm)	Barrier Thick. (μm)	Press. (psi)	LOS
1641	SB	100	2	6	12	across shield
1642	SB	100	2	6	12	across shield
1643	SB	100	2	6	10	20° to side of shield
1695	SB	300	2	13	10	across shield
1736	TB	300 (500?)	2	13	10	across shield

1641, 1642, 1695, 1736 diagnostics view across the shine shield

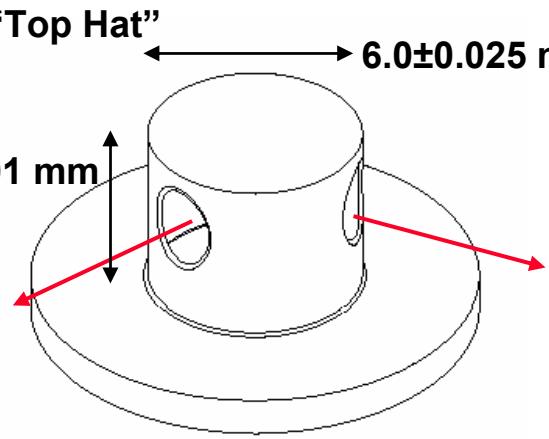

Aperture Area

Time resolved x-ray pinhole framing camera

Energy, Power, and Spectrum

3 fast pulsed bolometers
Filtered x-ray diode array (XRD)
Total energy and power (TEP)
Transmission grating spectrometer (TGS)

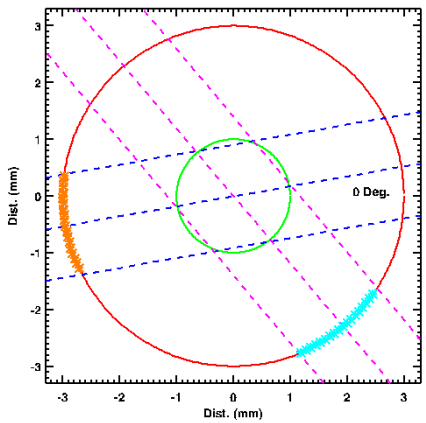

shine shield

LOS 29/30

LOS 5/6

- Apertures are ~4.4±0.4 mm^2 initially

1643 diagnostics views are rotated by 20° but half of the region above the shield is still visible

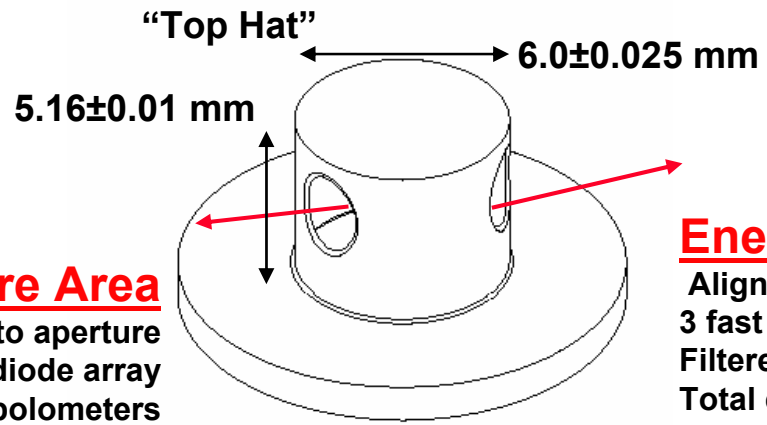

Energy, Power, Aperture Area

Aligned 20° from normal to aperture
Filtered X-ray diode array
2 fast pulsed bolometers
Multi-Layer Mirror Framing Camera

Energy, Power and Spectrum

Aligned 20° from normal to aperture
3 fast pulsed bolometers
Filtered x-ray diode array
Total energy and power
Transmission grating spectrometer

LOS 21/22

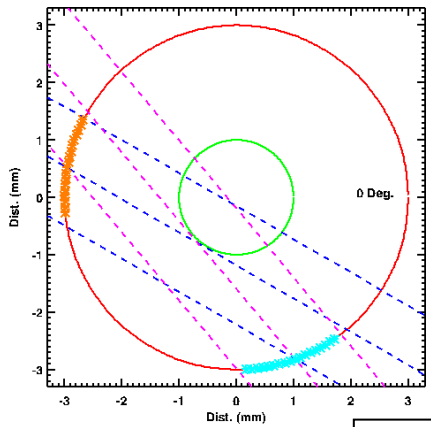

LOS 5/6

- Apertures are ~4.4±0.4 mm^2 initially
- Views might include aperture on opposite side - need to do a 3D layout

Comparison of brightness temperatures determined with time-dependent aperture closure measurements

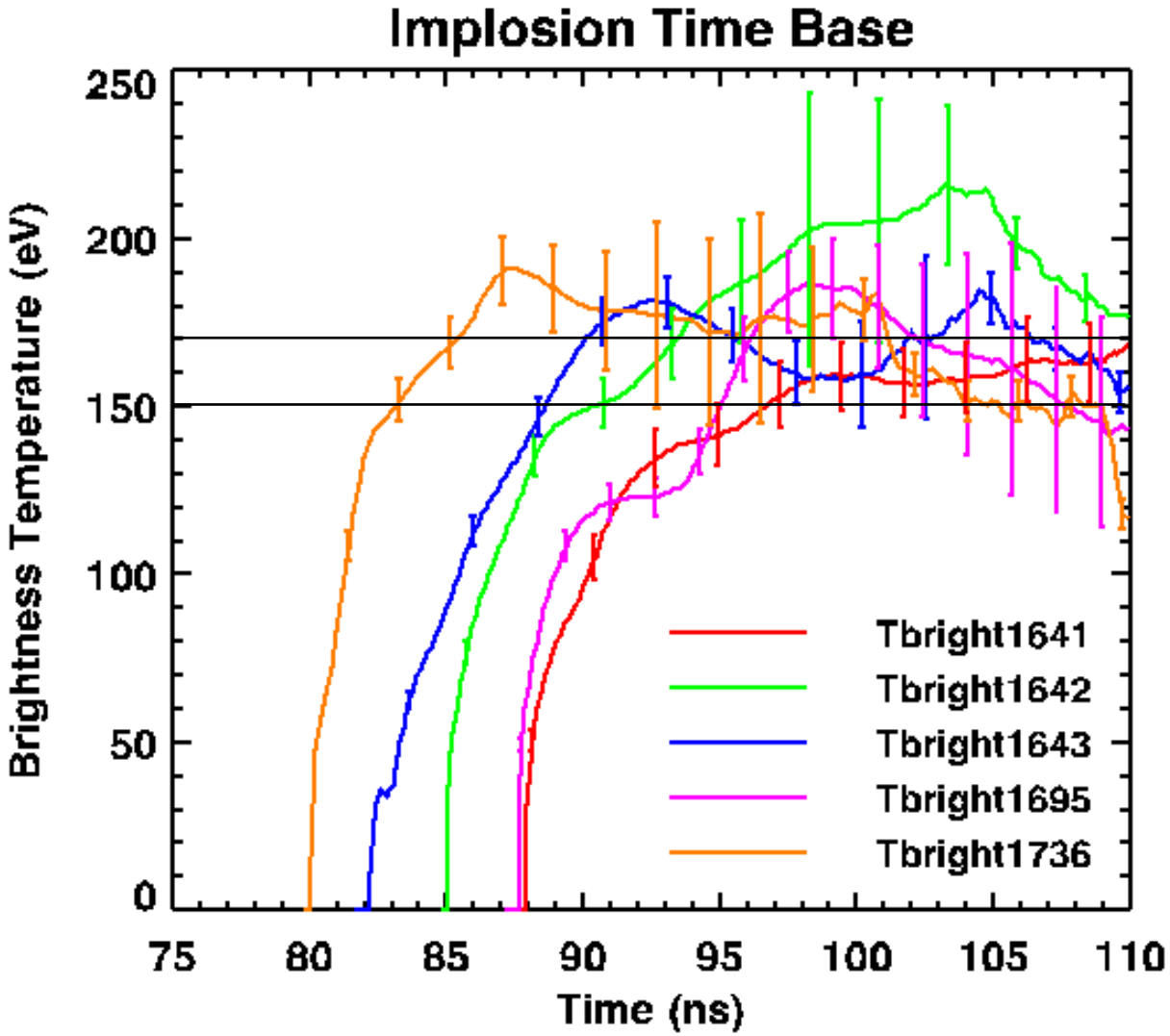

- All 5 experiments are above 150 eV
- 4 of 5 are above 170 eV
- ZR experiments are needed to measure the hydro-isolation time in the secondary

Sandia National Laboratories

Dynamic hohlraum driven 6 mm x 7 mm hohlraums reached 122±6 eV in experiments by Sanford et al

T.W.L. Sanford et al., PRL, 83, 5511 (1999)
T.W.L. Sanford et al., PoP, 7, 4669 (2000)

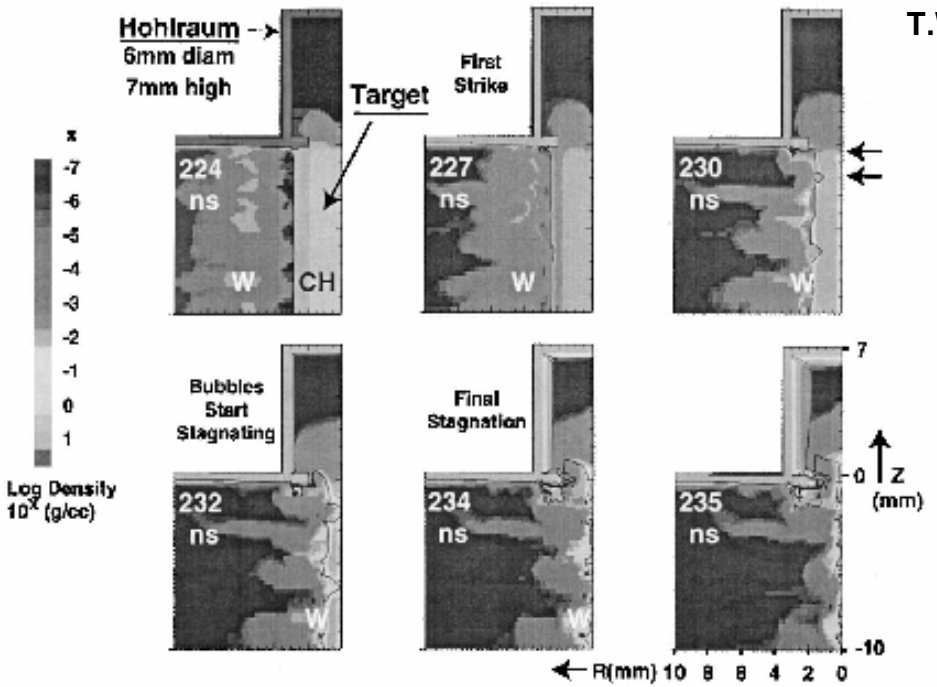

FIG. 5. Log density plots of the imploding tungsten plasma and foam target, showing the expansion of the gold walls of the NIF-scale hohlraum in the baseline E-RMHC model. The two arrows in the 230 ns plot correspond to the axial location of the bubble and spike whose radii are plotted in Fig. 4(D).

- T = 122 ± 6 eV, P = 13 ± 4 TW, E = 60 ± 20 kJ coupled in DH (scales to 130 eV for 6 mm diam. x 5.18 mm long)
- Probably has marginal hydro-isolation
- Compare these results T ~ 170 eV, 170 kJ, 50 TW coupled to secondary

Initial comparison (Feb 06) of brightness temperature assumed apertures were 75% open, constant with time

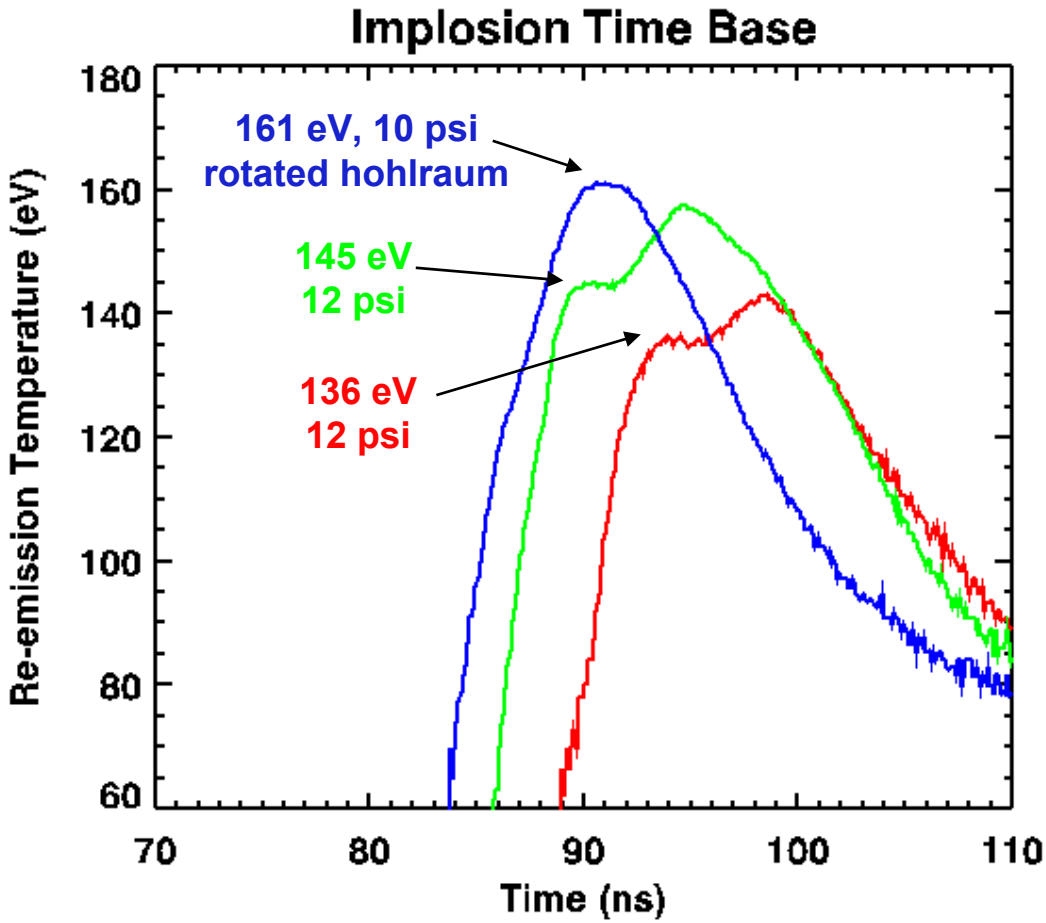

- This is the preliminary analysis from Feb 2006.
- Hole closure estimated from raw film and from Hammer simulations after ts+5 ns
- The temperatures on the plot for 1641 and 1642 are quoted at the first plateau (ts + 5 ns), since we thought the later ramp might be the z-pinch punching through.
- The time-dependent analysis has apertures at ~47% open *and* quotes values at ~ ts + 11 ns (except for 1736).

Summary of "peak" brightness temperatures and measured aperture closure

February 2006

Shot	T "peak" (eV)	T lower (eV) (Ti filter and geometric method)	@ ts + Δ Δ (ns)	Fraction aperture open at ts + Δ	T	Fraction open
1641	157 ± 10	147	10.6	*0.47 ± 0.11*	136 (Δ =5 ns)	0.75
1642	186 ± 17	169	10.6	0.36 ± 0.12	146 (Δ =4.3 ns)	0.75
1643	181 ± 9	172	10.5	0.49 ± 0.12	164 (Δ =10 ns)	0.75
1695	187 ± 13	174	10.9	0.49 ± 0.12	NA	NA
1736	191 ± 10	181	7.3	0.55 ± 0.08	NA	NA

We use ns-resistive-bolometry as an intrinsic standard that is calibrated via known properties of the Ni film

Method for small ΔT

$$mc_p \frac{dT}{dt} = \frac{dF}{dt} A$$

$$F \cong \frac{mc_p \Delta T}{A} = \rho_m x c_p \Delta T$$

$$\Delta\rho = \alpha \Delta T \cong \frac{wx\Delta V}{I I_o}$$

Exact

$$\rho(T(t)) = \frac{A}{l} \frac{V(t)}{I(t)}$$

$$F = \frac{m}{A} \int_0^{T(t)} C_p(T(t)) dT$$

D. L. Hanson et al., BAPS, 25, 890 (1980)
D. L. Hanson et al., BAPS, 26, 910 (1981)
R. B. Spielman et al., Rev. Sci. Inst., 70, 651 (1999)

- These two methods give results within 5% of each other for typical ΔT of 30 to 60° K reached at 400 to 800 kJ on film
- Typical ΔT for liners is 5° K at 25 kJ

High quality vapor deposited Ni films show bulk Ni density, resistivity and thermal coefficient

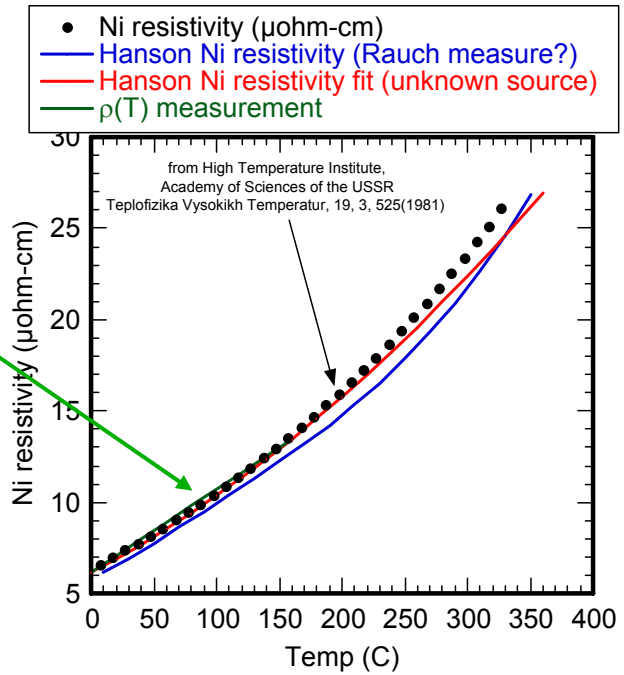

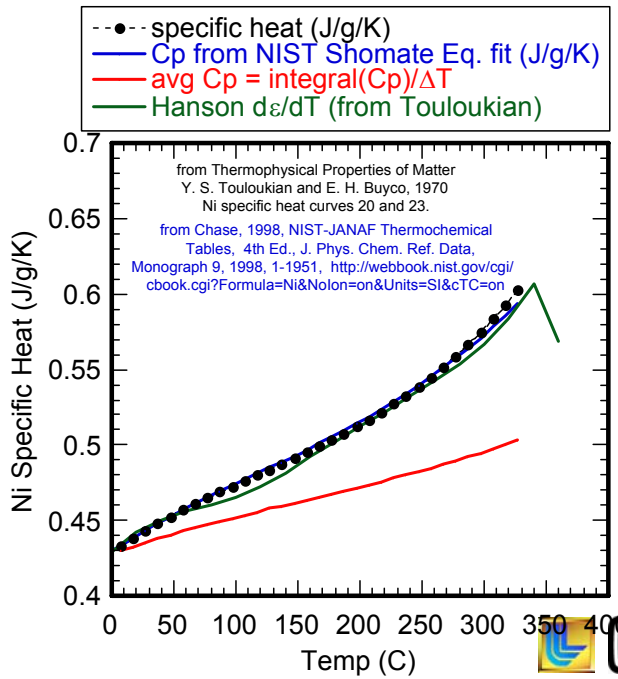

1642 Bolometer Energy Analysis LOS 5/6 (50°)

1642

error bars here from average over 18 ns window

TEP =
"total energy and power"
a flat energy response Si PIN diode
matched to bolometers flat response

Integral of TEP normalized to bolo energy

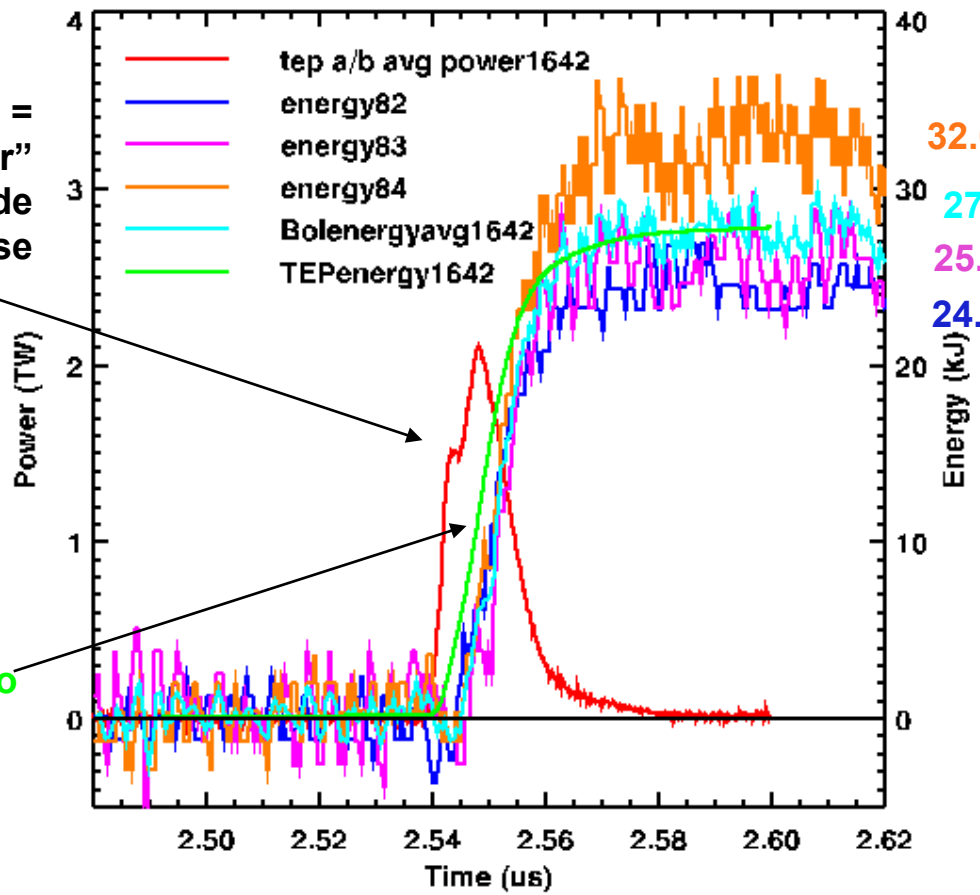

32.6 ± 2.2 kJ
27.8 ± 0.9 kJ
25.8 ± 1.6 kJ
24.9 ± 1.3 kJ

- Ebolo_avg = 27.8 ± 4.2 kJ
- Corrected for photon transmission through Ni bolometer film (assume Tsource = 150 eV) and for electrons that leave the front and back of the film, Ebolo_avg = 29.1 ± 4.4 kJ

Total energy measured through apertures is 25 to 30 kJ with ns-bolometry

Shot	Pressure (psi)	Energy (kJ)	Instrument	Average Energy (corrected by 1.046, exclude TGS) (kJ)	Initial Aperture Area (cm^2)
1641	~12	21.4±1.2 *26.8±1.6*	Bolo 82 LOS 5/6 *Bolo 84 LOS 5/6*	22.4 *25.2 ± 4.0*	0.0502
1642	12	24.9±1.3 25.8±1.6 *32.6±2.2*	Bolo 82 LOS 5/6 Bolo 83 LOS 5/6 *Bolo 84 LOS 5/6*	26.6 ± 0.7 *29.1 ± 4.4*	0.0409
1643	10	22.2±1.0 24.7±1.5 *30.0±1.3* 20.9±1.0 23.4±1.2	Bolo 82 LOS 5/6 Bolo 83 LOS 5/6 *Bolo 84 LOS 5/6* Bolo 65 LOS 21/22 Bolo 66 LOS 21/22	23.8 ± 1.7 *25.4 ± 3.7*	0.04142 0.04247
1695	10	21.6±1.1 28.6±1.4 *32.6±1.6*	Bolo 82 LOS 5/6 Bolo 83 LOS 5/6 *Bolo 84 LOS 5/6*	26.3 ± 5.2 *28.9 ± 5.9*	0.04215
1736	10	25.9±1.3 28.5±1.4 *31.1±1.7*	Bolo 82 LOS 5/6 Bolo 83 LOS 5/6 *Bolo 84 LOS 5/6*	28.5 ± 1.9 *29.8 ± 2.7*	0.04177

- Error in flux is ±15% with element 84, ±9% without
- Bolometer 84 is 23±3% higher than other bolometers

Power is obtained by normalizing XRD and TEP signals to bolometer energies, and by a spectrally-equalized combination of XRD signals

1643

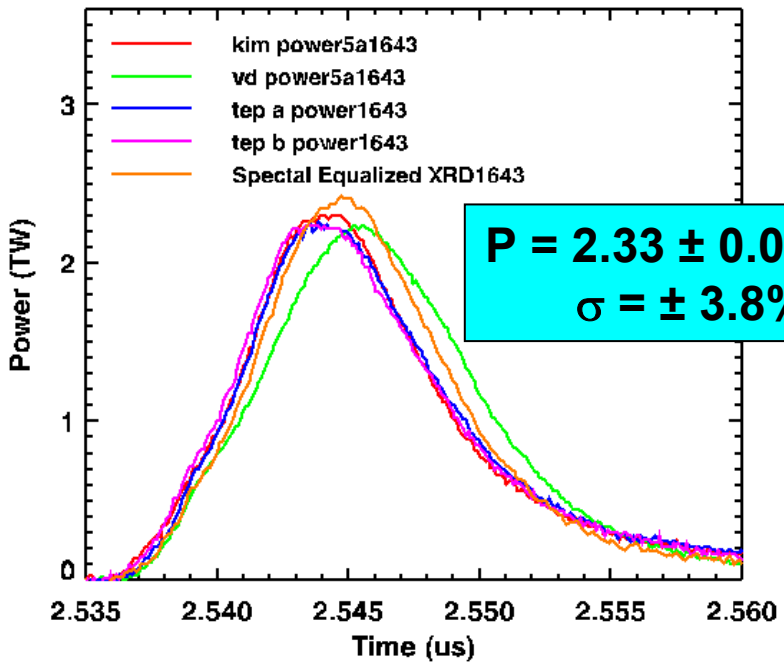

P = 2.33 ± 0.09 TW
σ = ± 3.8%

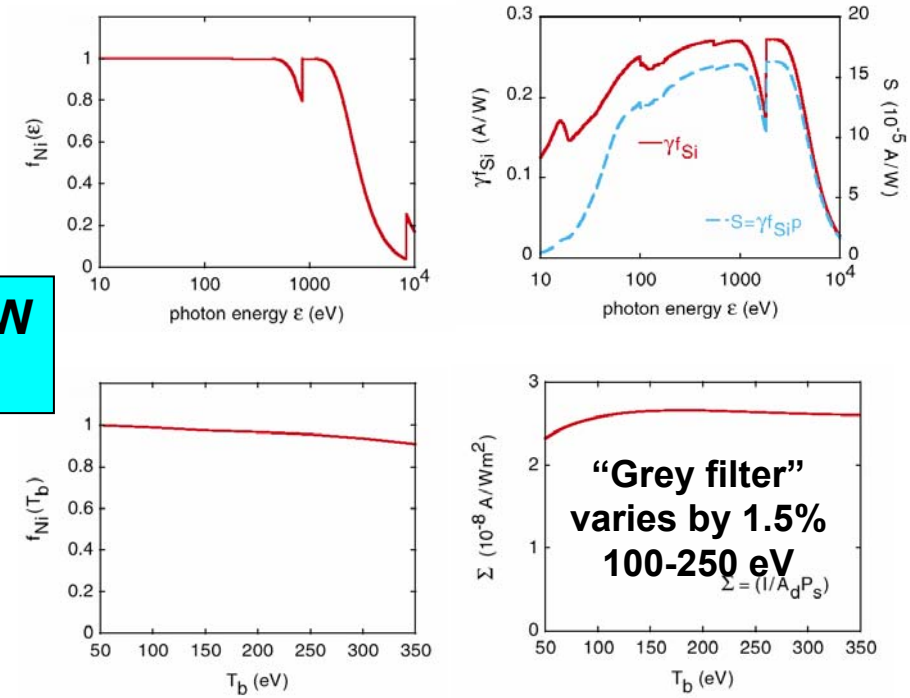

R. B. Spielman et al., Rev. Sci. Instrum., 70, 651 (1999)
D. L. Fehl et al., Rev. Sci. Instrum., 76, 103504 (2005)
H.C. Ives et al., Phys. Rev. ST A and B, 9, 110401 (2006)

- The TEP has a flat energy response, matched to the Ni bolometer
- The 5 μm Kimfol filtered XRD and TEP signals overlay

Hole closure data is obtained from filtered time-resolved x-ray pinhole cameras with 1 ns gates

1642

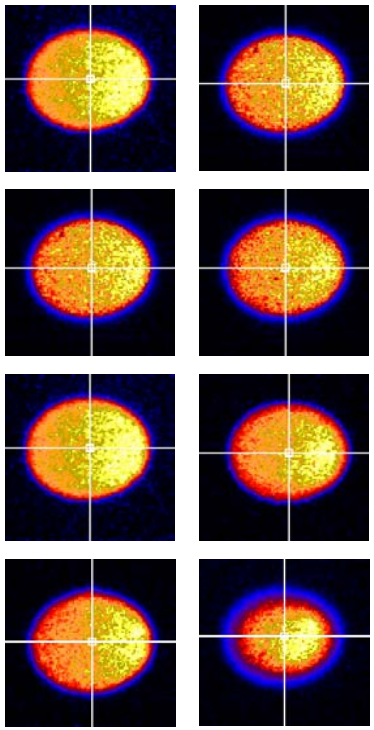

J. L. Porter, BAPS, 42, 1948 (1997)
R. E. Chrien et al., Rev. Sci. Instrum., 70, 557 (1999)
K. L. Baker et al., Phys. Plasmas, 7, 681 (2000)

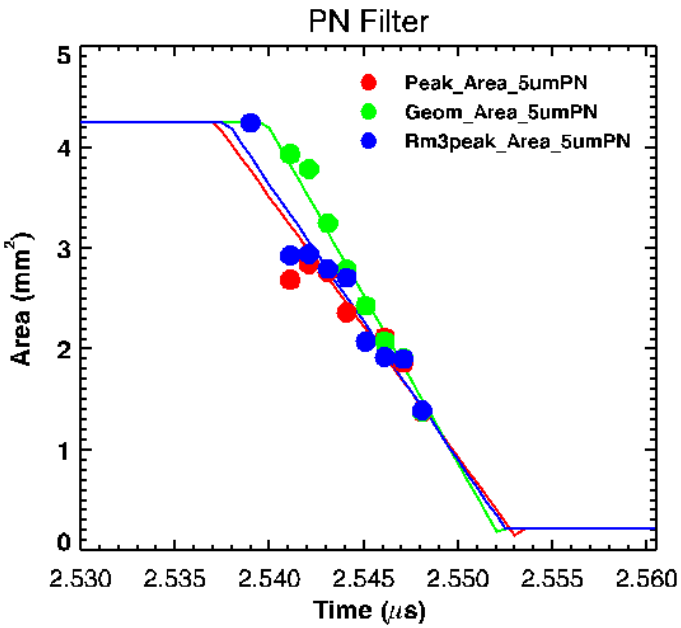

- The aperture area is calculated by:

$$\text{Area} = A_{\text{pixel}} \frac{\sum_{\text{pixels}} I}{I_o}$$

- The unattenuated intensity, I_o, is given by:
  - peak pixel,
  - or by peak removing the top 3 pixels,
  - or by a region averaged over a 5 pixel x 5 pixel square region at the geometric center of the aperture

On ZR we are planning 200 ps gates

The gradient of emission along the aperture makes the proper choice for I_o the unattenuated intensity uncertain

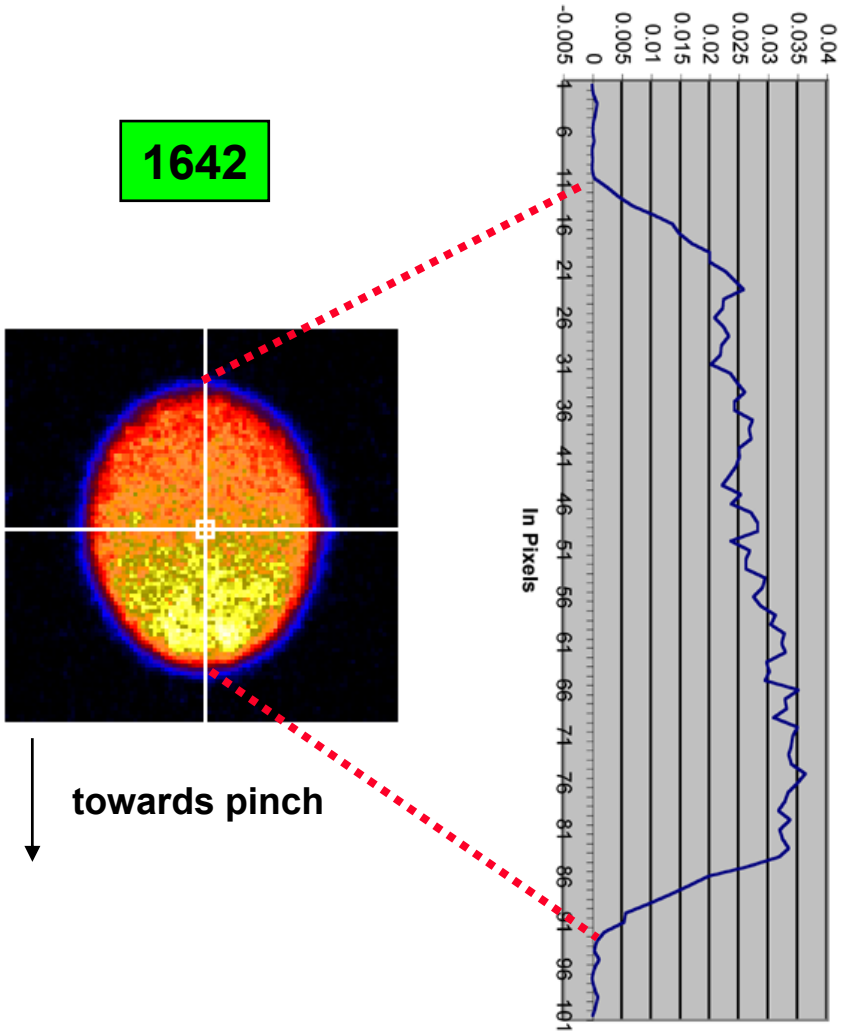

- Gradient in emission along the aperture is 40% in flux (10% in temperature)
- Earlier experiments with much larger hohlraums had ~10% gradient in flux across larger apertures
- The intensity at geometric center may make more sense - its like the average intensity $I_o \sim \langle I \rangle$

$$\text{Area} = A_{\text{pixel}} \frac{\sum I_{\text{pixels}}}{I_o}$$

What is the proper treatment of the closure data? The geometric method gives a larger aperture area

1642

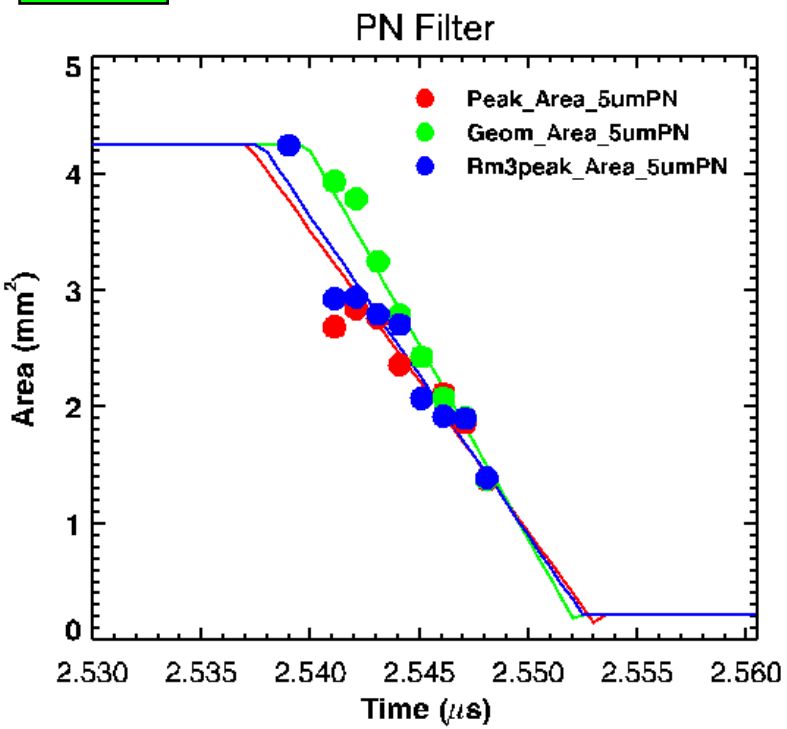

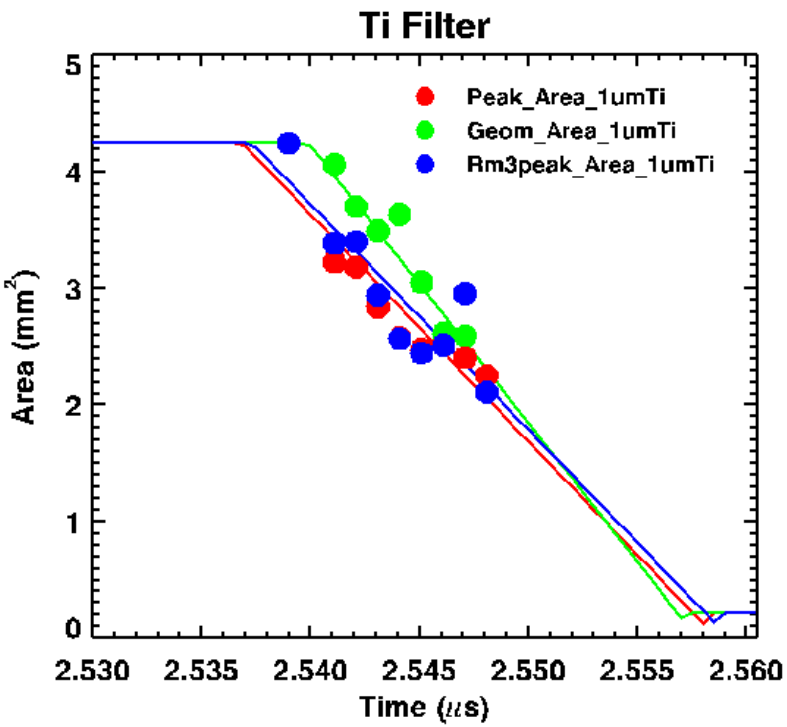

What is the proper treatment of the closure data? The harder filtered 1 μm Ti shows a larger aperture area

1642

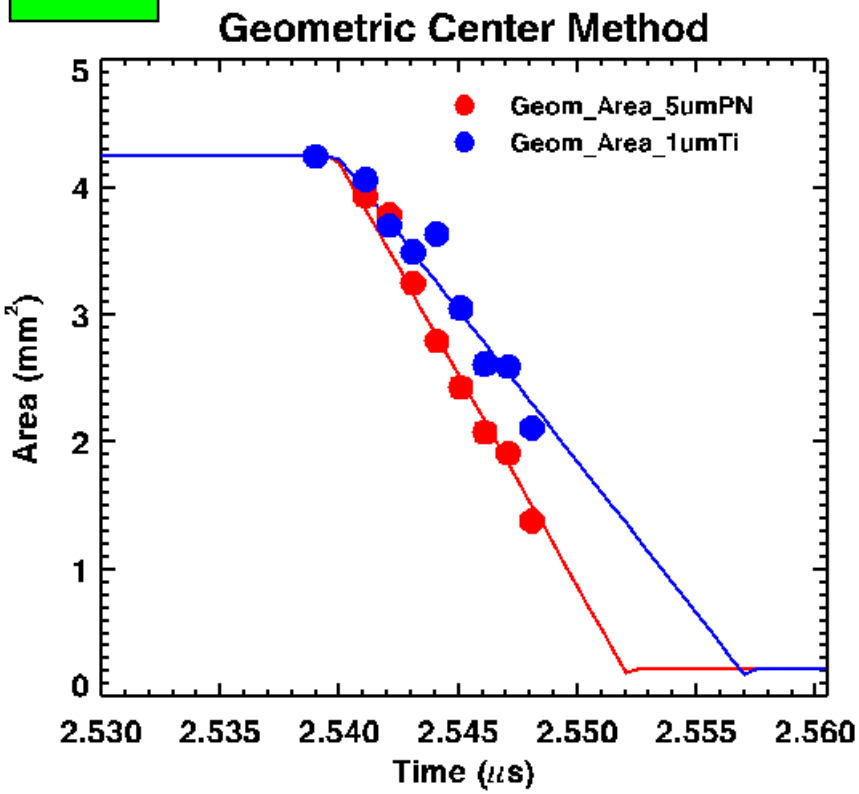

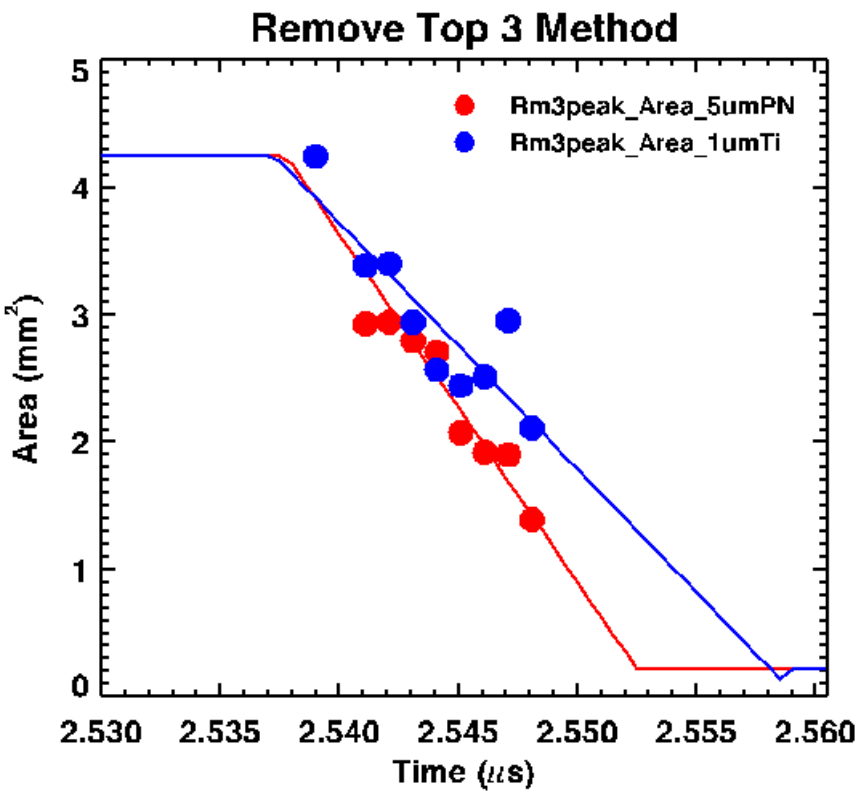

The Ti filter samples near the peak of the Planckian

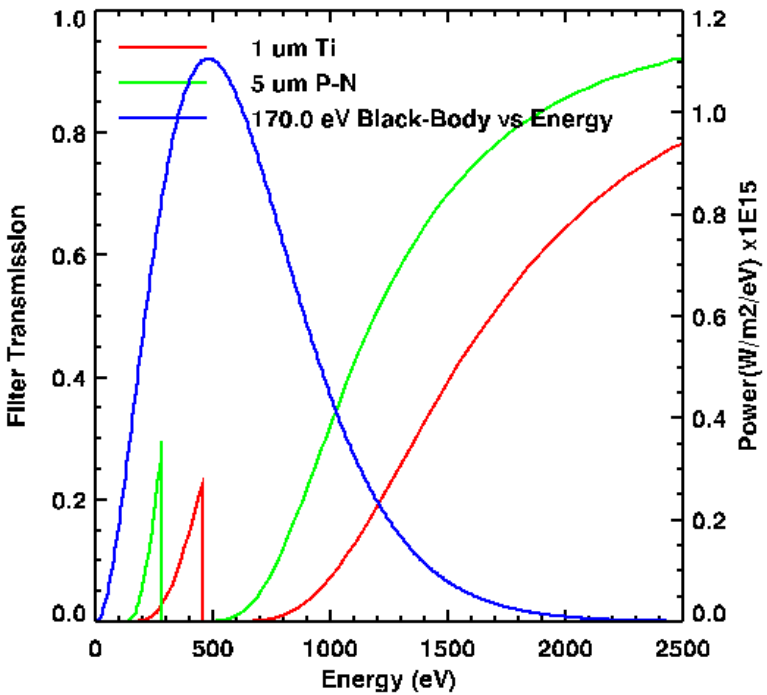

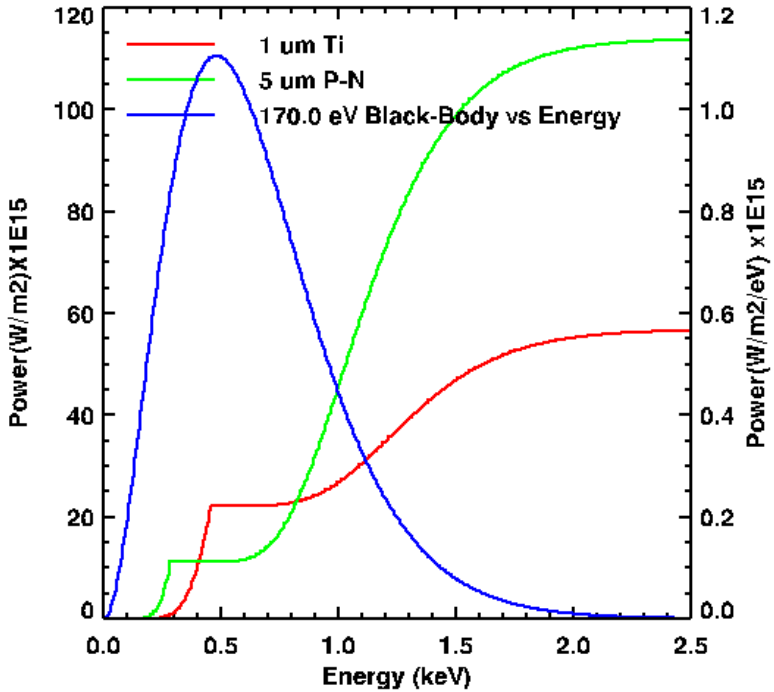

- **Softer cuts (like the Parylene-N) or the multi-layer-mirror camera with reflective crystal show smaller area**

The aperture closure measurements on 1642 overlap with peak emission

1642

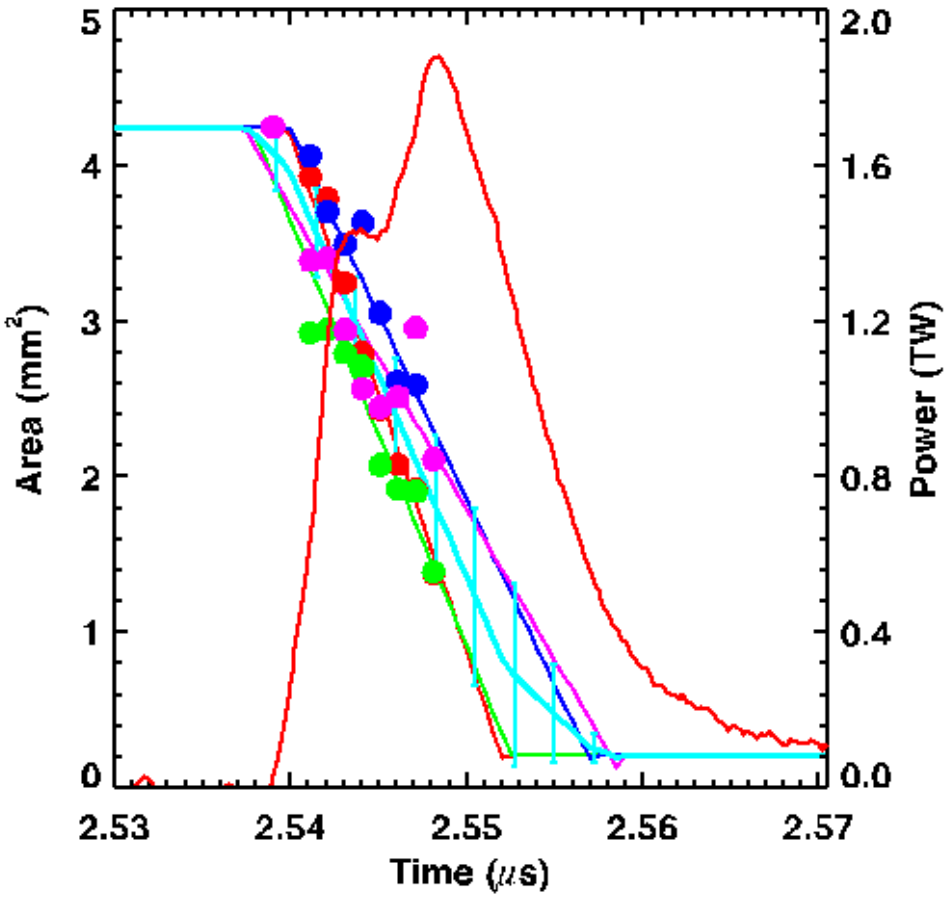

The uncertainty in aperture size at t_s+5 ns (at plateau) is ±10% in flux for 1642

1642

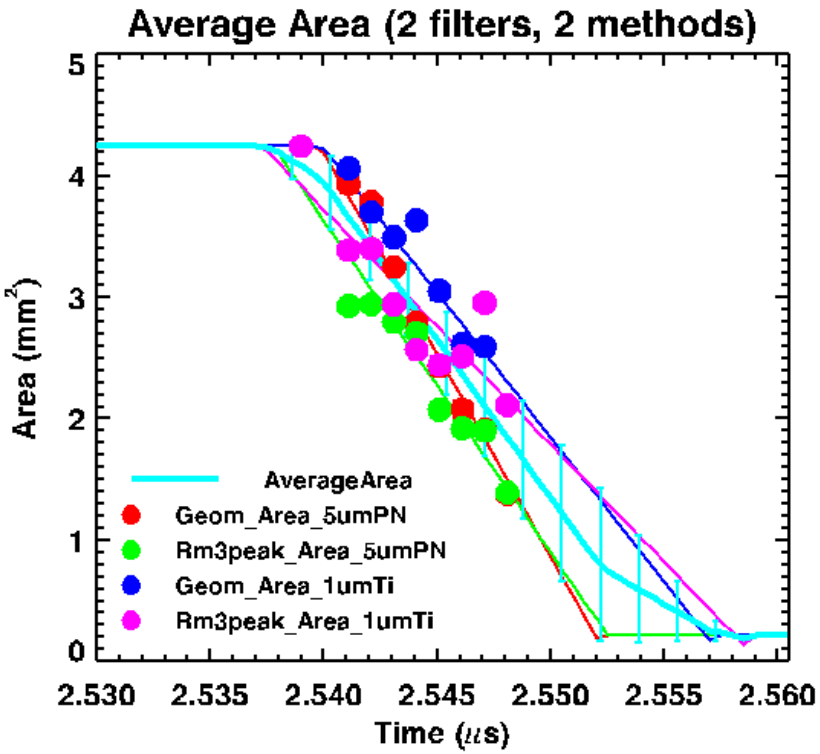

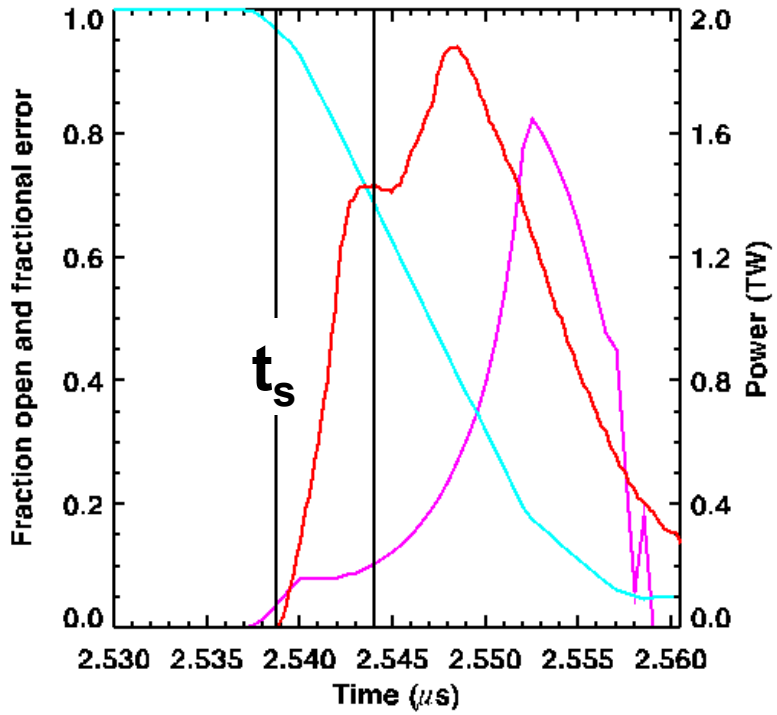

- Rapid closure, no late time data, and uncertainty of data treatment degrades measurement after ~ t_s+12 ns
- On ZR extend this window with a circular aperture initially 7 to 10 mm² area, rather than elliptical at 4.4 mm²

The measured aperture closure on 1642 is smaller than simulations by about 10% at t_s+5 ns

1642

Hammer calculation of $A(t)/A_o$ with 170 eV thermal drive

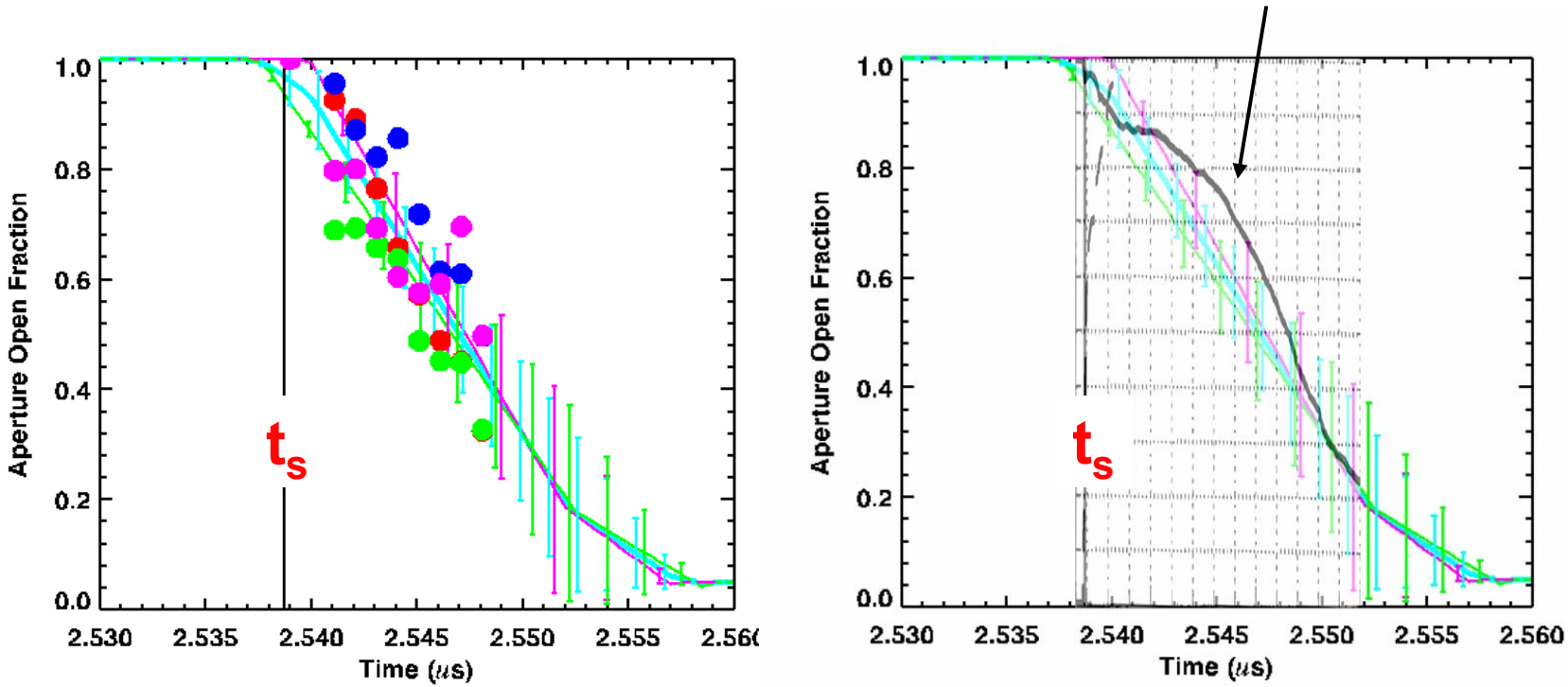

- Average closure rate is 6.1% of the initial area per ns, starting at t_s
- We use the average of all four methods (2 filters and 2 estimates for I_o

The Hammer simulation shows reasonable agreement with the Ti filter and the geometric center method

1642

Hammer calculation of $A(t)/A_o$ with 170 eV thermal drive

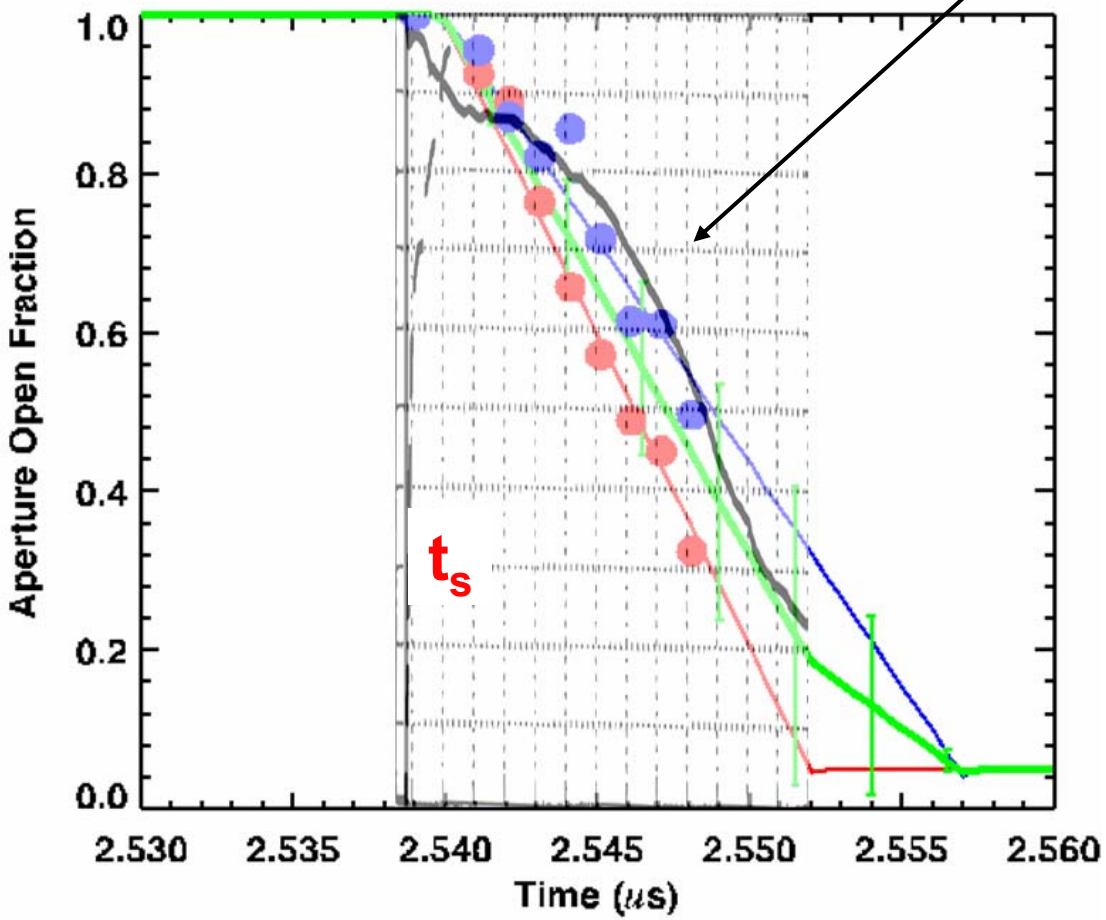

- If Ti filters with the geometric method is the right treatment this means that the brightness temperatures are closer to the lower end of the quoted error ranges
- Need 2D simulations and synthetic aperture pinhole camera images with actual filters to do better

Peak brightness temperature was 186 ± 17 eV at ts + 10.6 ns for 1642

Z-pinch on axis punching though the 100 μm shine shield?

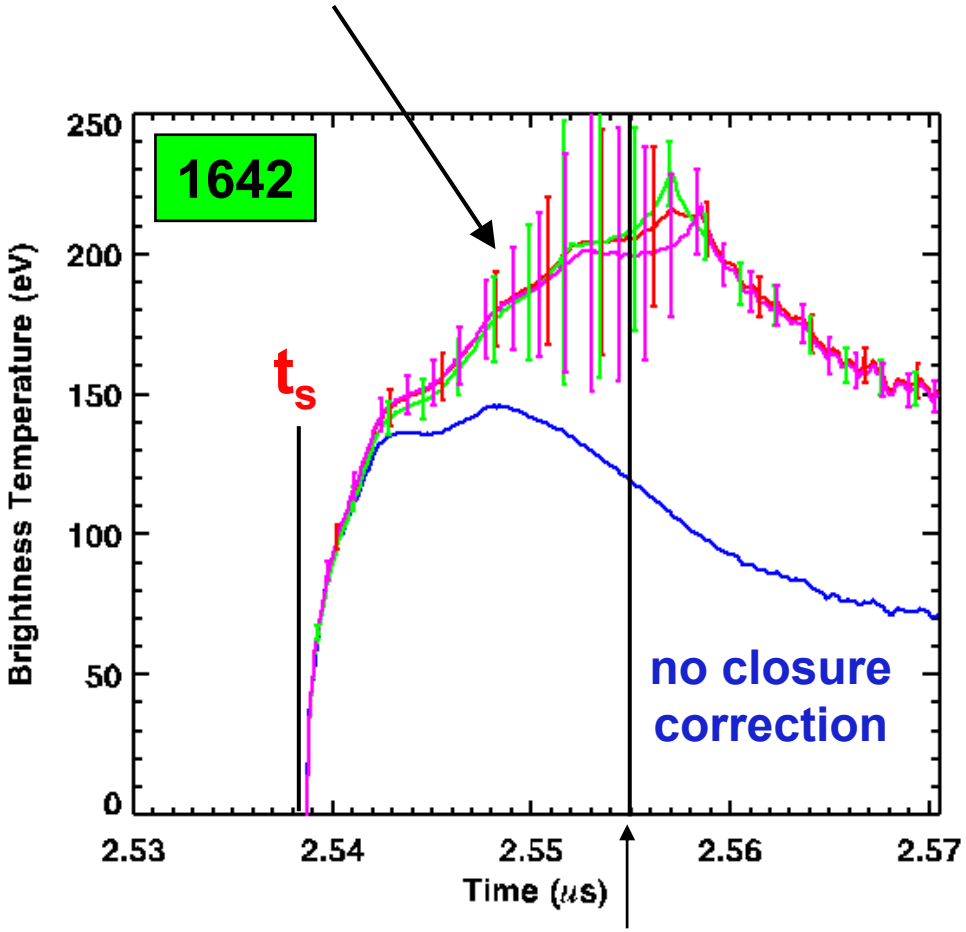

- Twall
  - at ts+5 ns = 149 ± 7 eV
  - at ts+10.6 ns = 186 ± 17 eV
- Error in re-emission flux at t_s+5 ns is ±18%, but at ts+10.6 ns is ± 37%
  - energy (±15%)
  - power (±4%)
  - hole closure (±10% to ±33%)
- On ZR improve secondary hohlraum temperature measurements with larger circular apertures and using shock breakout techniques

aperture estimated completely closed

The aperture closure data overlaps the time of peak emission for 1643

1643

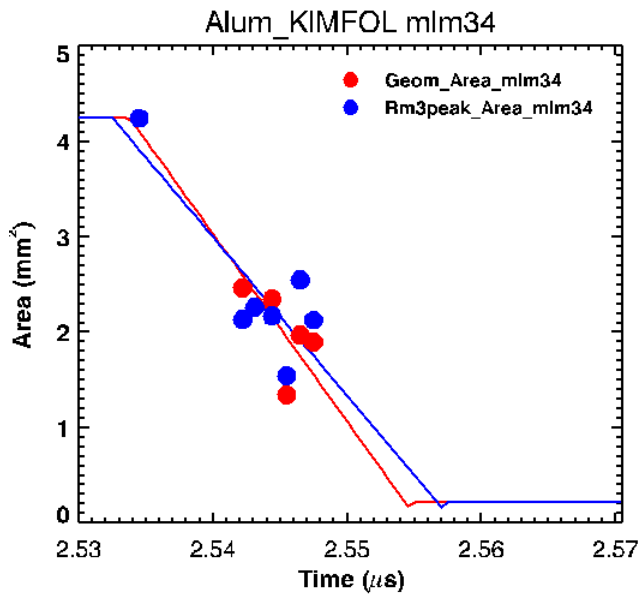

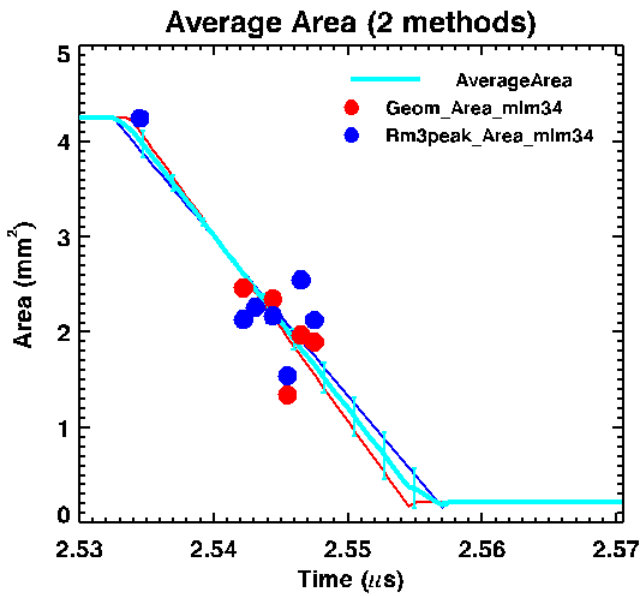

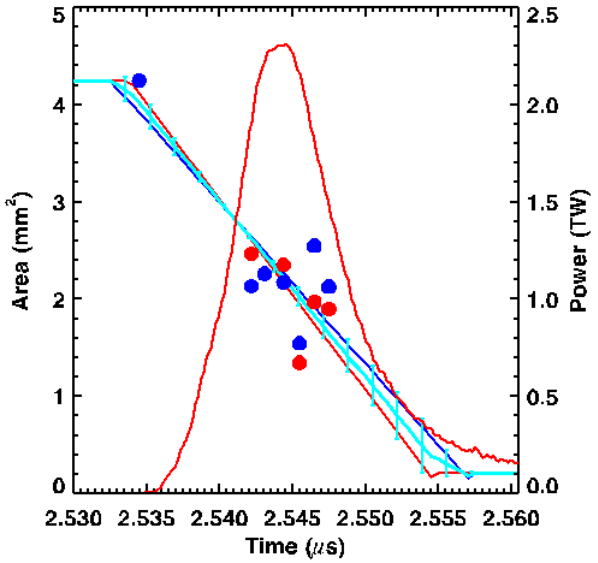

- **The average closure rate is 4.1% of the area per ns starting at ts**

Peak brightness temperature was 181 ± 9 eV at ts + 10.5 ns for 1643

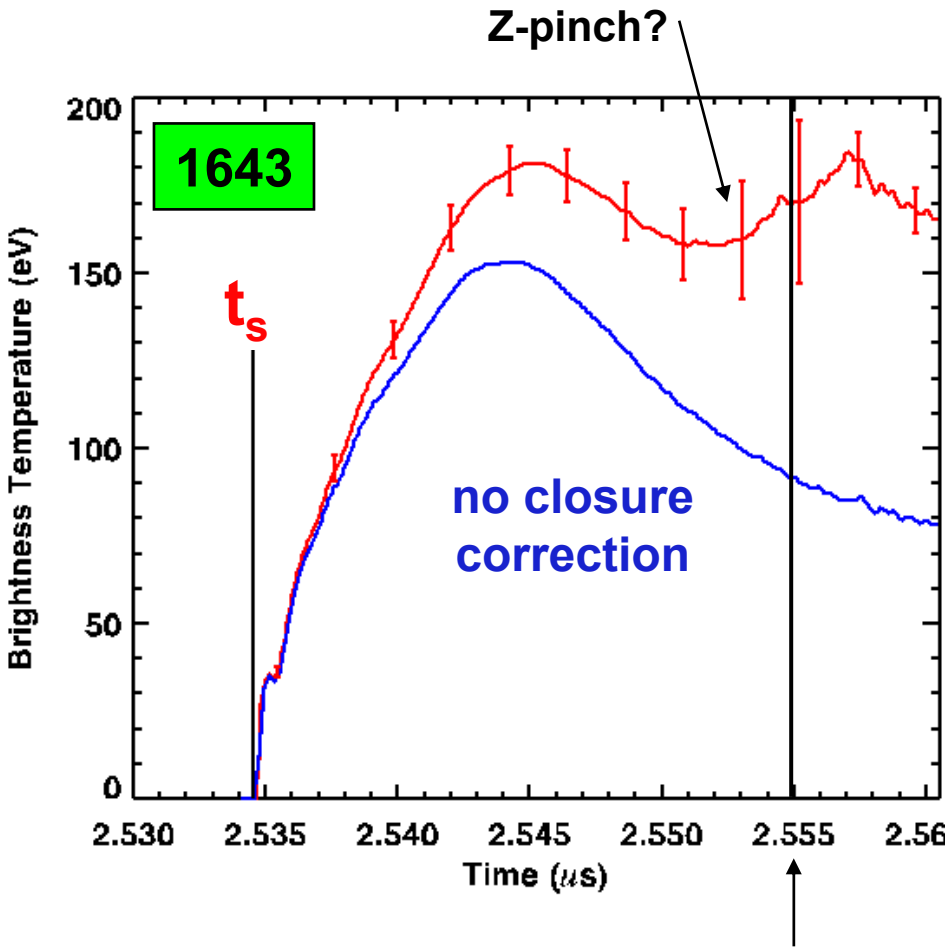

- Twall
  - at ts+10.5 ns = 181 ± 9 eV
- Error estimates at peak T (±20% in flux)
  - energy (±15%)
  - power (±4%)
  - hole closure (±12%)

The aperture closure data does not overlap the time of peak emission for 1695

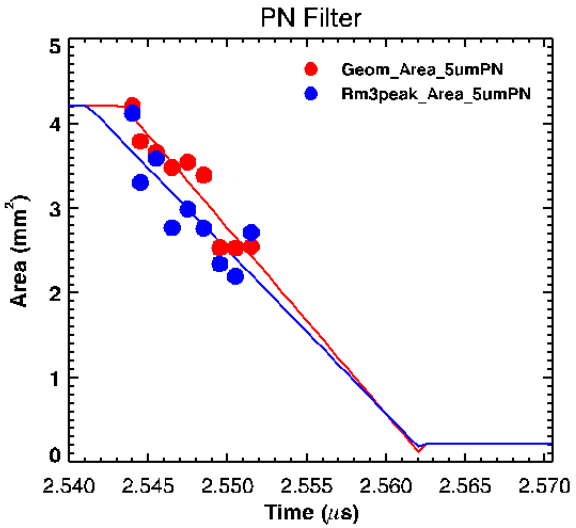

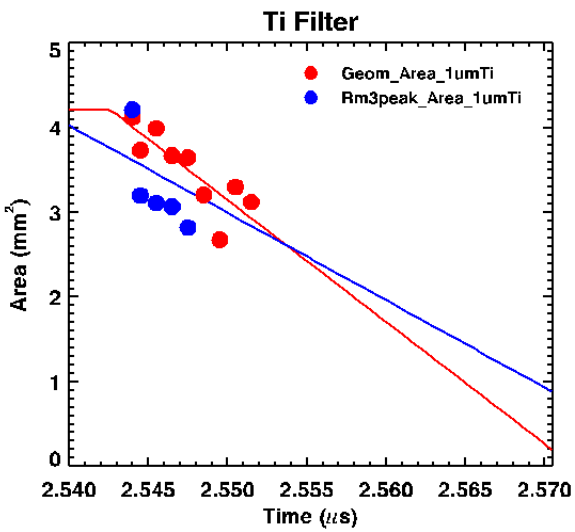

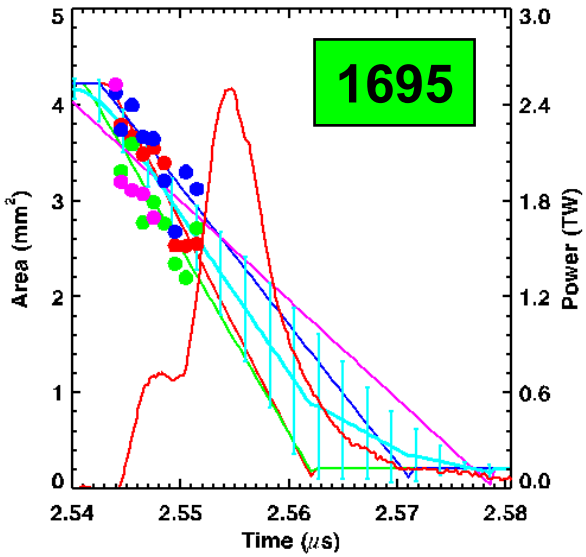

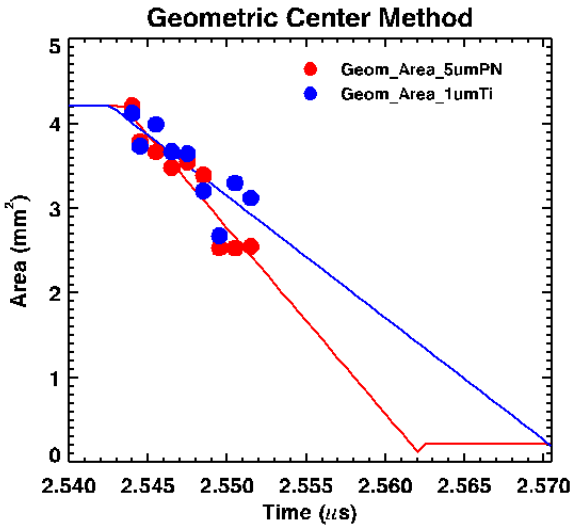

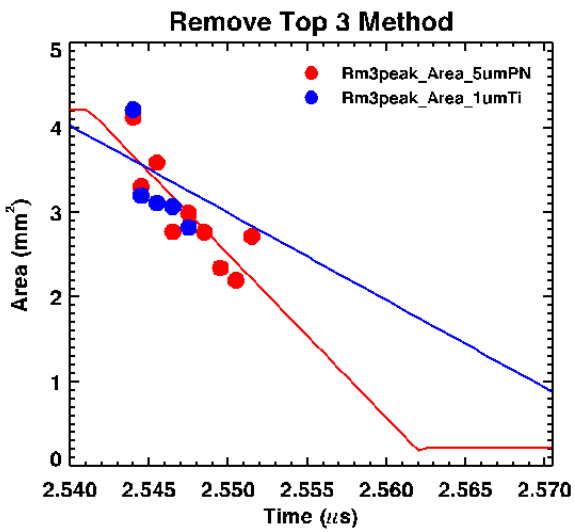

- We planned for the timing of the identical shot 1643 but the pulse came 8.3 ns later than 1643

Sandia National Laboratories

The uncertainty in aperture size at ts+10.7 ns (peak power) is ± 23% for 1695

1695

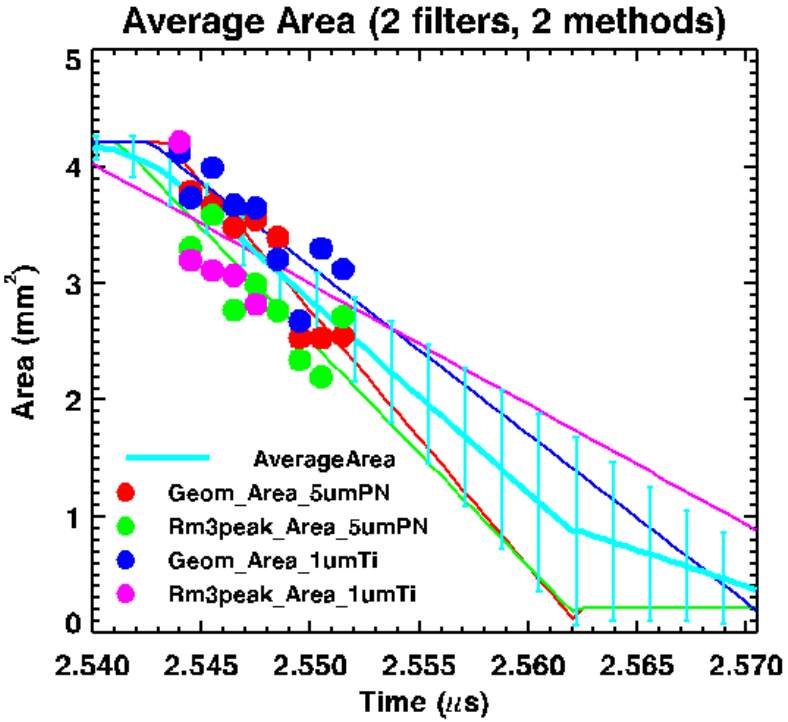

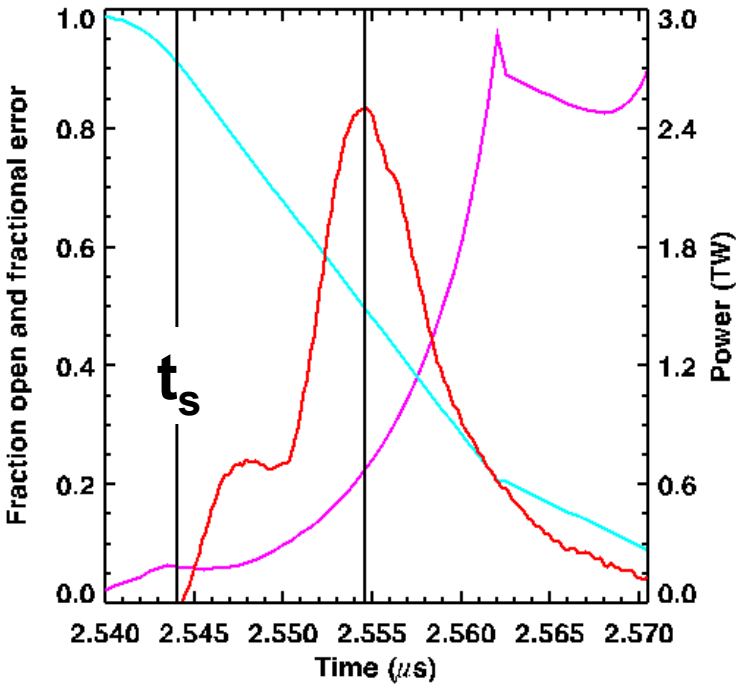

- Average closure rate is 4.2% of the initial area per ns
- Hole closure at peak based on extrapolation, thus larger uncertainty

Peak brightness temperature was 187 ± 13 eV at ts + 10.9 ns for 1695

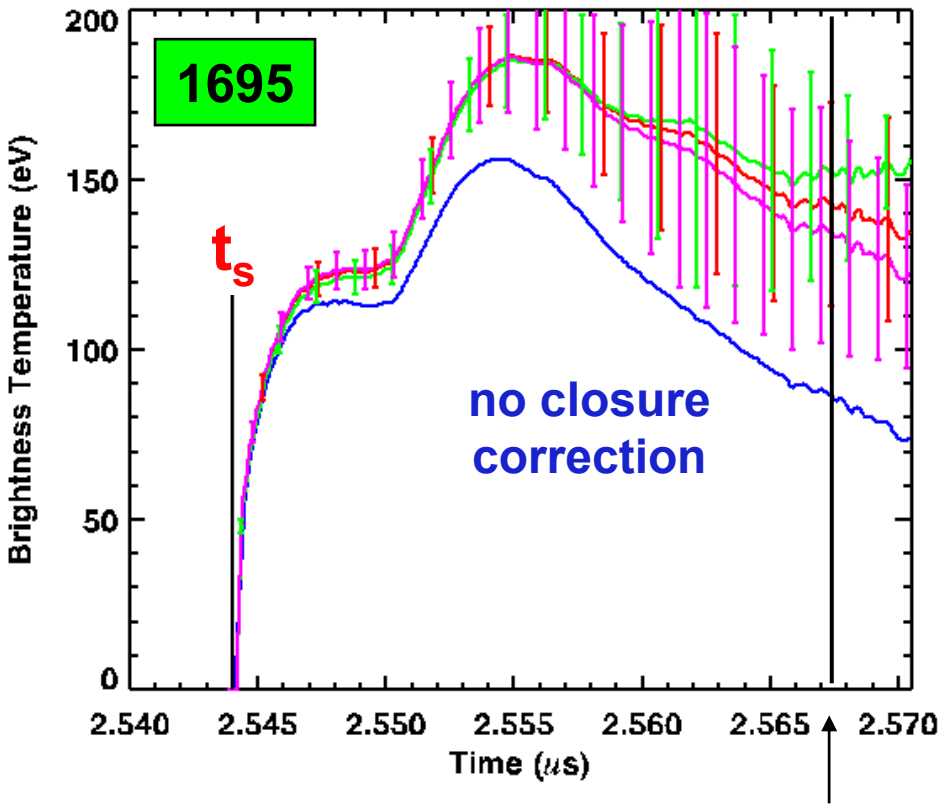

- Twall
  - at ts+8 ns = 158 ± 8 eV
  - At ts+10.9 ns = 187 ± 13 eV
- Large error in re-emission flux at t_s+10.7 ns is ±28%, because closure is extrapolated beyond end of data
  - energy (±15%)
  - power (±4%)
  - hole closure (±23%)

aperture estimated completely closed

The aperture closure data overlaps peak emission for shot 1736

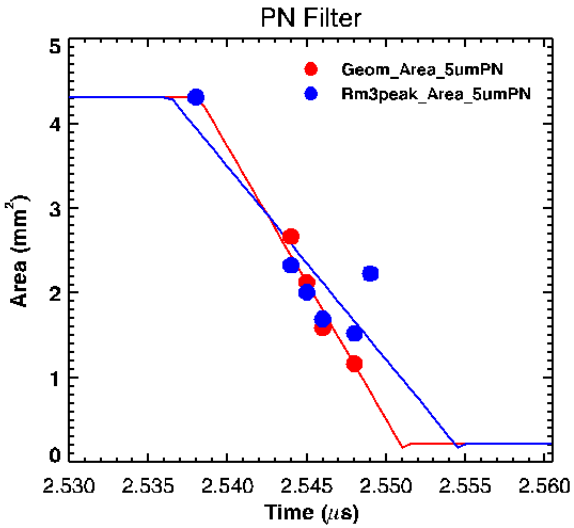

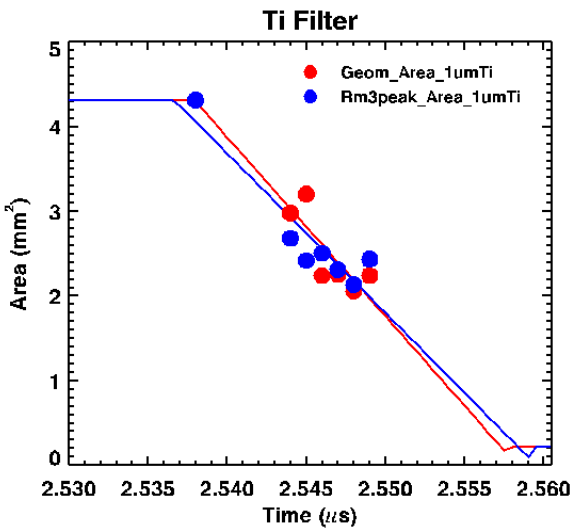

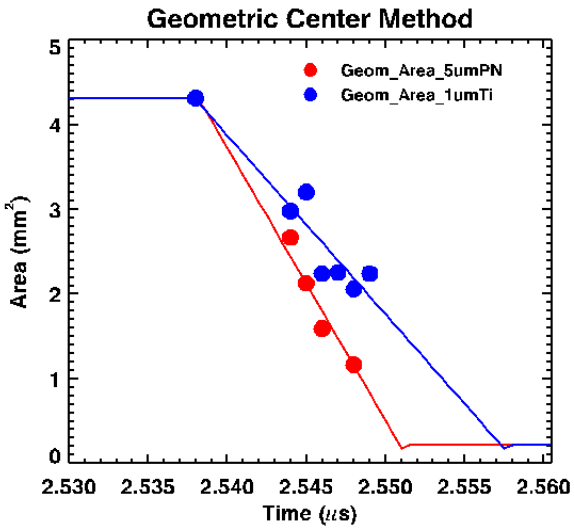

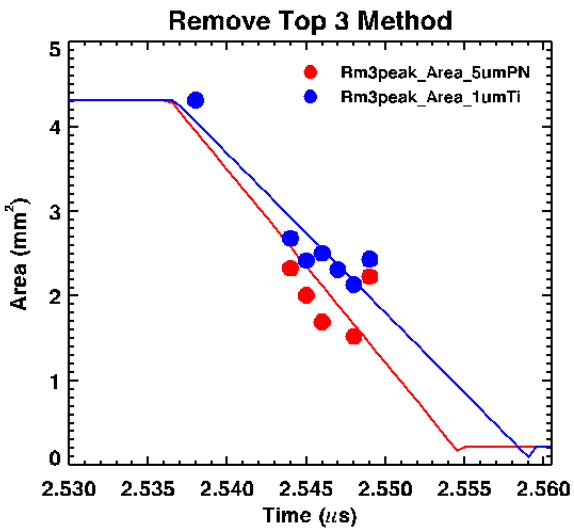

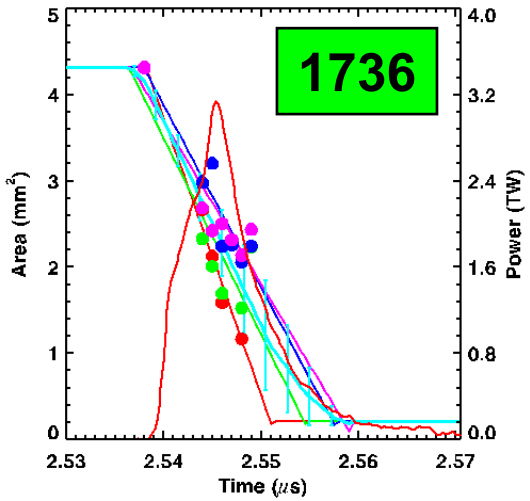

- **This is the latest we acquired closure data**

The uncertainty in aperture size at ts+7.1 ns (peak power) is ± 14% for 1736

1736

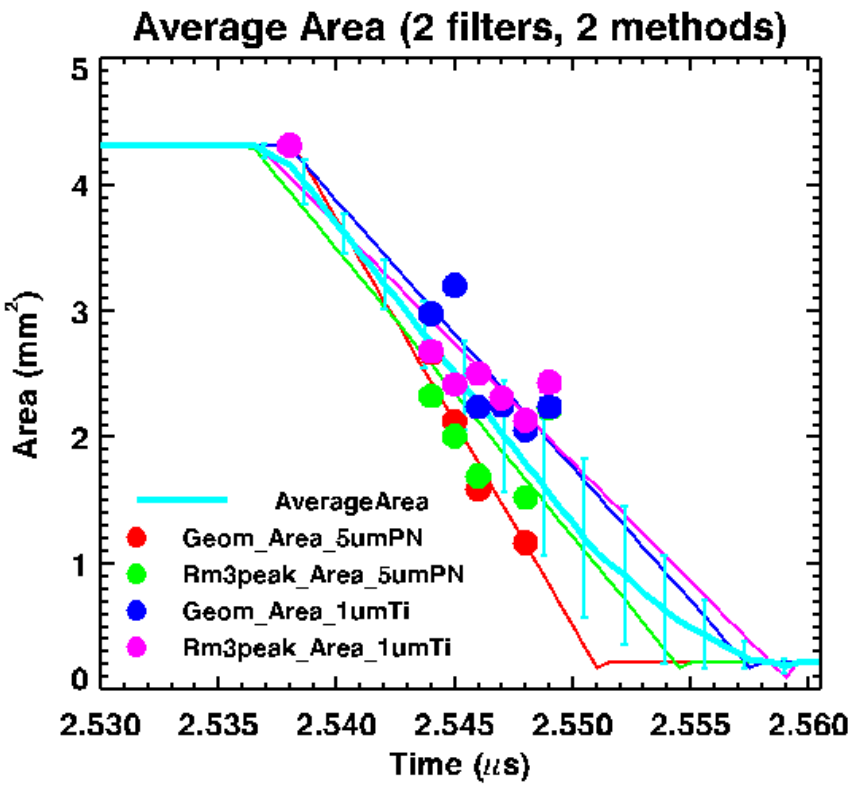

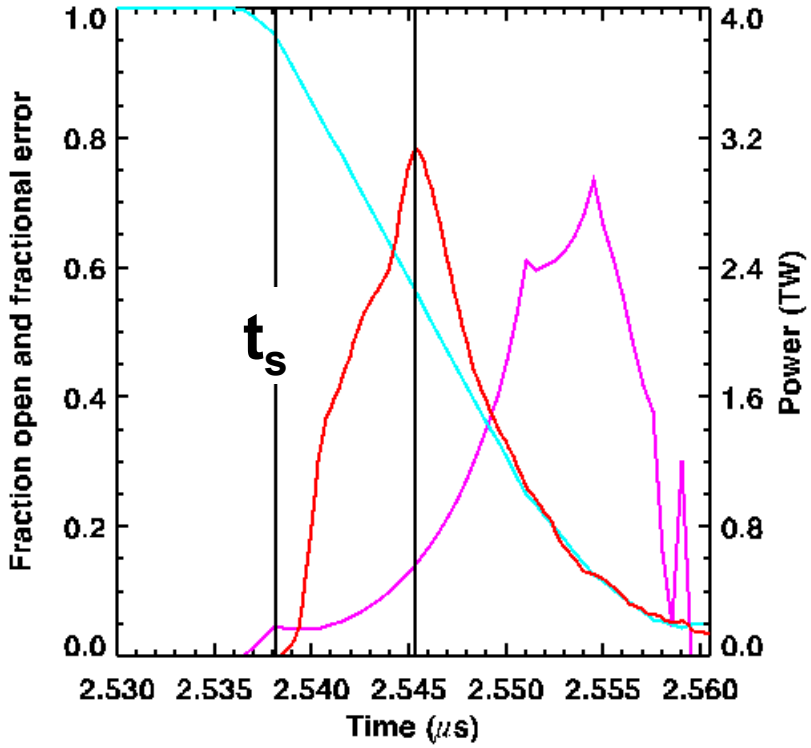

- Average closure rate is 5.4% of the initial area per ns

Peak brightness temperature was 191 ± 10 eV for 1736 at ts + 7.3 ns

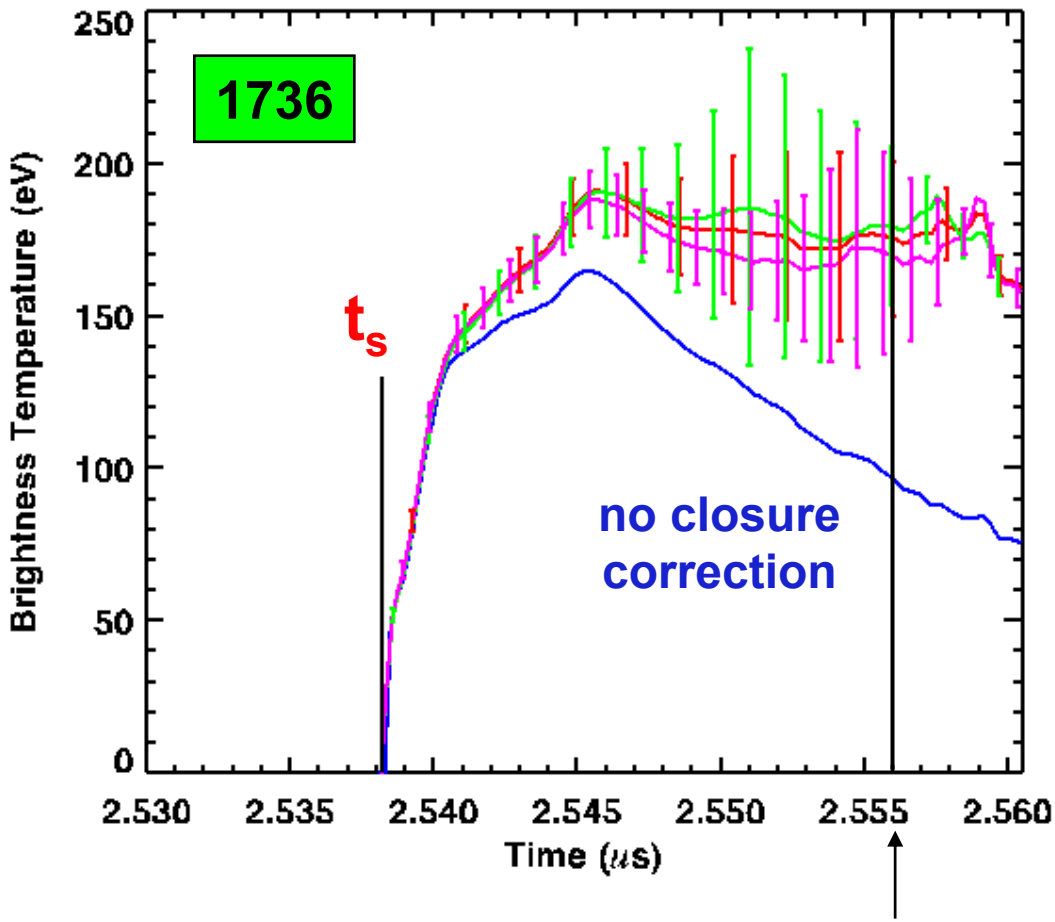

- Twall
  - at ts+5 ns = 159 ± 7 eV
  - At ts+7.3 ns = 191 ± 10 eV
- Error budget at ts+7.3
  - energy (±15%)
  - power (±4%)
  - hole closure (±14%)

aperture estimated completely closed

The aperture closure framing camera data was very weak (10x lower) on 1641 so use the measured average rate from other 4 shots

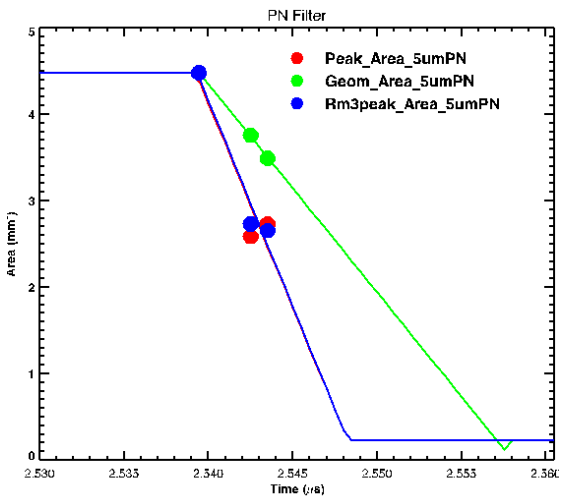

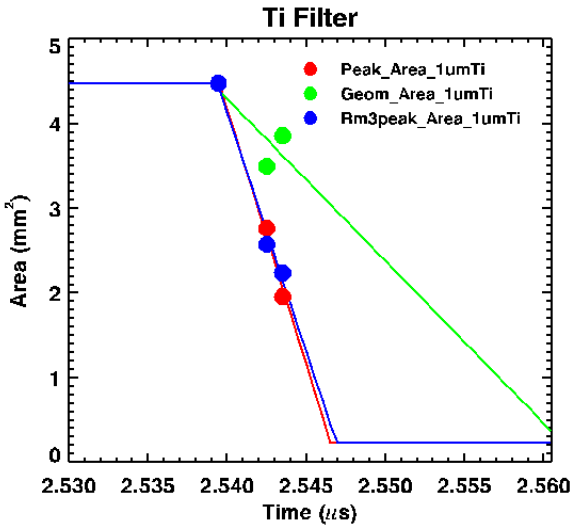

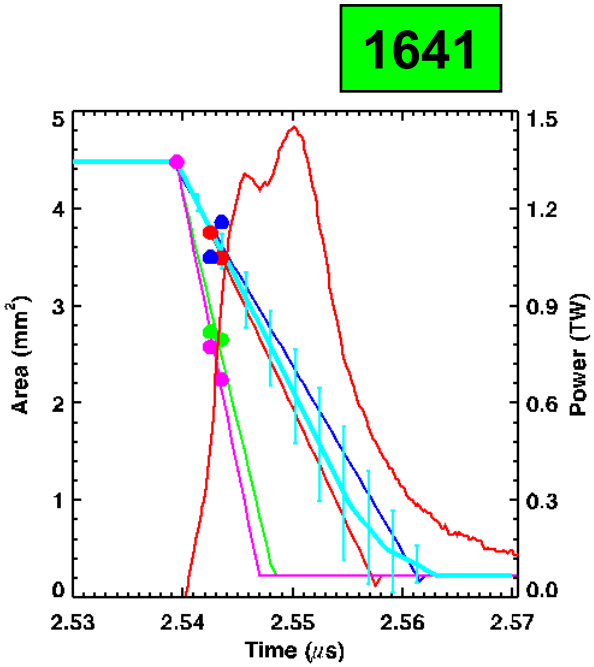

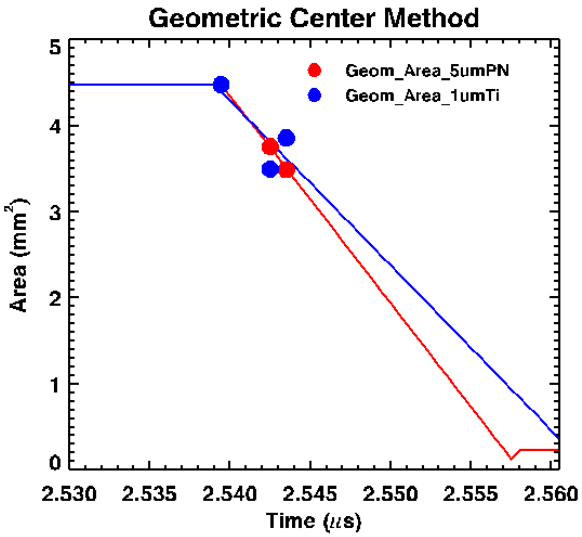

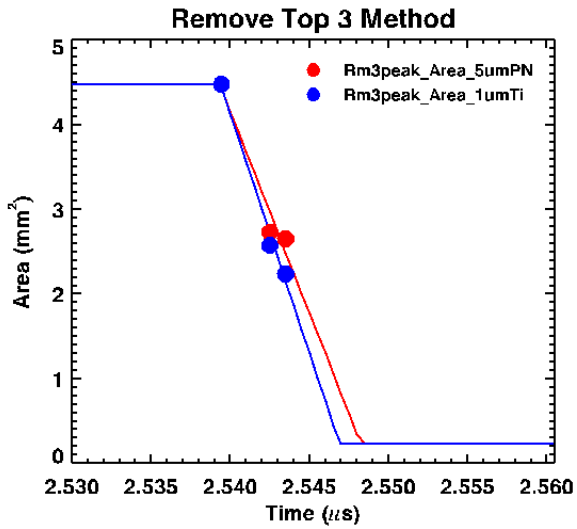

- Measured average rate (1642, 1643, 1695, 1736) is 5±1% of the initial area per ns starting at ts

Sandia National Laboratories

The uncertainty in extrapolated aperture size at ts+10.6 ns (peak power) is ± 23% for 1641

1641

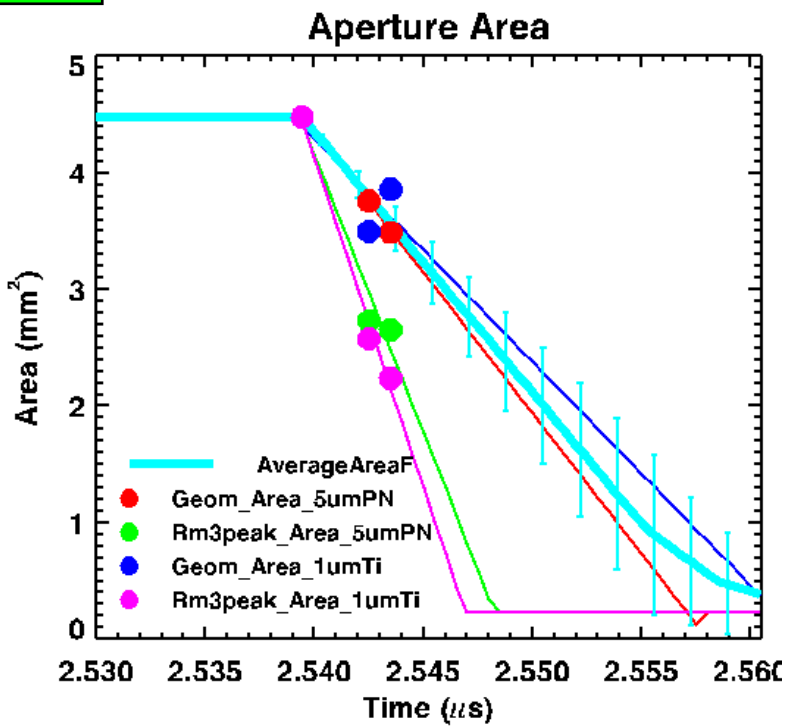

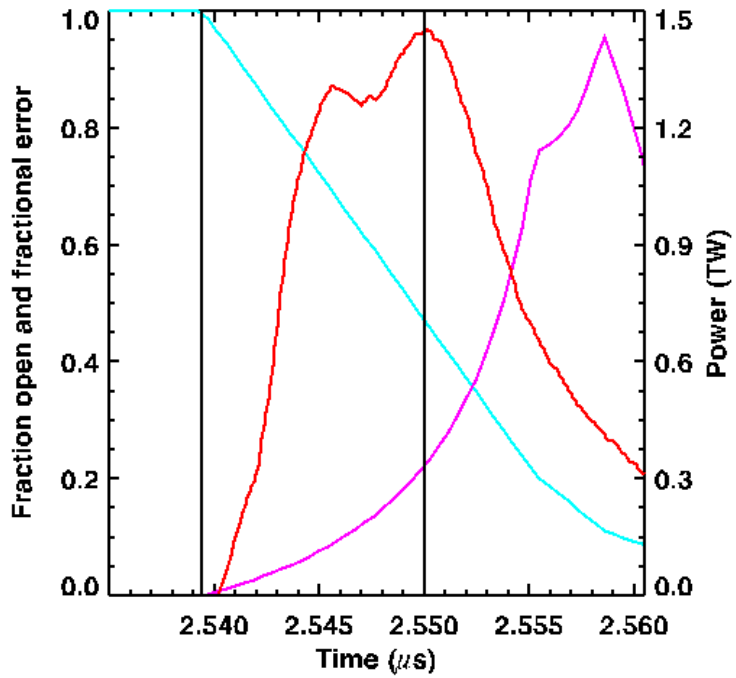

- Average closure rate is 5.0% of the initial area per ns, based on the average of 1642, 1643, 1695, 1736.
- This agrees with the geometric analysis of closure data from both filters for shot 1641

Peak brightness temperature was 157 ± 10 eV for 1641 at ts + 10.6 ns

missing one Marx bank on this shot (either early or late)

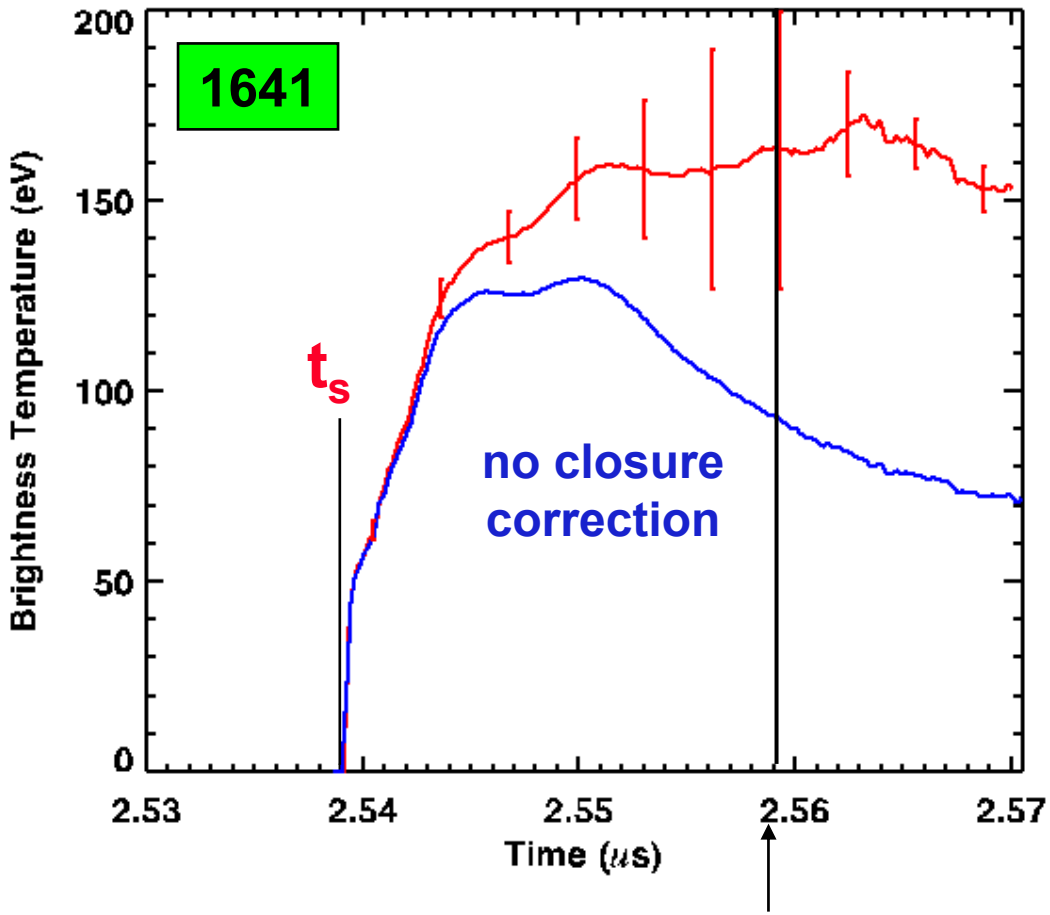

- Twall
  - at ts+6 ns = 138 ± 9 eV
  - At ts+10.6 ns = 157 ± 10 eV
- Error budget at ts+10.6
  - energy (±15%)
  - power (±4%)
  - hole closure (±23%)

aperture estimated completely closed

Structure is observed in the hohlraum *and/or* on the bottom edge of the aperture 2.3 ns after peak temperature

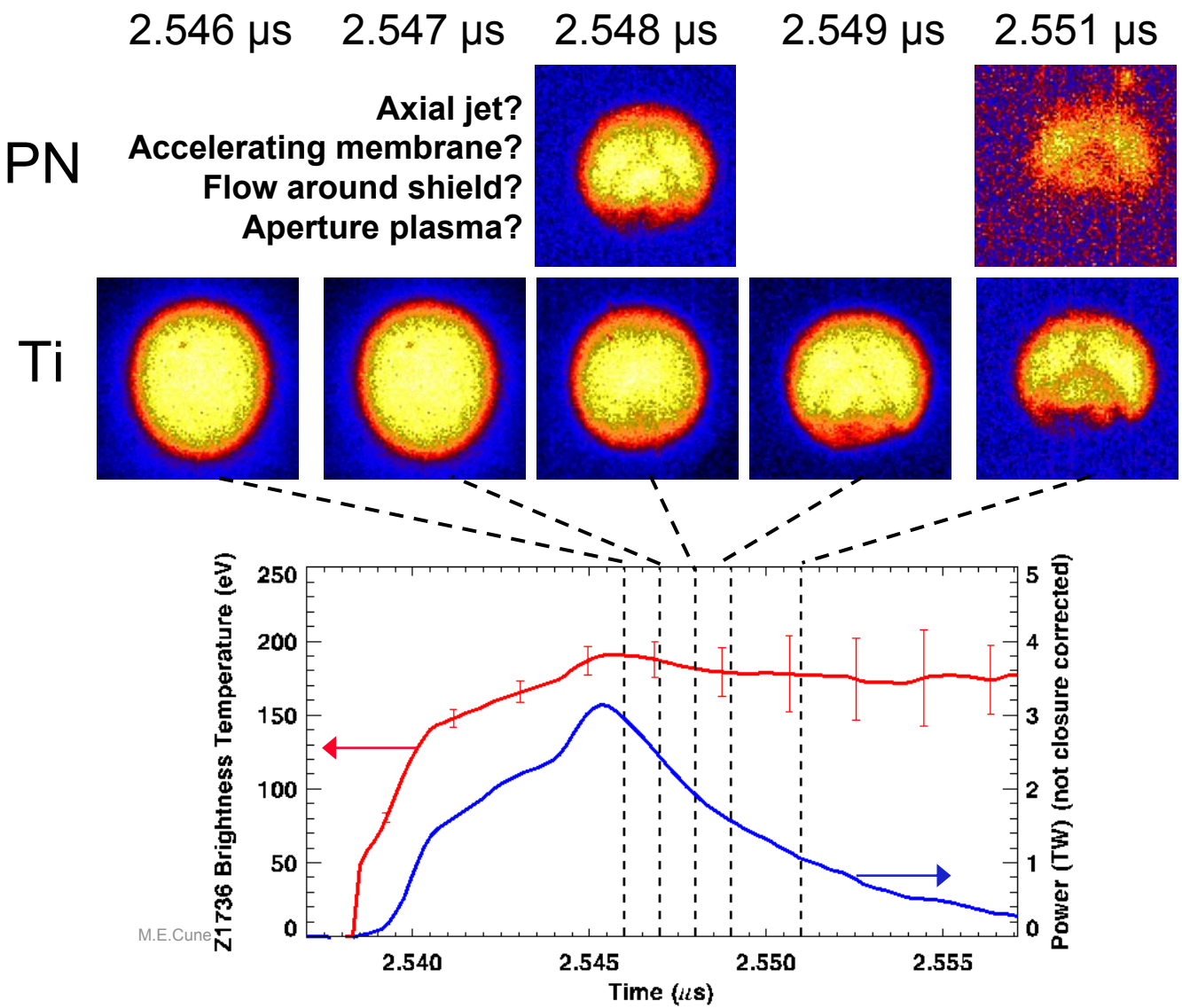

1736

- Not observed on any other shots (all SB). Last frame times:
  - 1642 (9.4 ns)
  - 1643 (13 ns)
  - 1695 (7.5 ns)
- Observed here 9.8 ns after ts
- Last frame is at ts + 12.8 ns

Sandia National Laboratories

LOS is 0.7 to 1.2 mm above the shine shield and 1.1 to 1.4 mm above the primary entrance

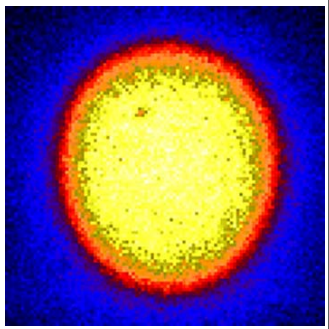

tp

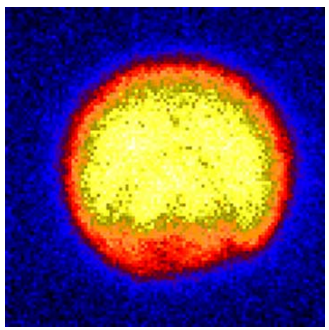

tp+3

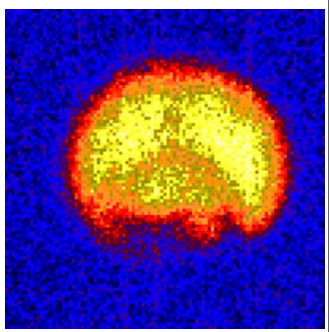

tp+5

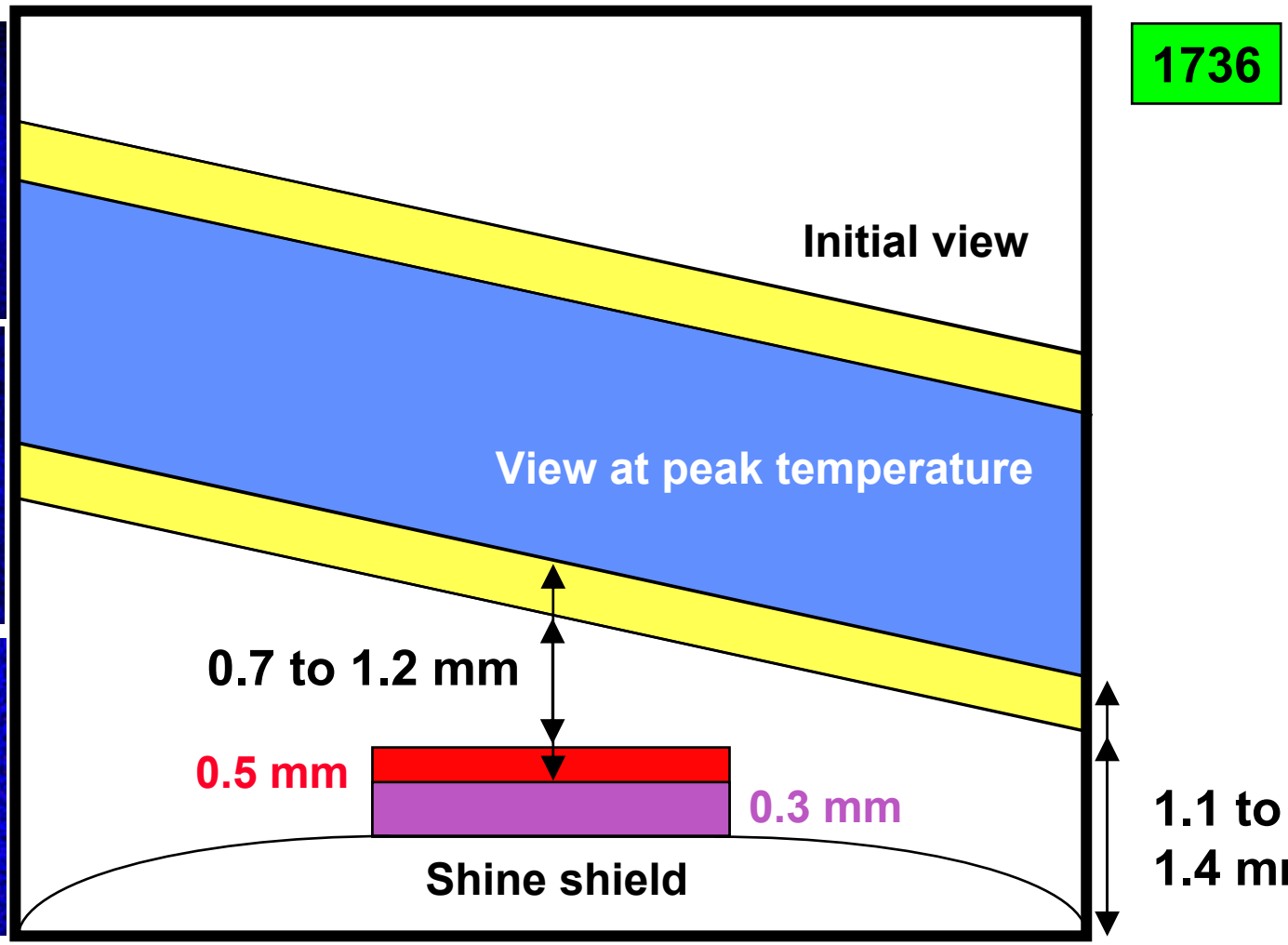

Preliminary analysis of transmission grating spectrometer on LOS 5/6 - 1

1643
Feb 2006 analysis

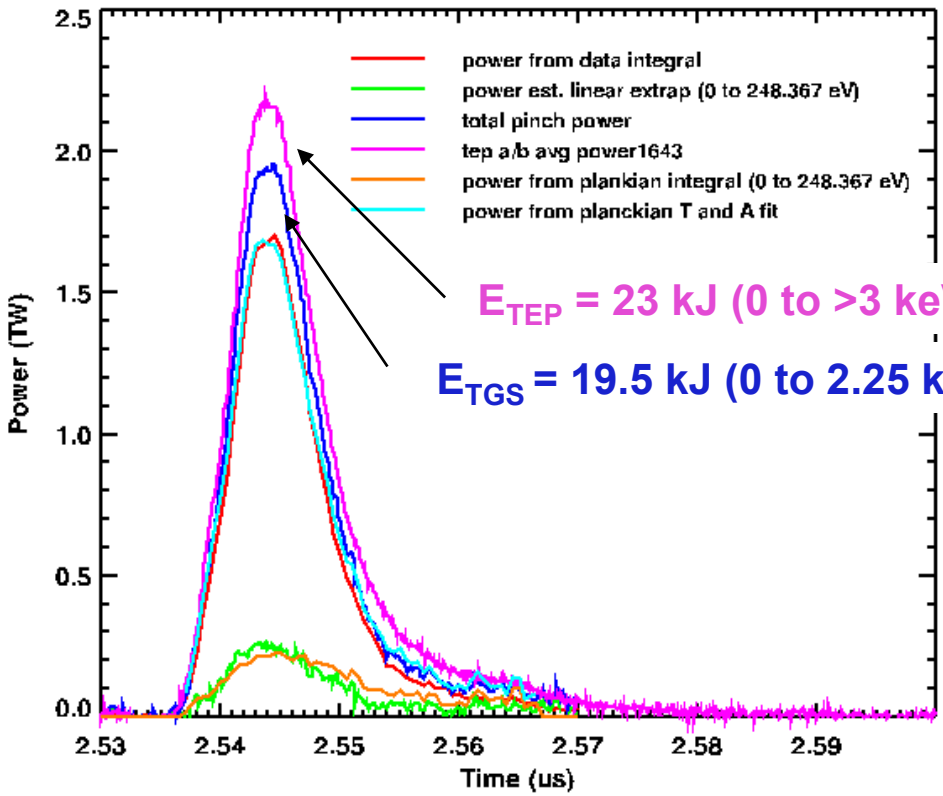

E_{TEP} = 23 kJ (0 to >3 keV?)

E_{TGS} = 19.5 kJ (0 to 2.25 keV)

- We installed a pristine calibrated grating for this shot (HS18)
- Agreement between peak powers and energy are encouraging

Preliminary analysis of transmission grating spectrometer on LOS 5/6 - 2

- Unfold method fits both temperature and area

Tpeak_fit = 148 eV
Apeak_fit = 0.03258 cm^2
(79% of initial area)

- Errors in these fits are much larger than previously obtained. This needs looking into
- A much better method might be to define the area from the hole closure measurement, and just fit for temperature. This will take some time to modify the code.
- This data requires 2-4 weeks of effort: different unfolding techniques and various cross checks to do it justice. These preliminary results were a 1 day effort.

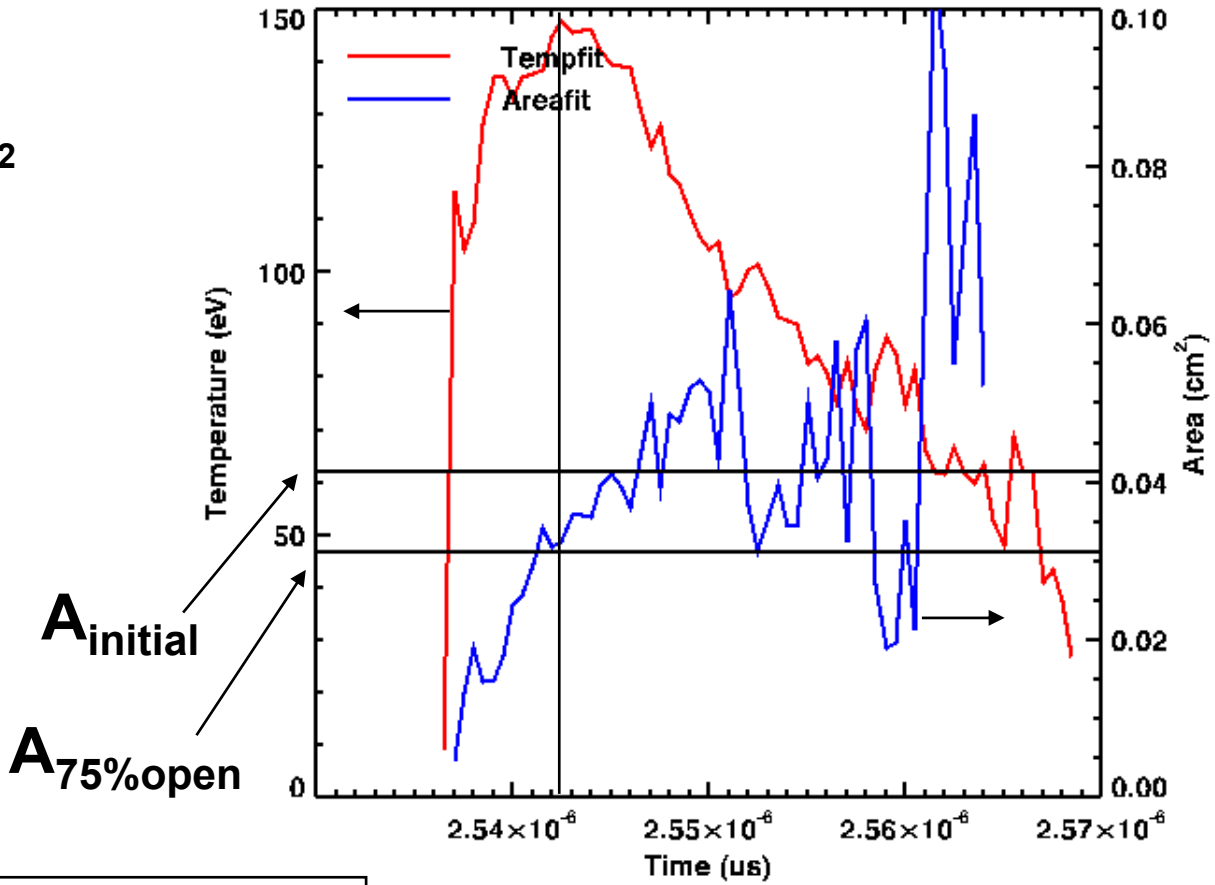

1643
Feb 2006 analysis

Preliminary analysis of transmission grating spectrometer on LOS 5/6 - 3

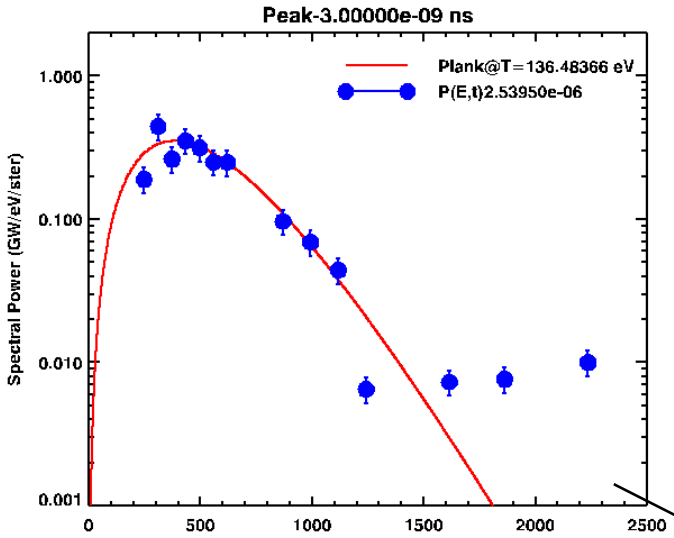

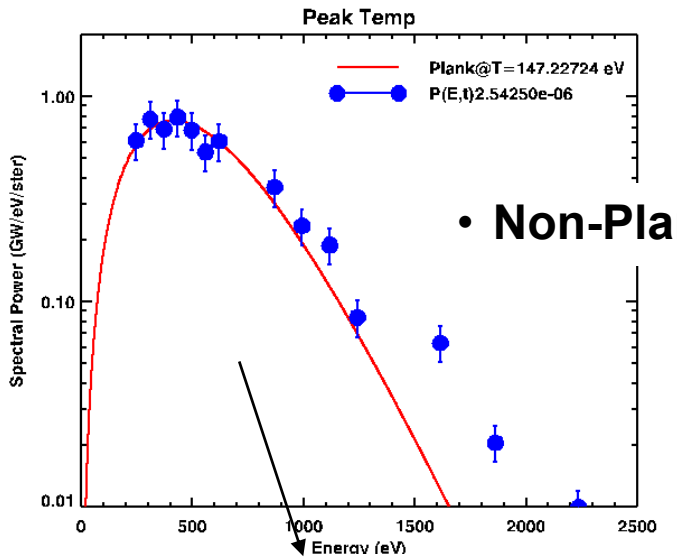

- Non-Planckian tail

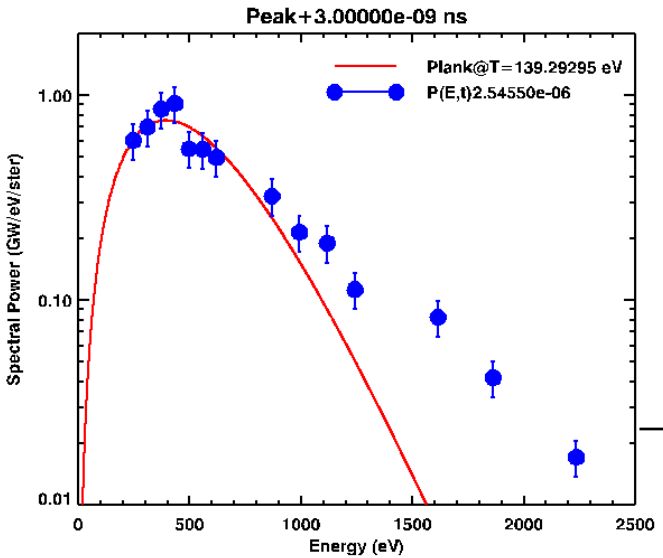

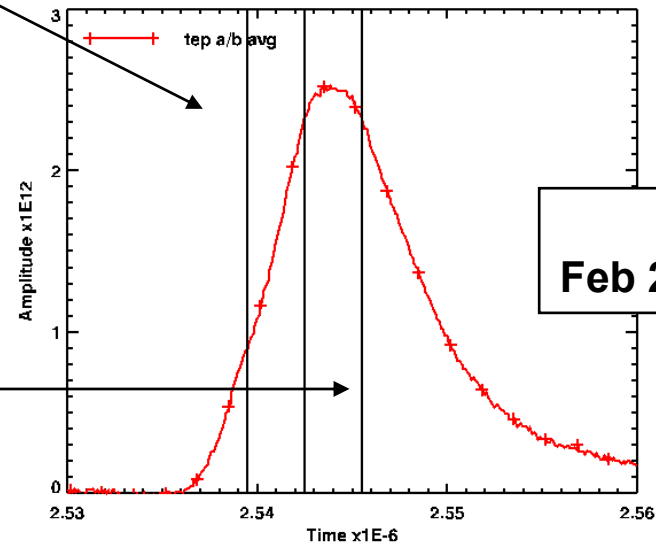

1643
Feb 2006 analysis

Sandia National Laboratories

What do simulations predict for expansion of z-pinch into secondary or through shine shield?

- As viewed from this LOS?
- For 100 μm shield?
- For 300 μm shield?
- For 500 μm shield?
- At the far wall around the membrane?

Comparison of brightness temperatures with time-dependent aperture closure

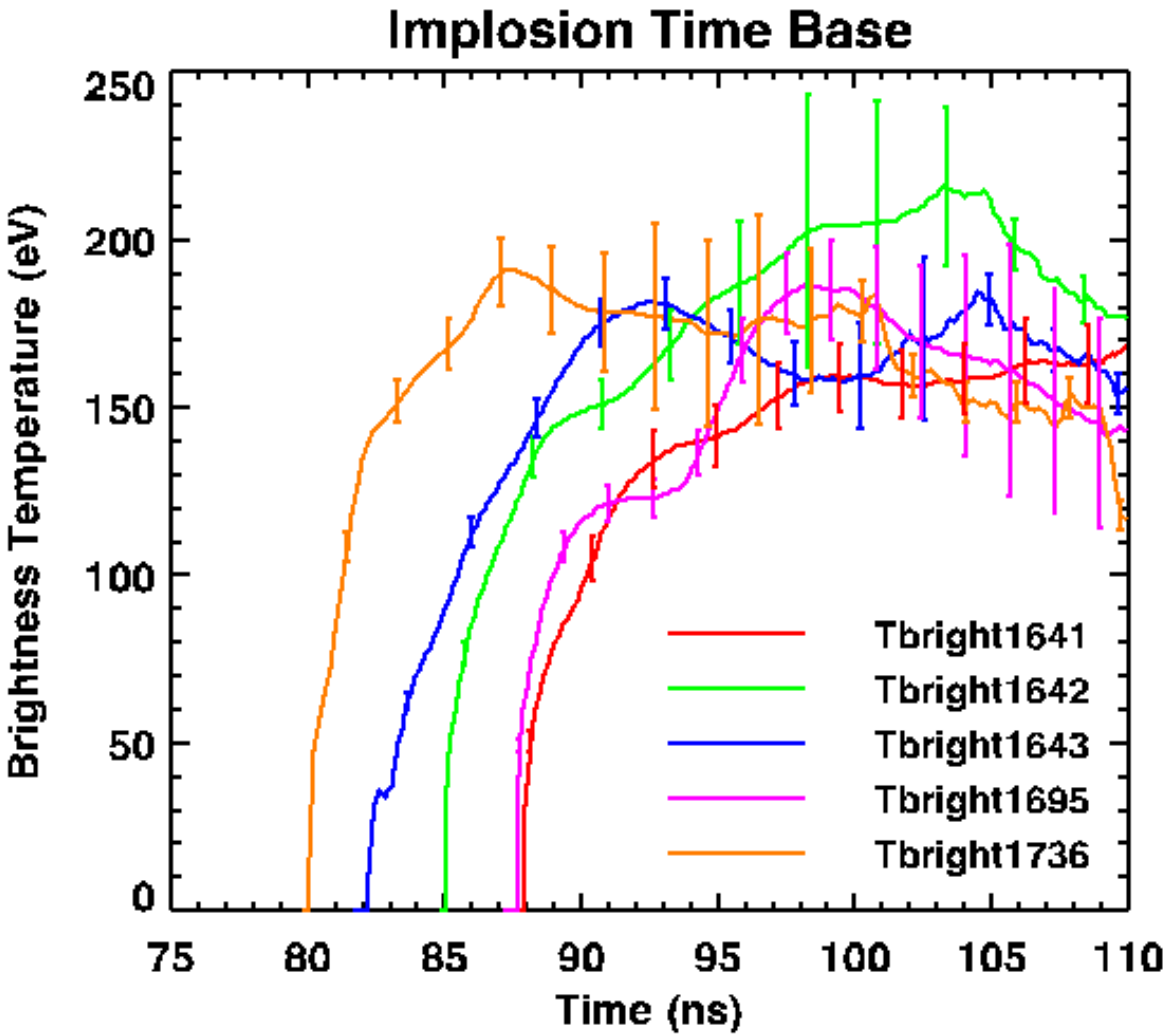

- How long does the secondary remain isolated from the pinch plasma?

There is a large shot-to-shot variation in the pulse shape

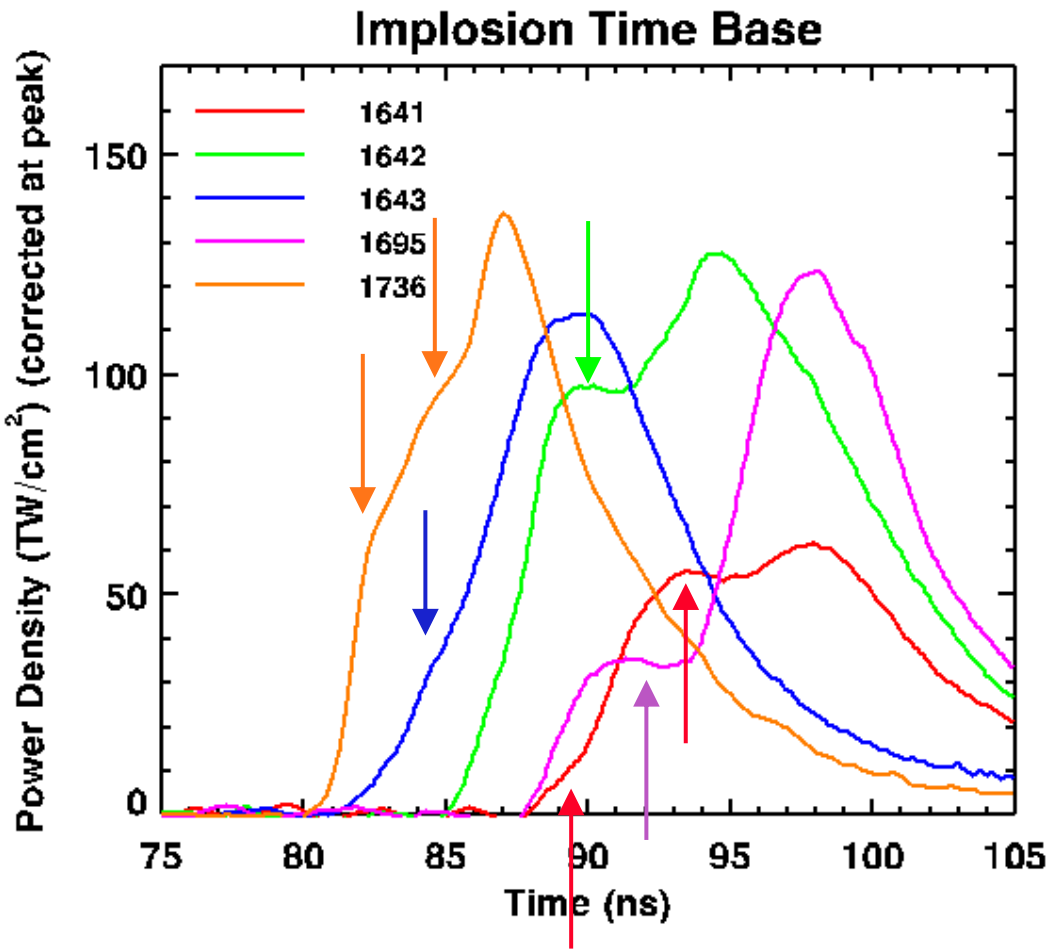

- This “foot pulse” is 130 to 150 eV
- Surprising variation between 10 and 12 psi
- Significant shot-to-shot variation of pulse shape, implosion time, and detailed structure during the rise.
- LOS difference between 1643 and the others is unlikely to be the cause
- Weak correlation of implosion time with mass
- This structure may result from variations in load dynamics

The Z accelerator has a comprehensive set of electrical monitors

W. A. Stygar et al., 11th Pulsed Power Conference
W. A. Stygar, et al., 11th Pulsed Power Conference
P. A. Corcoran, et al., 11th Pulsed Power Conference
W. A. Stygar et al., to be published

Z Equivalent Circuit Model

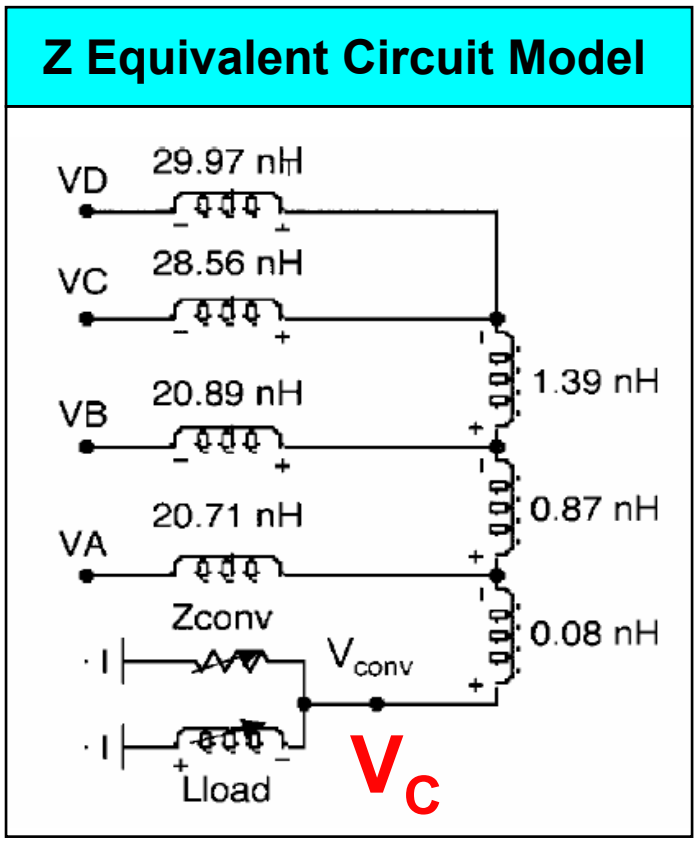

E. M. Waisman et al., Phys. Plasmas, 11, 2009 (2004)

$$V_C = \sum_k \alpha_k V_k - L_e \frac{dI_M}{dt}$$

$$\alpha_k = [0.306, 0.291, 0.206, 0.197]$$

$$L_e = 6.84 \text{ nH}$$

- The inductances have ± 5% 1σ random and systematic errors
- The voltage, stack current, MITL current have 1σ random ad systematic errors of ± 7%.
- 12 Stack Bdots, 24 Stack Vdots
- 12 (to 24) MITL Bdots
- Circuit model and monitors checked with an independent inductive wire probe to measure convolute voltage V_C

The load Bdots require a decrease of 0% to 10% to match the Z Idot measured on 36 other monitors

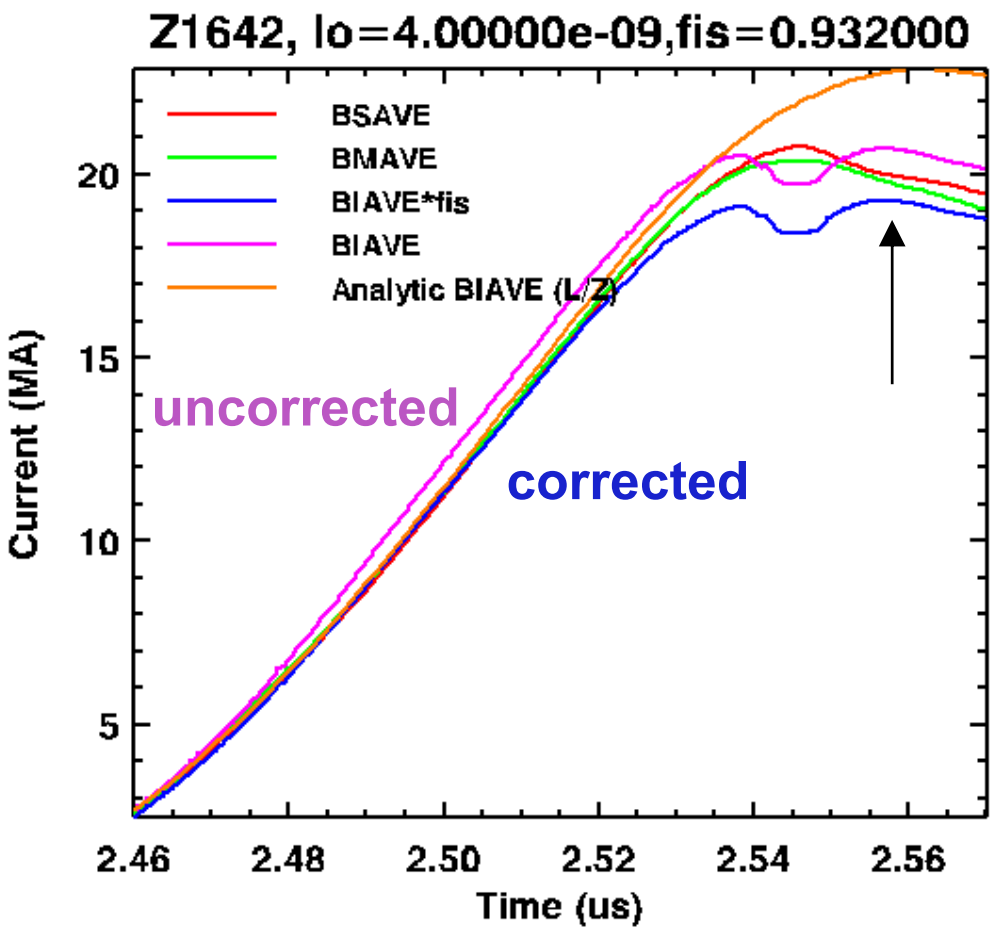

This is likely due to inadequate and variable rejection of common mode noise

There are only 2 to 4 load Bdots

On this shot we reduced the load Bdot by 7.8%

The load dI/dt now agrees with

- the avg. stack current
- the avg. MITL current
- an analytic load current for fixed L/Z calculated with the measured forward going voltage

$$I_{LA}(t) = e^{-(tZ/L)} \int_{t_o}^{t} dx V_{OC}(x) e^{(xZ/L)} / L$$

All four Bdots consistently show the jump of current after peak current

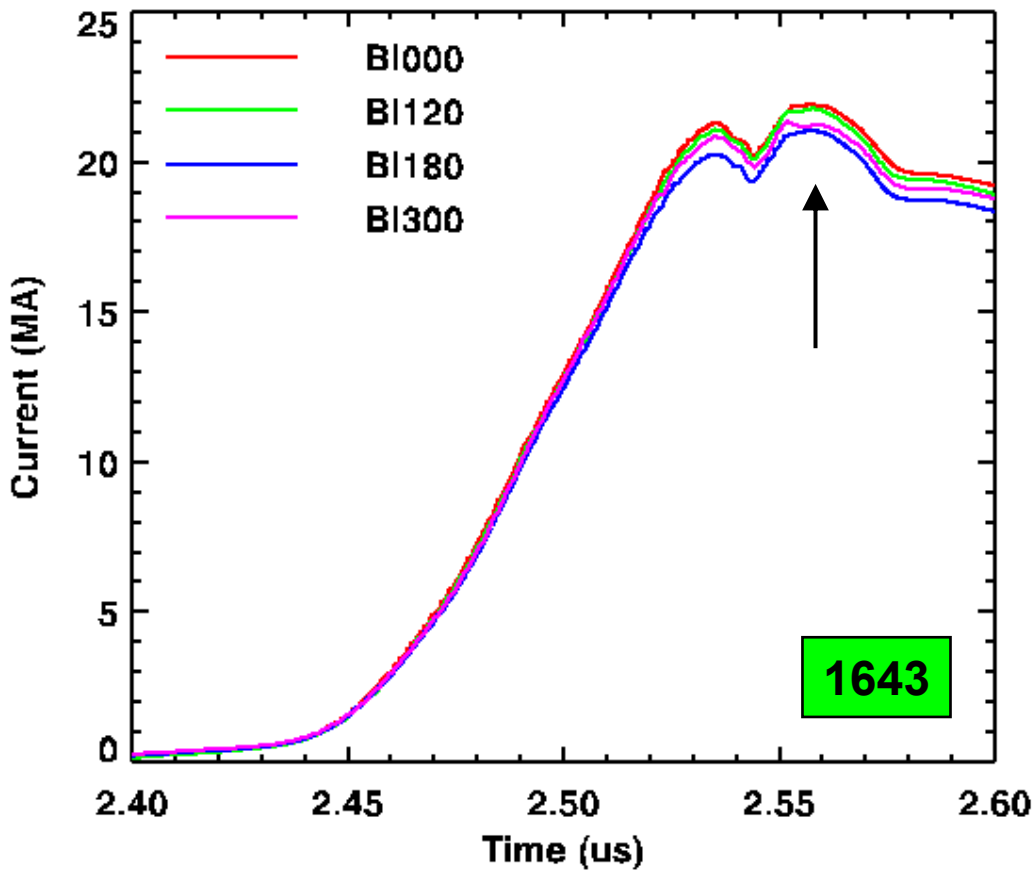

Vacuum gaps of 1 to 2 mm short on the timescale of the current pulse with peak magnetic pressure of 0.2 - 0.5 MBar

W. A. Stygar et al., Phys.Rev. E,69, 046403 (2004)

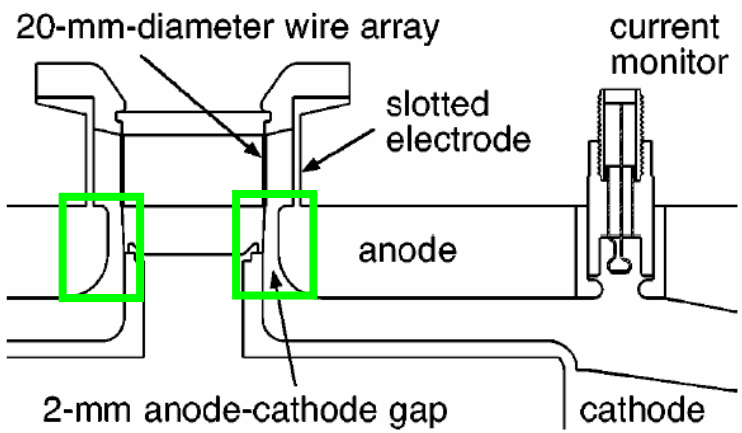

- **Small magnetically-insulated gaps that are initially bridged by material may also show these effects**
- **Wire arrays have higher ΔL and voltages, higher total soft and hard x-ray powers and yields and faster risetimes**

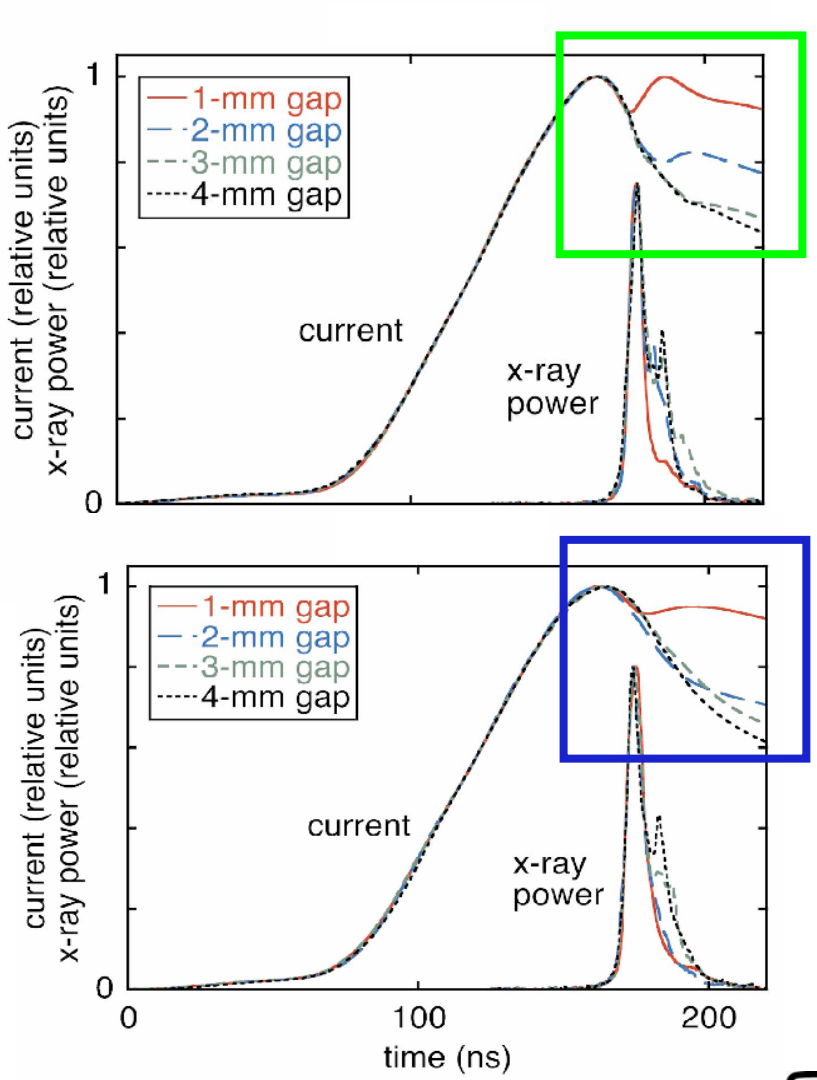

The entire set of electrical data* is systematically consistent to within ±10% with the initial load inductance

*with the load Bdot correction

$$V_C = V_S - L_e \frac{dI_M}{dt} = \frac{d}{dt}\left(L_L(t) I_L(t)\right)$$

$$V_{CO} = L_o \frac{dI_L}{dt}$$

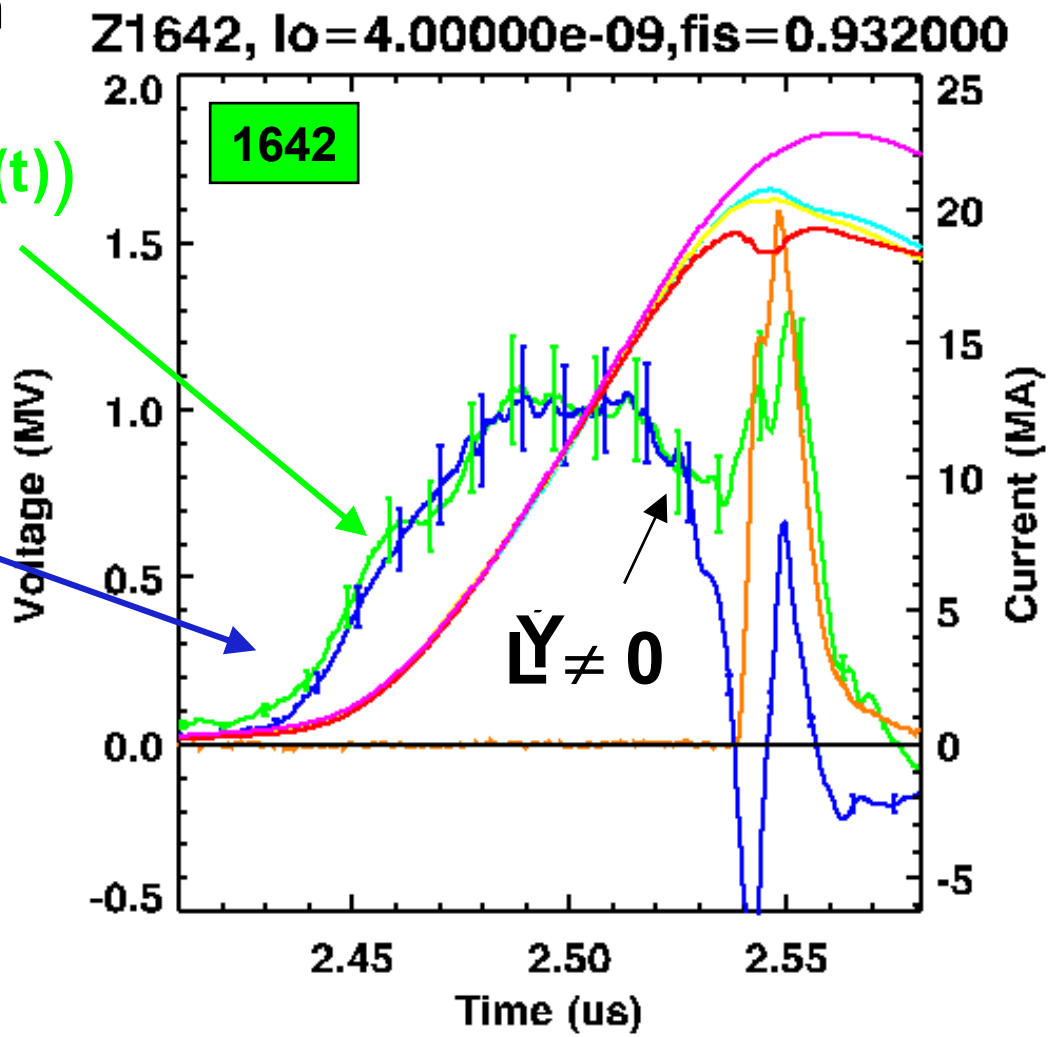

- The load voltage is the difference V_C - V_{CO}
- dL/dt changes late into the pulse

Similar agreement is obtained for the other 4 experiments

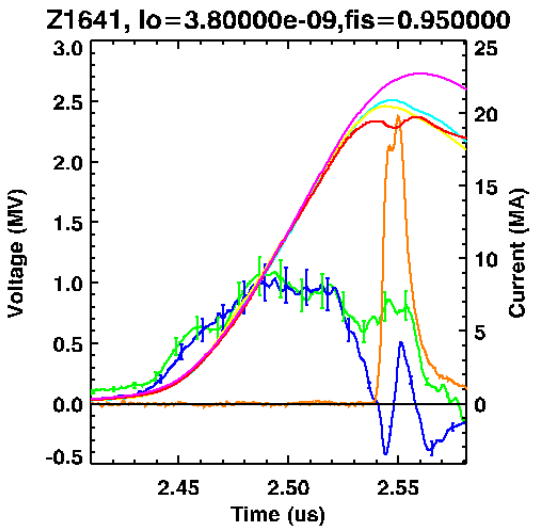

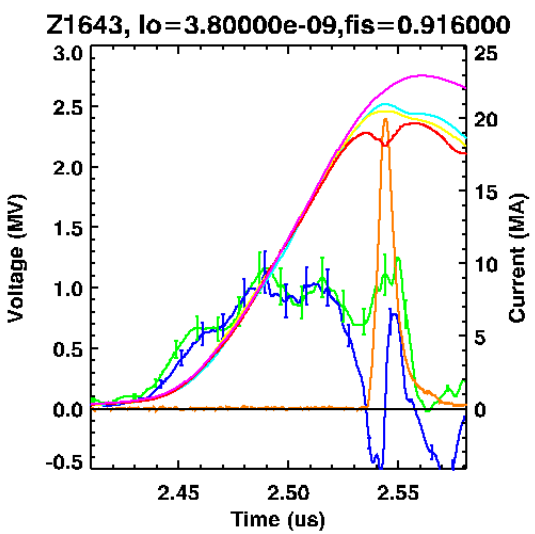

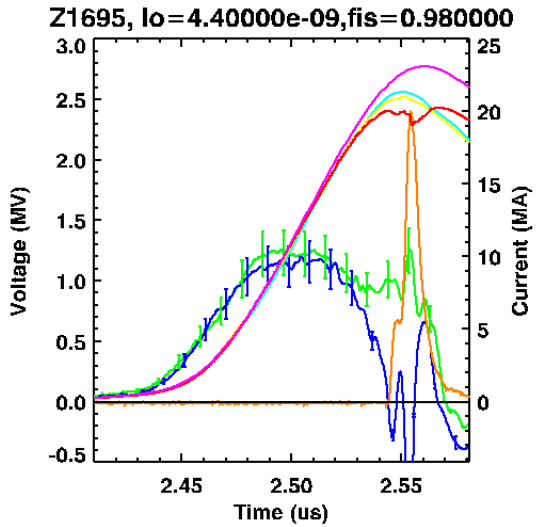

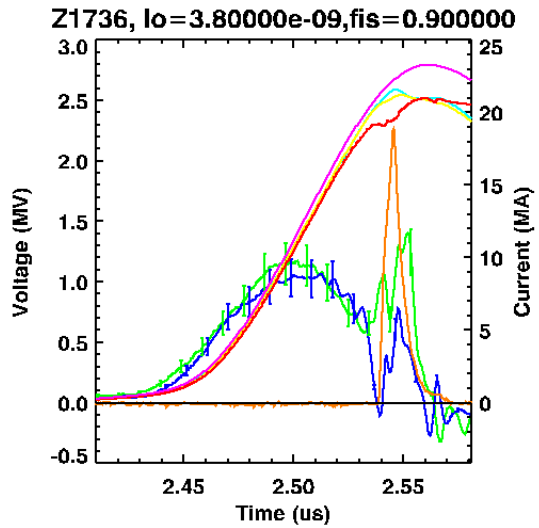

- **The average BIAVE correction for the 5 shots is <fis> = 0.94 ± 0.03**

The load voltage peaks and falls during the rising portion of the hohlraum power pulse

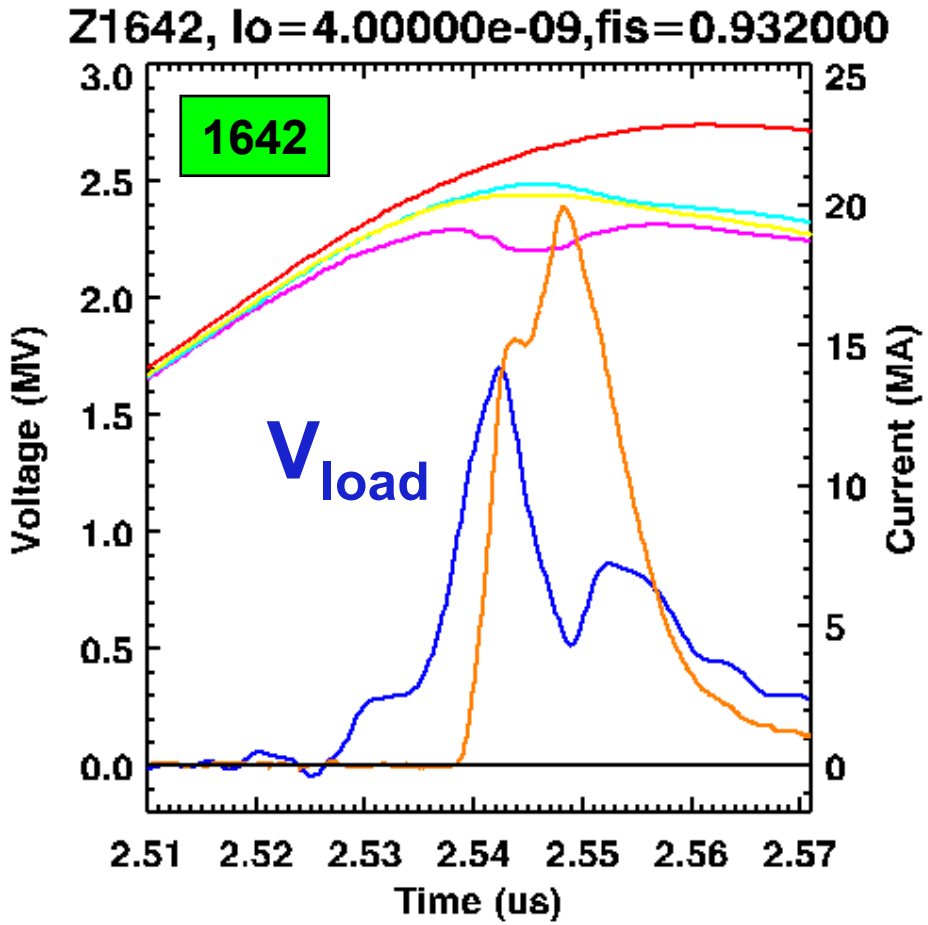

- Here the peak voltage of 1.7 MV is reached only 3.8 ns after the power pulse begins to increase
- This occurs on all five of shots

The electrical data is consistent with rapid decrease of the L-dot of the implosion near stagnation

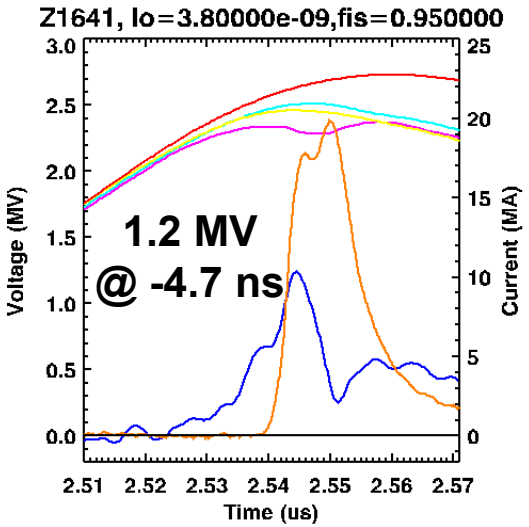

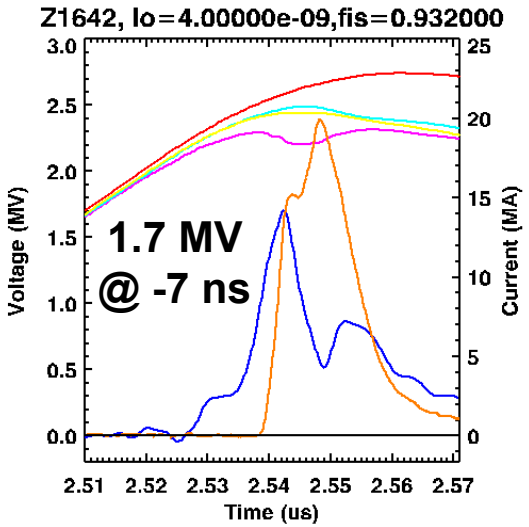

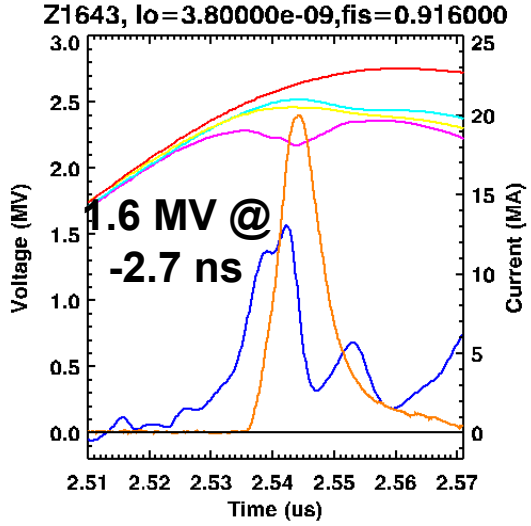

- Gap shorting?
- Implosion of trailing mass and current?
- Material back-pressure at stagnation?
- A bounce?

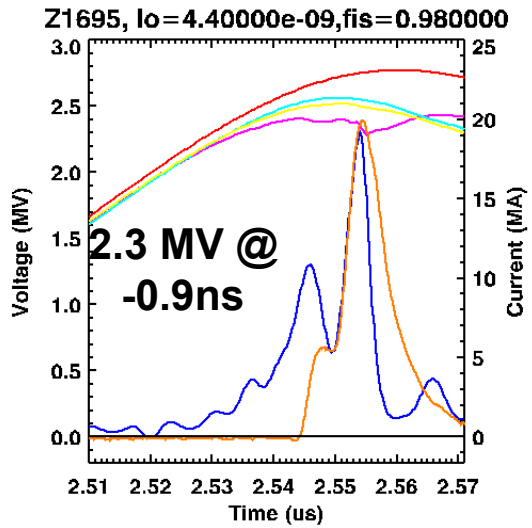

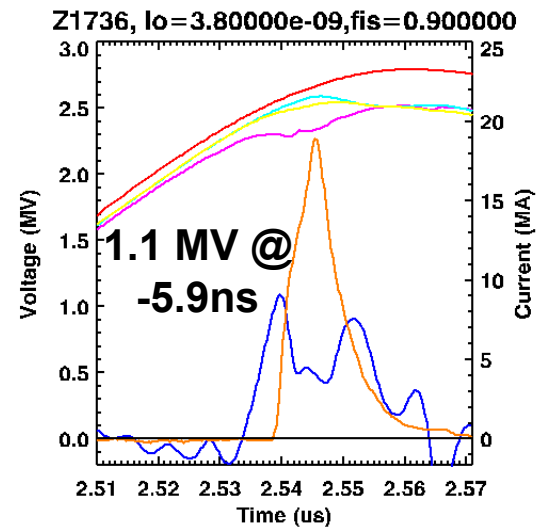

The electrical energy delivered to the load is ~300 kJ at peak temperature

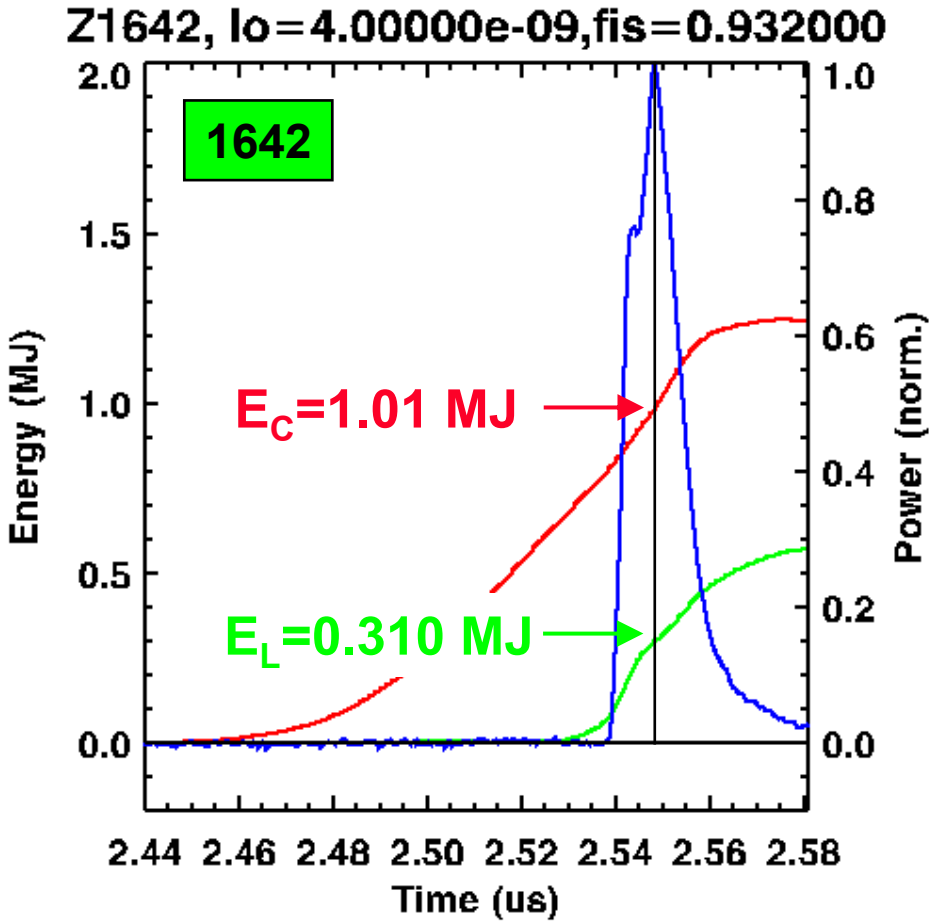

- For all five shots at peak secondary temperature:
  - $\langle E_C \rangle$ = 1.01 ± 0.15 MJ
  - $\langle E_L \rangle$ = 0.31 ± 0.08 MJ
- We should be able to increase this efficiency
  - L_O = 4, ΔL ~ 1, $\Delta L/L_O$ = 0.25 ~ E_L/E_C ~ 0.31
  - L_O = 2, ΔL ~ 1, $\Delta L/L_O$ = 0.5, E_L ~ 0.5 MJ

The other shots are similar

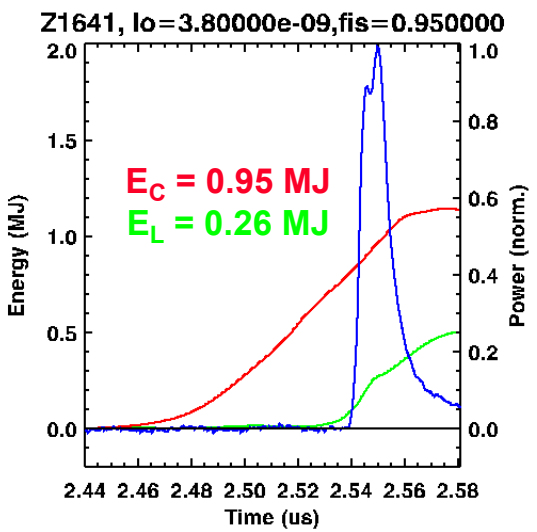

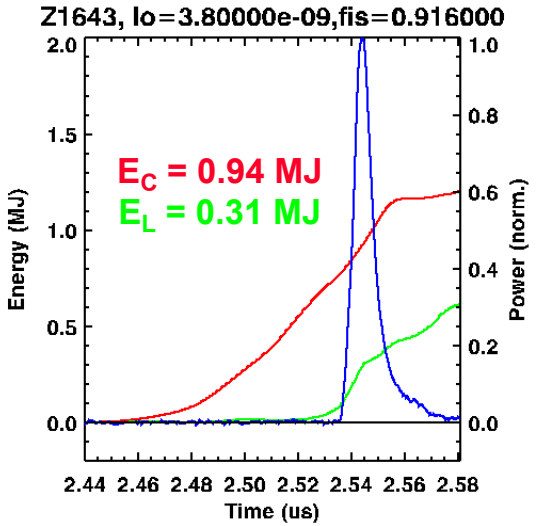

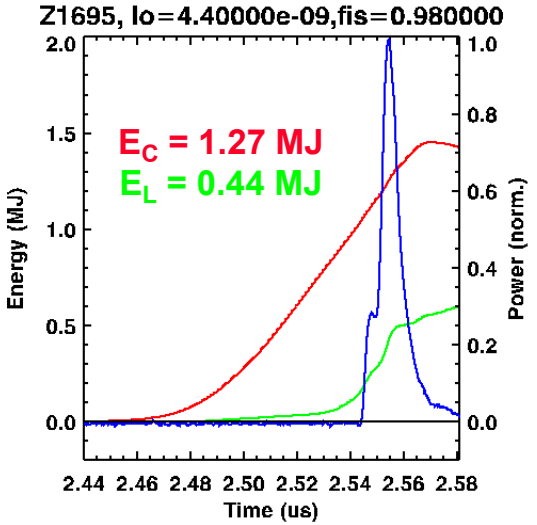

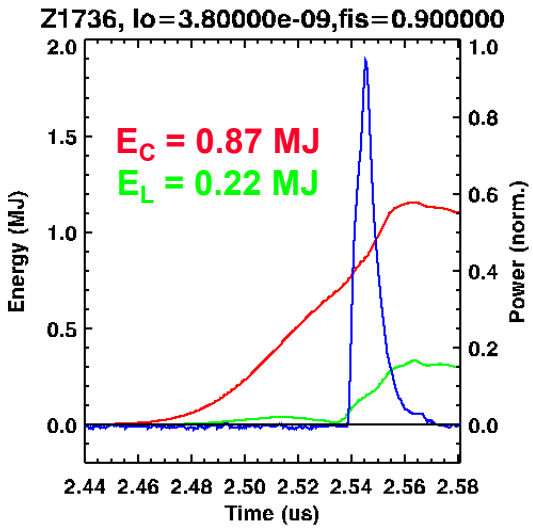

We calculate the load inductance

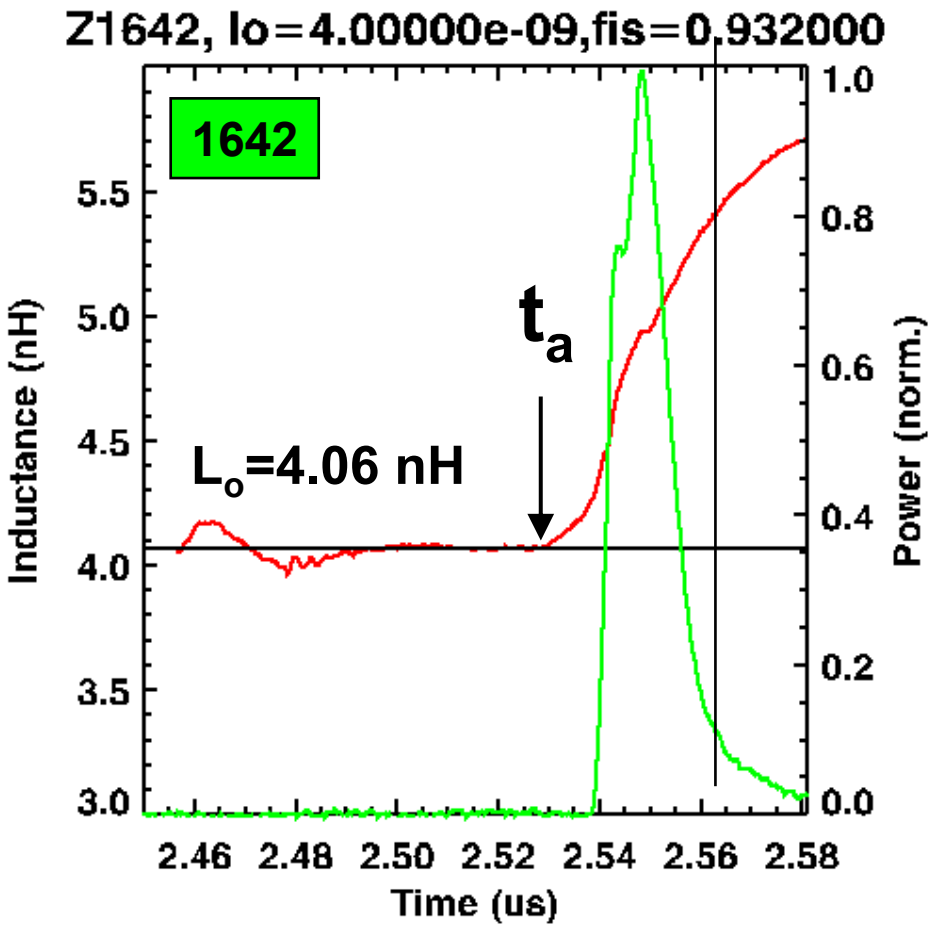

E. M. Waisman et al., Phys. Plasmas, 11, 2009 (2004)

$$L_L(t) = \left(\sum_k \alpha_k \phi_k + \phi_o - L_e I_M \right) \Big/ I_L$$

$$\phi_k = \int_{t_o}^{t} V_k$$

$$\phi_o = L_e I_M(t_o) + L_L(t_o) I_L(t_o)$$

- $\Delta L \sim 1$ nH by the time of peak hohlraum temperature
- The load rapidly accelerates at 74 ns into the current pulse

Similar agreement is obtained for the other four experiments

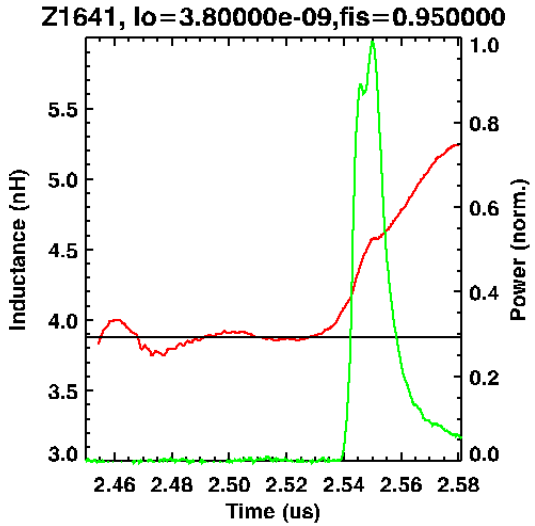

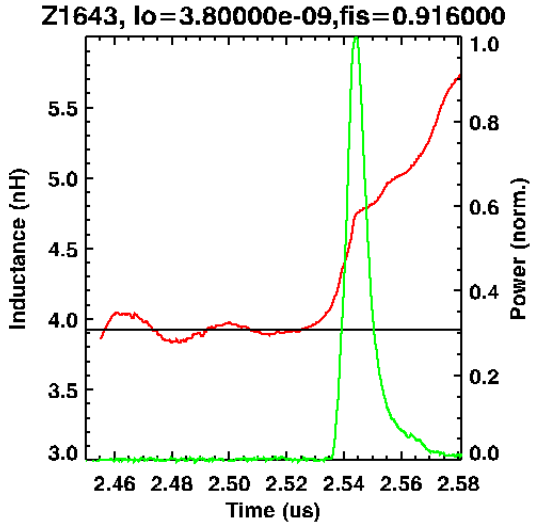

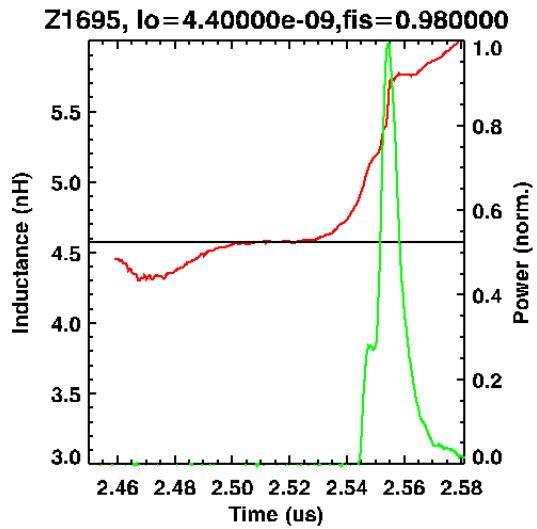

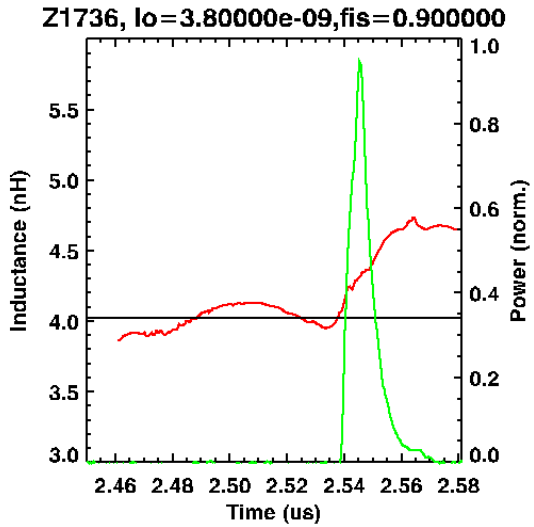

- Agreement is poorer for 1695 and 1736
- The electrical data from five shots is consistent with L_o = 4.1 ± 0.3 nH within 2.5% of the initial 4 nH geometric inductance
- In a sense this is an in-situ calibration of the load Bdot

From the change in load inductance we calculate the effective normalized radius of the current

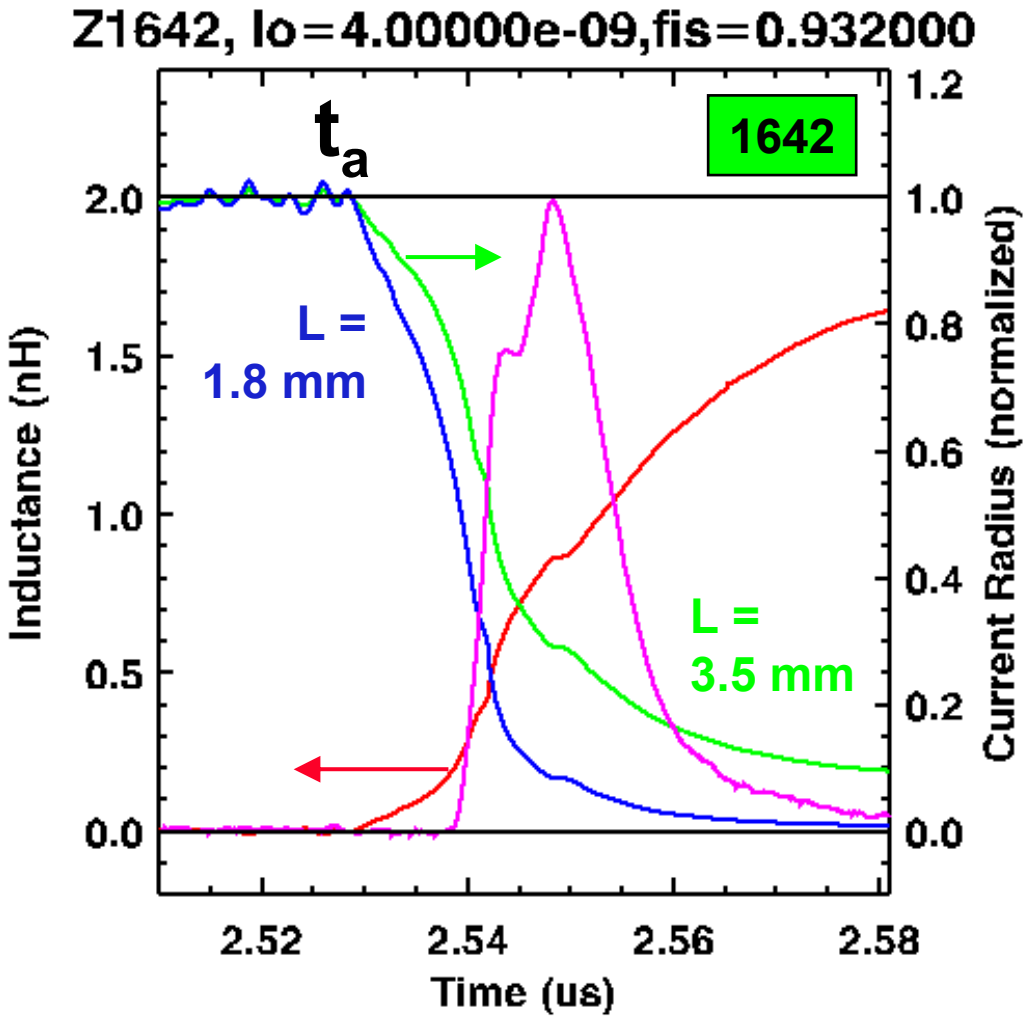

- We assume a range of pinch lengths, *l*
  - $r(t)/r_o = \exp[-\Delta L/2l]$
- This data could be analyzed with the time-dependent source length from simulations

We calculate the effective radius of the current

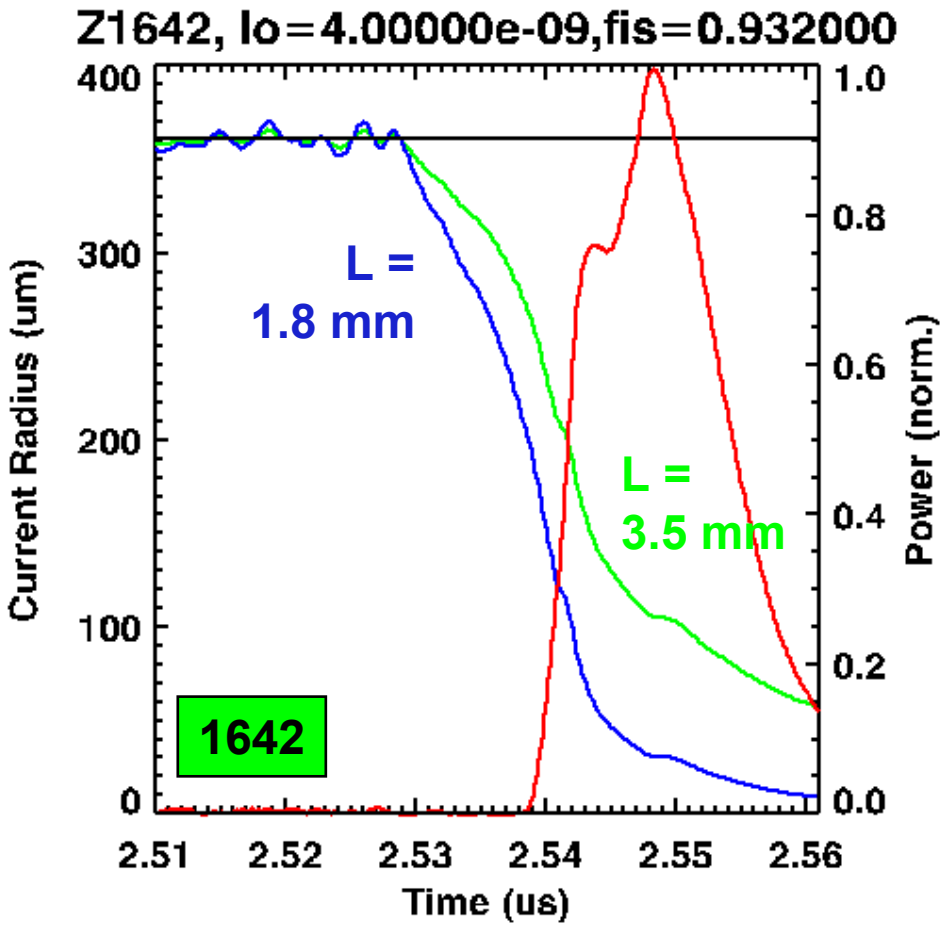

- Assumes r_o ~ 3.6 mm
- At the rising edge of the power pulse the effective radius is 1.7 to 2.5 mm
- At peak temperature the effective radius of the current is 0.3 to 1.0 mm
- We estimate a peak velocity of up to 45 cm/μs at the rise of the power pulse:
  - Vpeak ~ $2*\Delta R/(t_f - t_a)$
  - ΔR ~ 1 to 2.5 mm

We calculate the effective velocity of the current

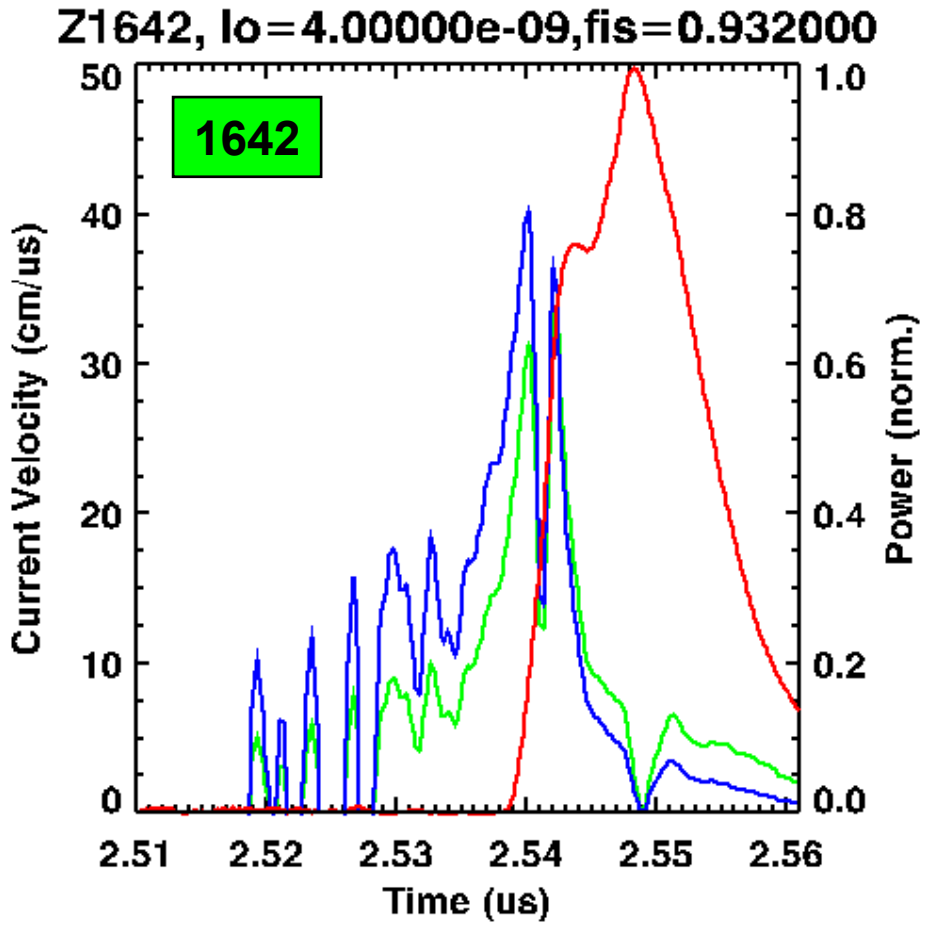

- The peak velocities are 35 to 41 cm/μs at a time 1.4 to 3.4 ns after the power begins to increase

We calculate the effective velocity of the current

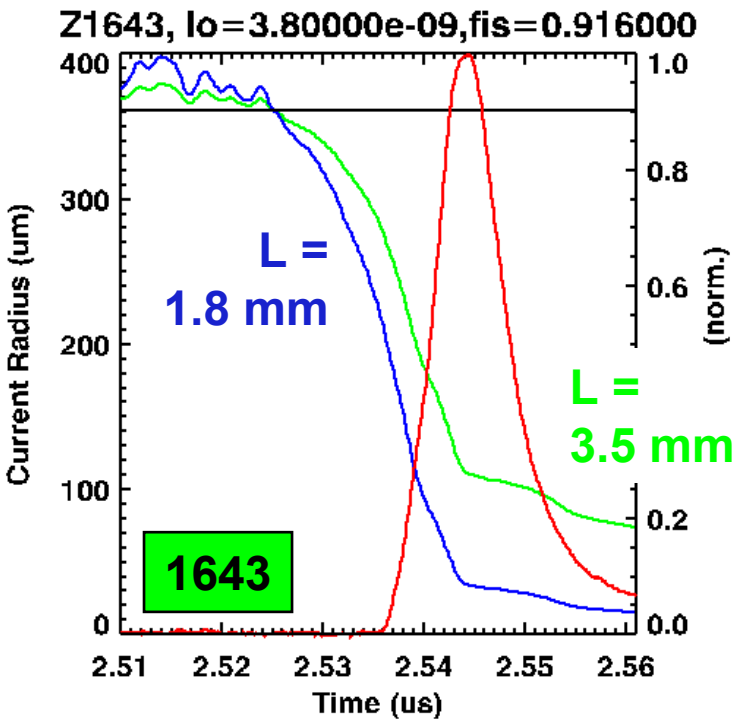

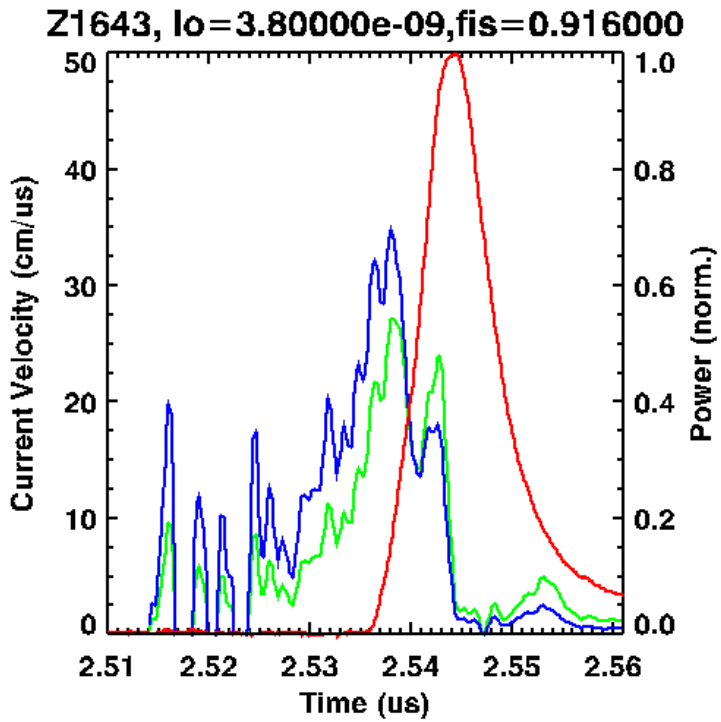

- **Veff ~ 25 to 35 cm/μs**

Typical Z-pinch radiation conversion efficiency on Z for 1 mm feed gap, 20 mm diam. array

W. A. Stygar et al., Phys.Rev. E,69, 046403 (2004)

At peak power:

E_{RAD}/E_L=57%

E_{RAD}/E_C=30%

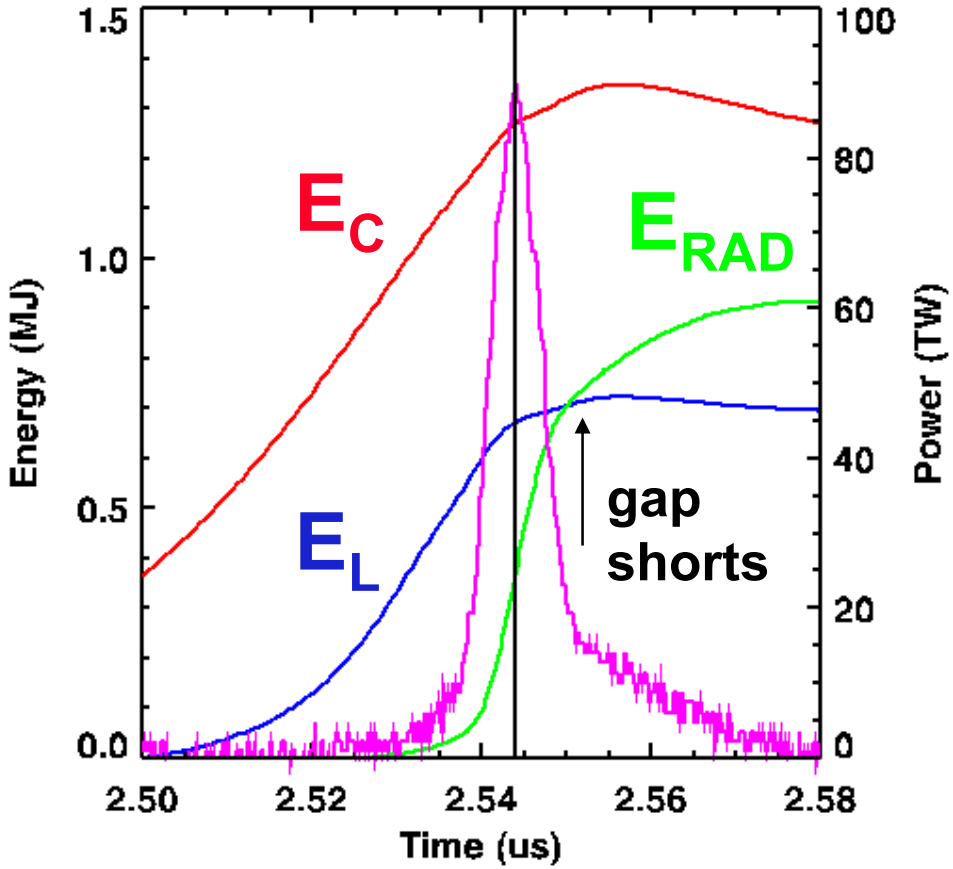

Vacuum gaps of 1 to 2 mm short on the timescale of the current pulse with peak magnetic pressure of 0.2 - 0.5 MBar

W. A. Stygar et al., Phys.Rev. E,69, 046403 (2004)

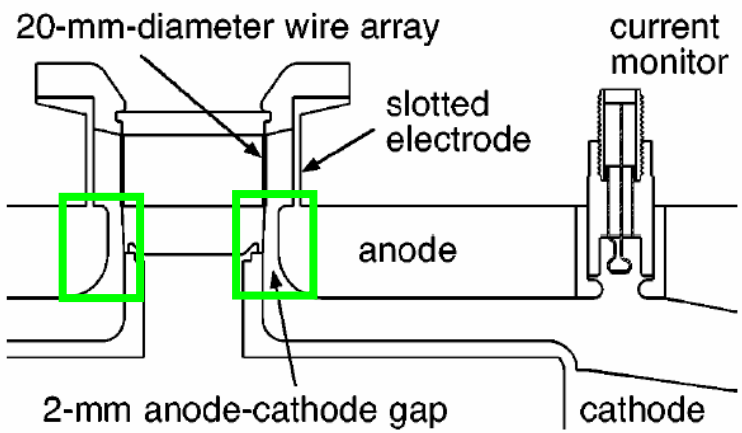

- **Small magnetically-insulated gaps that are initially bridged by material may also show these effects**
- **Wire arrays have higher ΔL and voltages, higher total soft and hard x-ray powers and yields and faster risetimes**

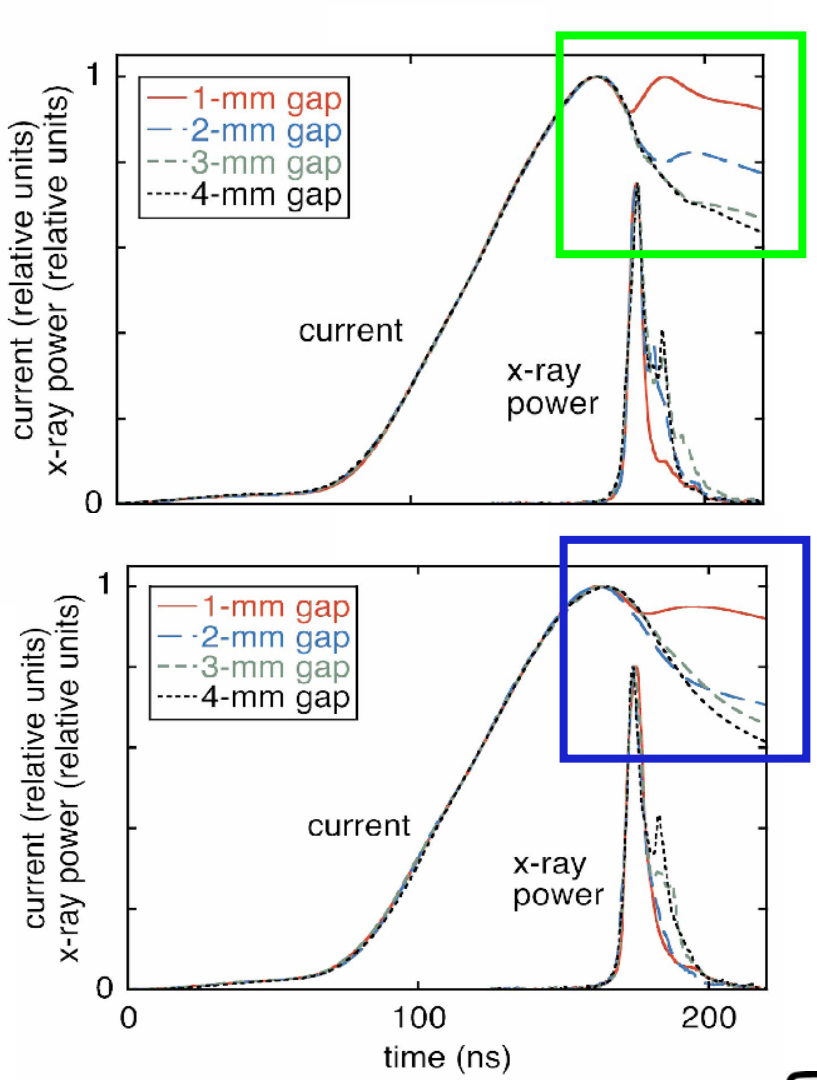

Z-pinch radiation conversion efficiency

W. A. Stygar et al., Phys.Rev. E,69, 046403 (2004)

E_{RAD}/E_C
(end of pulse)

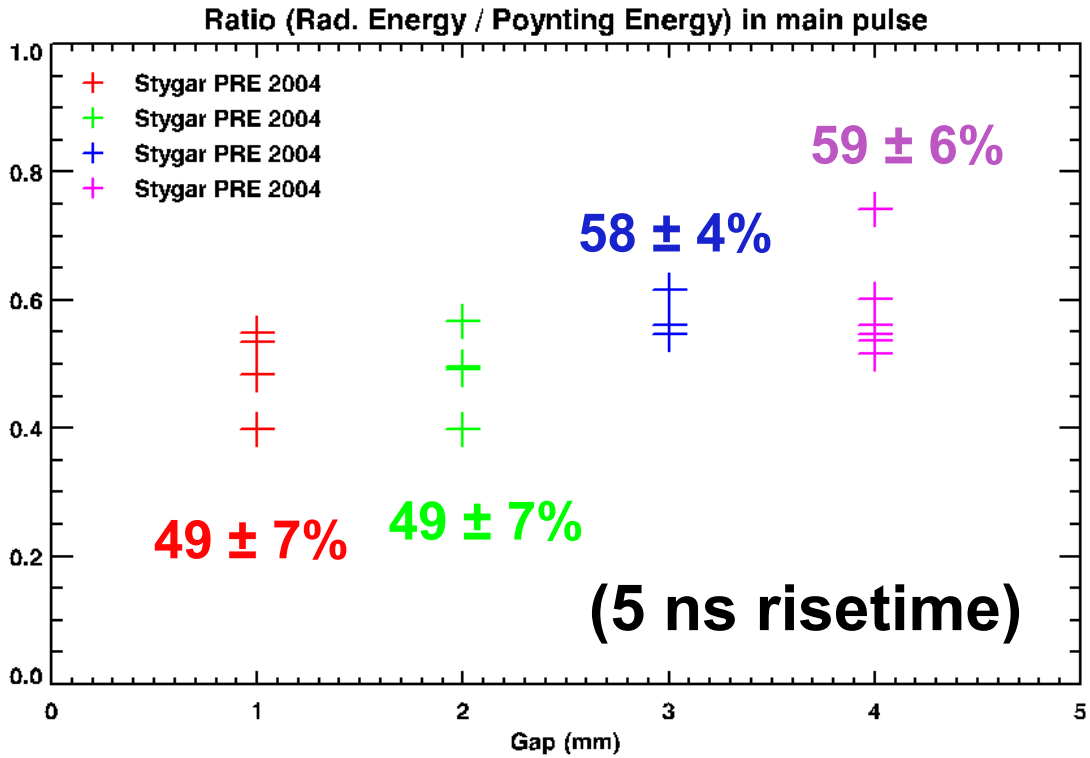

E_{RAD}/E_C ~ 50 ± 7 % with 1 to 2 mm gaps

E_{RAD}/E_L ~ 63 ± 7% at 1 to 2 mm gaps

Pinch power estimates for these experiments

Shot	τ_{rise} (ns)	E_L (kJ)	Estimated P_{max} (TW) (100% E_L)	Estimated P (TW) (63% E_L)	Tlower (eV)	T "peak" (eV)
1641	7.9	264	67	42	147	157 ± 10
1642	7.2	322	89	56	169	186 ± 17
1643	5.5	309	112	71	172	181 ± 9
1695	7.95* 5.0	444	120	76	174	187 ± 13
1736	5.2	222	85	54	181	191 ± 10

A previous 0D hohlraum energetics model can be applied to this data

M. E. Cuneo et al., Laser Part. Beams, 19, 481 (2001)

Primary $(1-f_s f_{ps})P_p - f_{ps}A_{ps}\sigma(T_p^4 - T_s^4) = A_p\sigma T_p^4$

Secondary $f_s f_{ps}P_p + f_{ps}A_{ps}\sigma(T_p^4 - T_s^4) = A_s\sigma T_s^4$

$A_p = (1-\alpha_p)A_{wp} - (1-\alpha_g)A_g$

$A_s = (1-\alpha_s)A_{ws} - A_h$

cm^2

$A_{wp} = 0.6597$

$A_g = 0.0314$

$A_{ws} = 1.0$

$A_{ps} = 0.2513$

$A_{hs} = 0.045$

The inferred pinch powers and measured secondary temperatures are consistent in the hohlraum model

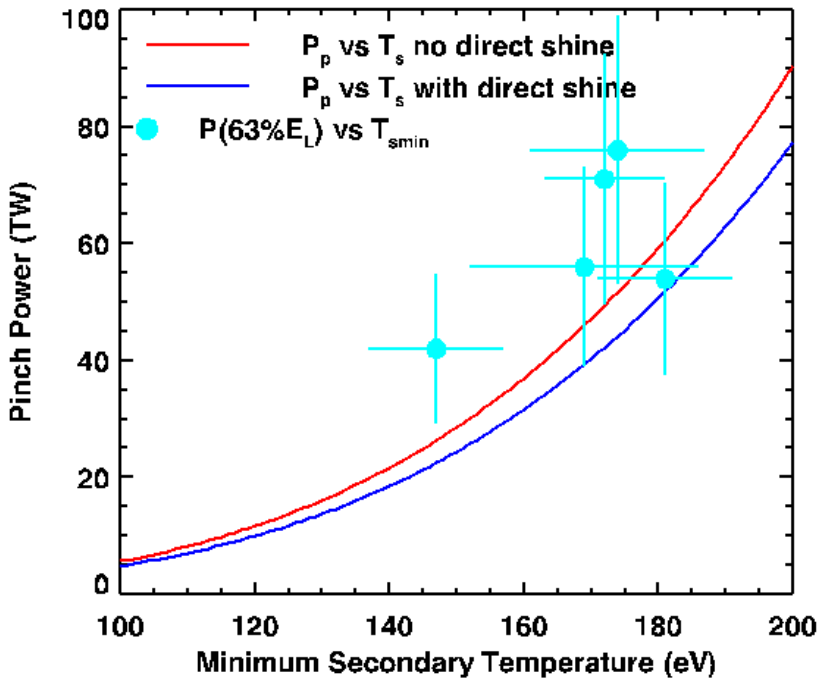

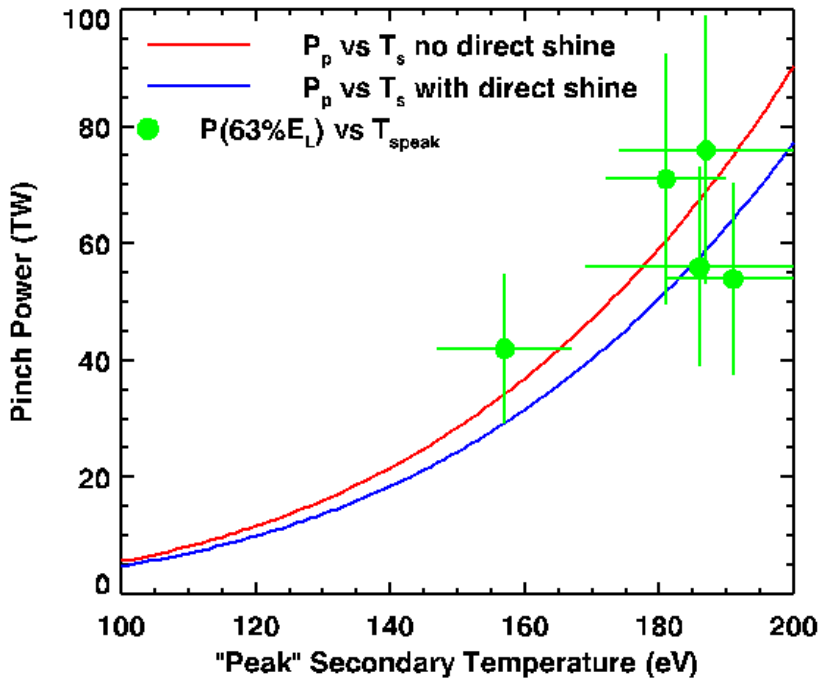

f_{ps} = 63% (coupling efficiency of primary to secondary)
f_s = 10% (direct pinch shine into secondary)
α_p = 0.85 (primary wall albedo)
α_s = 0.80 (secondary wall albedo)
α_{gap} = 0.34 (feed gap albedo)

Five experiments were performed in this experimental configuration before Z shut down

Shot	Liner Style	Press. (psi)	τ_{imp} (ns)	V_{peak} (MV) @ t (±30%)	T_{wall} (eV)	T_{wall} (eV)	$\tau_{gapshort}$ (ns)	$\tau_{aperture}$ at 20% open (ns)
1641	SB	12	89.0	1.2 (ts+5.9)	138±9 ts + 6	157±10 ts + 10.6	ts+6.1 ts+8.1	ts+16.1 *(5%)*
1642	SB	12	85.5	1.7 (ts+3.6)	149±7 ts+ 5	186±17 ts+10.6	ts+4.5 ts+8.4	ts+13.2 (6.1%)
1643	SB	10	84.6	1.6 (ts+7.8)	169±8 ts+ 8	181±9 ts+10.5	ts+6.1	ts+17.4 (4.1%)
1695	SB	10	87.9* 92.9	2.3 (t+10.0)* (ts+5.0)	158±8 ts+ 8	187±13 ts+10.9	ts+10.6* ts+5.6	ts+18.9 (4.2%)
1736	TB	10	79.6	1.1 (ts+1.5)	159 ± 7 ts + 5	191 ± 10 ts + 7.3	ts+3.5	ts + 14.2 (5.4%)

Improvements

- Improved current measurements
  - VISAR has shown precision of 1 to 2% in load current measurements (Lemke et al).
  - Local common mode rejection Bdots
  - Bdots with smaller area for higher bandwidth measurements near peak current
  - Measure L_L in-situ after vacuum gap compression

- Improved secondary energetics
  - larger, circular apertures
  - shock breakout
  - foam tamping at the secondary entrance

Improvements

- Optimize source performance
  - lower feed inductance
  - In-situ electrode cleaning techniques to reach the smallest Ak feed gaps (2 to 4 mm) and lowest feed inductances
    - >0.25 GHz RF reactive plasma discharge
    - In-situ DC heating 600-1000 °C for 20 minutes)
  - load gap/feed gap optimization
  - Nesting to increase power, reduce pulsewidth
  - WF_6 gas?

A lower inductance feed (3 nH) should be designed and implemented for the next experiments

Taper this feed from 6 to 2 mm gap at an angle of °15 from r=3.9 cm to r=0.375 mm

Z-Beamlet view at 2 to 10 mm (Z 16 to 18 mm)

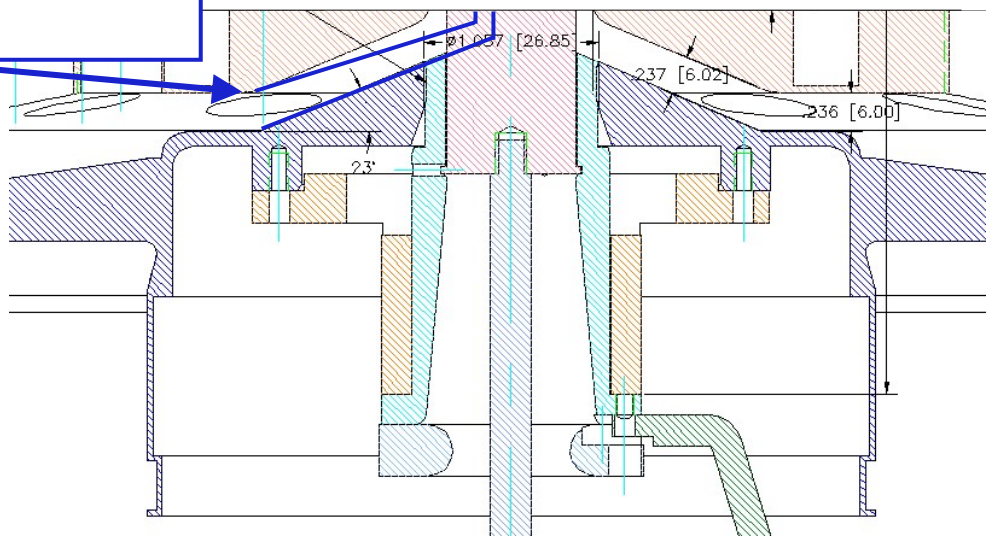

It might look something like this

- A feed with an avg. radial gap of 4 mm from 4 cm to 0.4 cm gives ~ 3 nH and saves about 1 nH.
- Would really like 2 nH. This requires a 3 mm avg. radial feed gap from 4 cm to 0.4 cm. This is probably impossible without in-situ (active) cleaning techniques, and may be impossible even with cleaning.
- Compatibility of a lower load height with ZR MITL's and backlighter line of sight must be assessed - should be no problem

The problem of contamination has been faced and solved in other programs

Magnetic Fusion

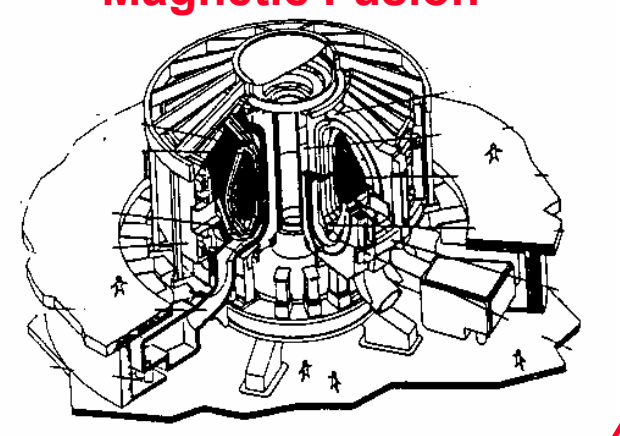

High Energy Physics

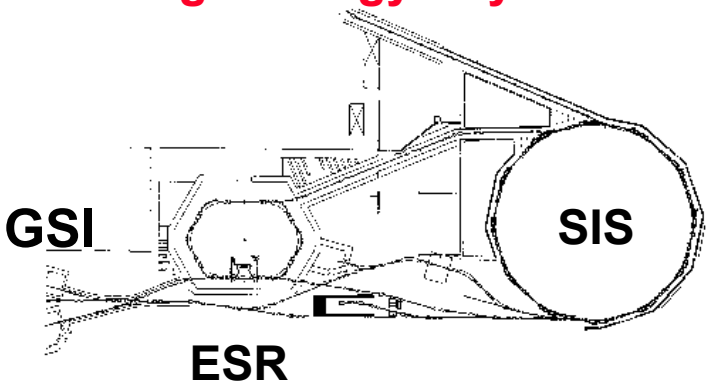

control of 50 - 100 monolayers surface/bulk contamination is critical

Ion Beam ICF

Z-pinches

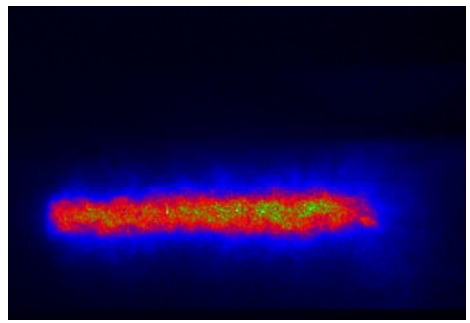

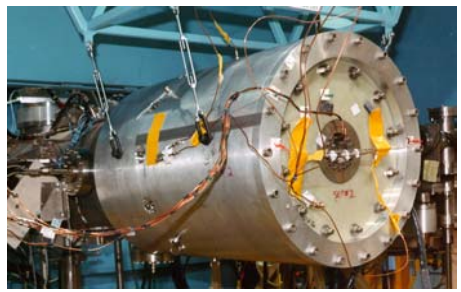

Radiography

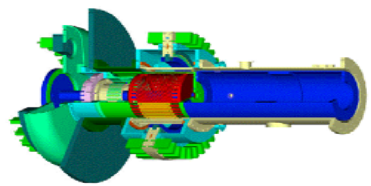

Decade

..... microwave tubes, RF cavities, MBE/plasma etching for micro-electronics, SEM resolution..... cold start problem in single shot devices

Large inventories (30-100 ml) of H_2, H_2O, C_nH_m, CO_2, CO, O_2 are found in bulk and surface layers

surface contaminant layer (< 30 Å)
H_2, H_2O, CO_2, CO, C_nH_m

porous oxides (100 - 300 Å)
FeO, Cr_2O_3, Fe_2O
C(H), H_2O

bulk
Fe, Cr, Ni, H_2

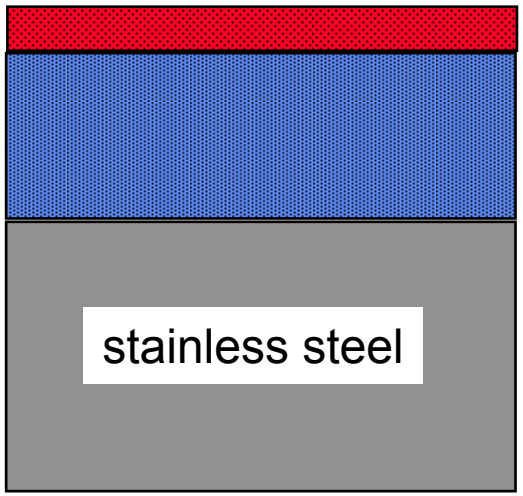

physisorbed and chemisorbed surface gases

physisorbed and chemisorbed gases in porous oxide layer

gases dissolved in bulk

contamintant binding energies	units (kcal/mole)
physisorbed on surface (and in oxide layer?):	Q ≈ 2 - 14
all gases (except H_2O)	Q ≈ 2 - 10
H_2O	Q ≈ 8 - 14
chemisorbed on surface (and in oxide layer?):	Q ≈ 10 - 50
C_nH_m	Q ≈ 20 - 30
H_2 (various metals)	Q ≈ 10 - 40
H_2 (stainless)	Q ≈ 21
stain. outgas. charac.	Q ≈ 22 - 25
CO (on stainless)	Q ≈ 22 - 47
oxide layers:	Q ≈ 50 - 100

M. E. Cuneo, IEEE Trans. on DEI, Vol. 6, No. 4, 469(1999)

Real surfaces have non-uniform coverage and density and are heterogeneous

Anode and cathode plasmas must be mitigated to meet 5-10 MV/cm required for ion beam fusion

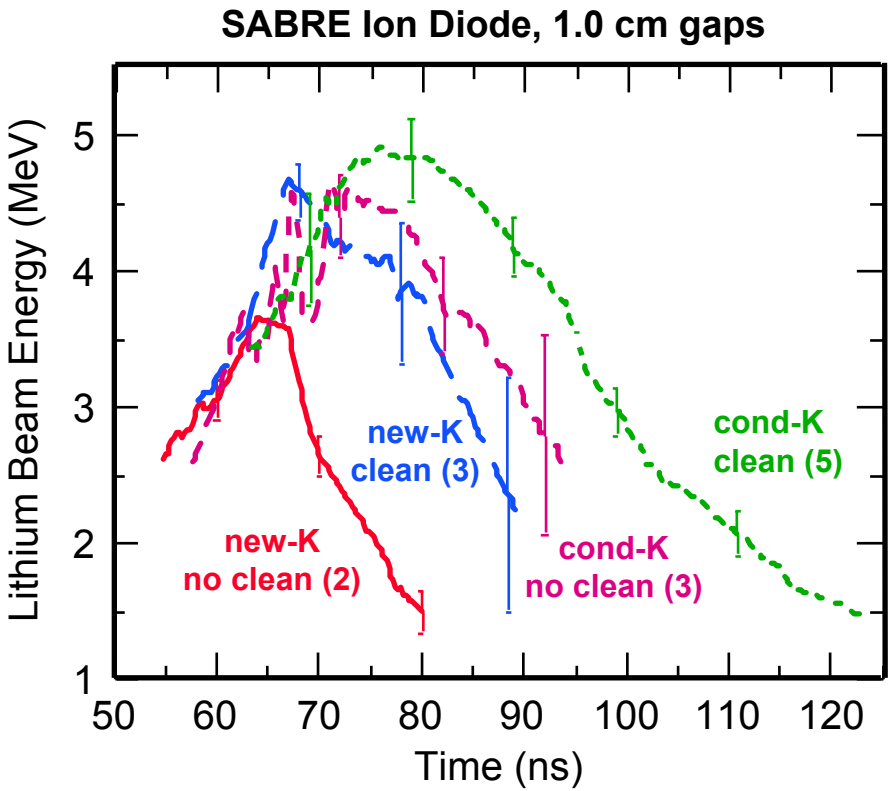

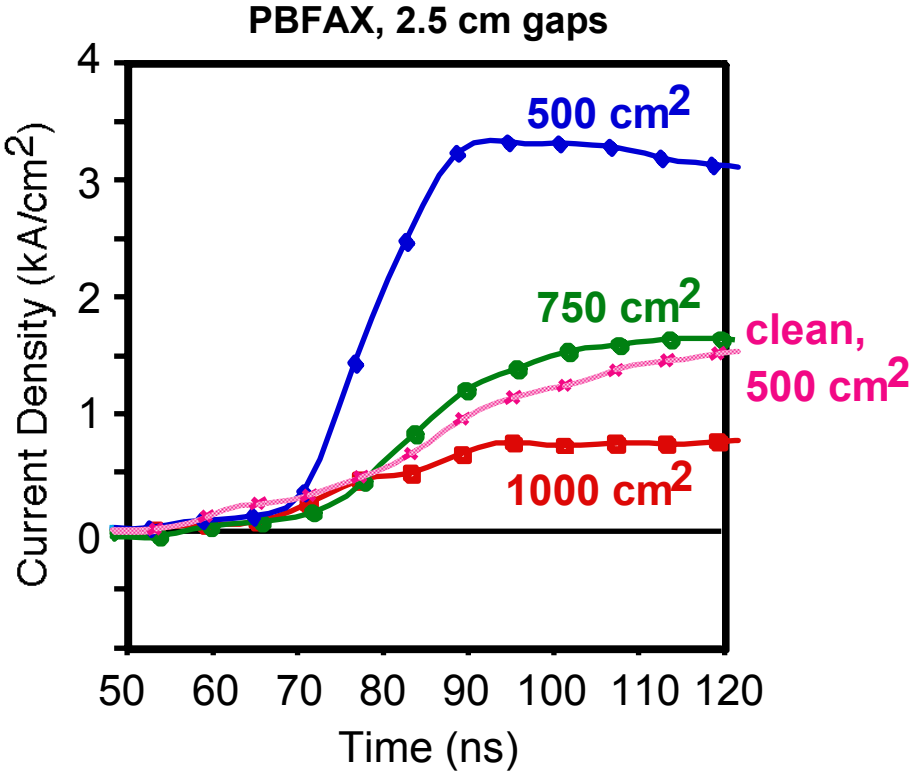

M. E. Cuneo, IEEE Trans. on DEI, Vol. 6, No. 4, 469(1999)

Cleaning and multiple pulse conditioning widen the applied-voltage pulse and decrease impedance collapse rate

There are other cleaning protocols shown to be successful in many fields

M. E. Cuneo, IEEE Trans. on DEI, Vol. 6, No. 4, 469(1999)

Method	Comments
pre-installation material selection	Materials have large differences of susceptibility to chemisorption, solubilities, diffusion, and binding energies for different contaminants [23].
pre-installation bake out	Vacuum forged metals, hydrogen firing followed by baking near melt effective for removal of oxide layer/bulk gases but oxide forms once removed from furnace.
pre-installation electric or chemical polishing	Dielectric residue has resulted in inconsistent results with electropolishing [18]. Results with chemical polishing methods better [18] but large improvements suggested by microprotrusion hypothesis not seen [4].
pre-installation water jets	Difficult to apply to pulsed-power. Effectively used for control of dust in RF cavities [18,39].
pre-installation clean room assembly	Difficult in typical pulsed power environment, but has shown large gains in RF cavities [18, 39], and in microelectronics.
low base pressure	Important, but difficult with pulsed power limitations. Local cryogenic differential pumping appears to be useful [103].
pre-breakdown e^- emission	Difficult to apply to pulsed-power. Very effective in conditioning gaps for high voltage breakdown on small experiments [2,59].
gas conditioning	Difficult to apply *in situ* in pulsed-power. Very effective in conditioning gaps for high voltage breakdown [2,59].
multiple breakdowns/arcs, repetitive operation	Some observations in low power pulsed-power experiments [9,85,86,100,115,127], but generally difficult to apply *in situ* except for rep-rate pulsed-power. Very effective in conditioning gaps for high voltage breakdown [59,69].
cryogenically-cooled electrodes	cryo-cooled electrodes do impact cathode plasma formation in pulsed-power experiments [17,104]. Not entirely understood.
surface coatings	Thick coatings are effective at controlling desorption from oxide and bulk where *in situ* cleaning of oxide and bulk not possible [17,80]. Material selection important [23]. Dielectric coatings have raised breakdown and flashover thresholds [65-67].
discharge cleaning	Large beneficial effects in pulsed-power experiments [16,17,87,88,93,98,99,101]. Physical and chemical sputtering is extremely effective at removing down to the last monolayer of tightly bound contaminants [19,20,53,54,73,74,135]. Discharges can also possibly remove inclusions. Reactive gases have large removal rates for hydrocarbon impurities [57,58]. Reactive gases lower field emission current [75], lower secondary electron emission current [76], raise operating field threshold [61,62,64,136]. Generation of a pure oxide layer [77] may be a factor [75,105].
in situ heating	Effective in pulsed-power experiments at 150 to 700°C at removing surface contamination contributing to the plasma [6,7,10,17,82-84,92-98,125,126,128]. Useful for bulk contaminant removal [72]. Effective in small-scale experiments at temperatures >1400°C at increasing breakdown fields on some materials [60] by control of particulate. Effective at reducing sticking coefficient to prevent recontamination after discharge cleaning [17,93,95]. Heating synergistic with discharges [30]. Will not remove the last monolayer without heating above oxide melt temperature or sputtering.
ion, e^- beam surface treatment	Shown to be very effective at increasing pulsed-voltage gap holdoff and decreasing effective surface microenhancement [69]. Not entirely understood: possibly from an increase in hardness, smoothing of surface, eliminating inclusions, surface cleaning, crystal structure and grain boundary changes.

Recommended priority for next experiments

(1) Hydro-coupling measurements
- Remove secondary and image at secondary entrance plane
  - Shadowgraphy
  - Backlighting

(2) Pinch energetics
- Can do this simultaneously with the above hydro experiment
- Measure pinch power, spectrum, and dynamics thru Be case
- Assess pinch L and K-shell emission

(3) Primary energetics
- Measure Twall (hard with a 2-3 mm high, 6 mm wide primary)

(4) Develop two-sided drive

(5) Long Pulse (28 MA, 240 ns) power scaling experiment (in-situ electrode cleaning becomes even more important with longer pulses)

Z-Pinch Source Experiments

- For various platforms, evaluate and compare optimized z-pinch sources at identical peak currents with widely different implosion times:
  - ZR in short pulse mode at 16-28 MA for τ_{imp} = 80-130 ns (2007-2009)
  - ZR in long pulse mode at 16-28 MA for τ_{imp} = 150-300 ns (2008-2009)
  - Goal: achieve same x-ray power at τ_{imp} = 250 ns as at 90 ns will reduce accelerator cost by more than a factor of 2*X*

$$\text{Cost} \propto E_{\text{Marx}} \propto \left(\frac{1}{\tau}\right)^{2/3}$$